Neuroprotection of Cone Photoreceptors in Retinitis Pigmentosa

A thesis submitted to the Medical Sciences Division and Nuffield Laboratory of Ophthalmology for the degree

DOCTOR OF PHILOSOPHY IN OPHTHALMOLOGY

Daniel M. Lipinski

Merton College

University of Oxford

Hilary Term, 2013

Abstract to

Neuroprotection of Cone Photoreceptors in retinitis Pigmentosa

By

Daniel M. Lipinski

Merton College, University of Oxford

D.Phil., Hilary Term, 2013

Retinitis pigmentosa (RP) is a genetically and phenotypically heterogeneous condition that affects approximately 1 in 4000 individuals worldwide. The most common presentation of RP is a rod-cone dystrophy, where the degeneration of cone photoreceptors occurs secondary to advanced rod loss, leading to a significant decline in central vision and a corresponding reduction in patient quality of life. The mechanisms underlying secondary cone loss are poorly understood, particularly in disorders where the gene defect is unknown or manifest only in rod photoreceptors. Consequently, the thesis presented herein proceeds on several fronts. First, in the long term a greater understanding of the causes underlying cone loss in RP is likely to be beneficial, and so in chapter one a dominant cone degeneration is characterized using intrinsically fluorescent cone photoreceptors to track the degenerative process. Second, as we develop a greater understanding of the genetic etiology underlying RP it is likely that the number of large genes identified as being causative will increase. As currently there is no efficient way to deliver large genes to photoreceptors, chapter two explores the use of alternate viral vectors that might be used to deliver a large therapeutic transgene. Lastly, whilst our understanding of cone loss in RP remains incomplete, it is necessary to develop a broadly applicable therapy to slow or attenuate further cone loss in RP patients regardless of the underlying cause. In chapters three and four we examine the use of low molecular weight 'growth factors', such as ciliary neurotrophic factor (CNTF), to preserve cone photoreceptors long-term using a rhodopsin knockout model of RP.

Contents

Acknowledgments

I would like to express my sincere thanks to Professor Robert MacLaren for his guidance and support throughout this research, and for tolerating my oftentimes wayward approach to lab politics and departmental bureaucracy. I am deeply grateful for the opportunity to have studied in Oxford under Robert's patient supervision, and for the many occasions on which he has gone out of his way to help make my start in academia a successful one. Additionally, and perhaps most importantly, Robert has taught me that buying group dinner is a perfectly legitimate use of 'discretionary' funding.

I owe a debt of gratitude to Fight for Sight UK, whose generous sponsorship made the work presented herein possible, and who are continuing to provide support for my post-doctoral research. Financial assistance (all non-refundable) was also gratefully received from 'The Bank of Mum and Dad', who kindly provided for more years of university education than one might think strictly necessary to get a 'real' job.

I am fortunate to have worked alongside many excellent scientists and clinicians during my short time in Oxford –deserving special mention are Alun R. Barnard, Mandeep S. Singh, Peter Charbel Issa, Stephen Hughes and Wayne I.L. Davies – each of whom contributed significant amounts of time and expertise to my research. They all taught me a great deal along the way, only some of which was actually related to ophthalmology. I also give thanks to my collaborators, Drs Emanuella Volpi and Mohamed Yusuf, who carried out the fluorescent in situ hybridizations presented in Chapter 1. Lastly, I would like to thank my examiners, Professors Dame Kay Davies and Glen Jeffery, for their time and guidance.

This thesis is dedicated to my parents, and to Rachel, for their continued love and support.

Abbreviations

AF	autofluorescence
CNTF	ciliary neurotrophic factor
cSLO	confocal scanning laser ophthalmoscope
DAPI	4',6-diamidino-2phenylindole
DsRed	Discosoma red fluorescent protein
EGFP	enhanced green fluorescent protein
ELISA	enzyme-linked immunosorbent assay
EIAV	equine infectious anaemia virus
ERG	electroretinography
FISH	fluorescent in situ hybridization
GCL	ganglion cell layer
GDNF	glial cell derived neurotrophic factor
GFAP	glial fibrillary acidic protein
HEK293	human embryonic kidney cell line, 293rd clone
HIV	human immunodeficiency virus
INL	inner nuclear layer
IPL	inner plexiform layer
IS	inner segment
LED	light emitting diode
MWS	medium wavelength cone opsin
NGF	nerve growth factor
NIR	near infrared reflectance
NCMD	North Carolina macular dystrophy
OCT	optimal cutting temperature (medium)

OKN	optokinetic nystagmus (response)
OLM	outer limiting membrane
OMR	optomotor response
ONL	outer nuclear layer
OPL	outer plexiform layer
OS	outer segment
PBCRA	progressive bifocal chorioretinal atrophy
PBS	phosphate buffered saline
PCR	polymerase chain reaction
PFA	paraformaldehyde
q-GL	quantitative grey level
rAAV	recombinant adeno-associated virus
RHO	rhodopsin
ROI	region of interest
RP	retinitis pigmentosa
RPE	retinal pigment epithelium
RPE65	retinal pigment epithelium specific retinal isomerase, 65kDa
RRD	rhegmatogenous retina detachment
S.D.	standard deviation
SWS	short wavelength cone opsin
TM	trabecular meshwork
UV	ultraviolet
VEEV-G	Venezuelan equine encephalitis virus glycoprotein
$VEGF_{165b}$	vascular endothelial growth factor, 165kDa b-isoform
VSV-G	vesicular stomatitis virus glycoprotein

Introduction

The Eye

The eye is a highly specialized organ which has evolved to transduce light stimuli into electrical signals and to relay those signals to the visual cortex. Light sensation and image formation is mediated through the activation of photoreceptor cells located in the outermost layer of the neurosensory retina, where incident light focused by the cornea and lens results in the activation of a signalling cascade and the propagation of an electrical impulse. This photoactivation is initiated by the isomerisation of light-sensitive 11-cis retinal within the photoreceptor outer segments, triggering the opening of cyclic-GMP gated ion channels. The continuation of the visual cycle is dependent on the constant replenishment of 11-cis retinal, a function performed by the retinal pigment epithelium (RPE), an underlying monolayer of cells in close contact with the photoreceptors. In addition to the isomerisation of photobleached retinoids, the RPE contributes directly to photoreceptor survival by the phagocytosis of spent outer-segment discs. Indeed, the maintenance of proper photoreceptor function is critically dependent on the RPE, and death of RPE cells invariably results in photoreceptor dysfunction and secondary degeneration. Maintenance of the complex photoreceptor-RPE interaction requires precise regulation of highly specialised intracellular protein interactions and the harmonic function of several hundred genes, any one of which can cause retinal dysfunction or cell death when mutated.

Despite its complexity the eye has many traits which make it an attractive organ for therapeutic intervention: it is immune privileged, of small size, easily visualized and examined, and readily accessible. The photoreceptors and the RPE are the primary targets for gene therapy treatments of retinal disease due to their importance for maintaining vision and susceptibility to common single gene disorders. The retina has a highly organized laminar structure which can be exploited for accurate spatial delivery of therapeutic material to the photoreceptors and RPE, where delivery is achieved through injection of fluid containing the therapeutic molecules into a potential space interposed between the two tissue layers, the subretinal space. Injection into the subretinal space results in a temporary detachment of the retina, but otherwise causes minimal damage. Alternatively, inner retinal neurons can be targeted

through administration of a therapeutic compound into the posterior chamber, which contains the vitreous humour and is largely self-contained, being separated from the anterior chamber by the lens and anterior hyaloidal membrane.

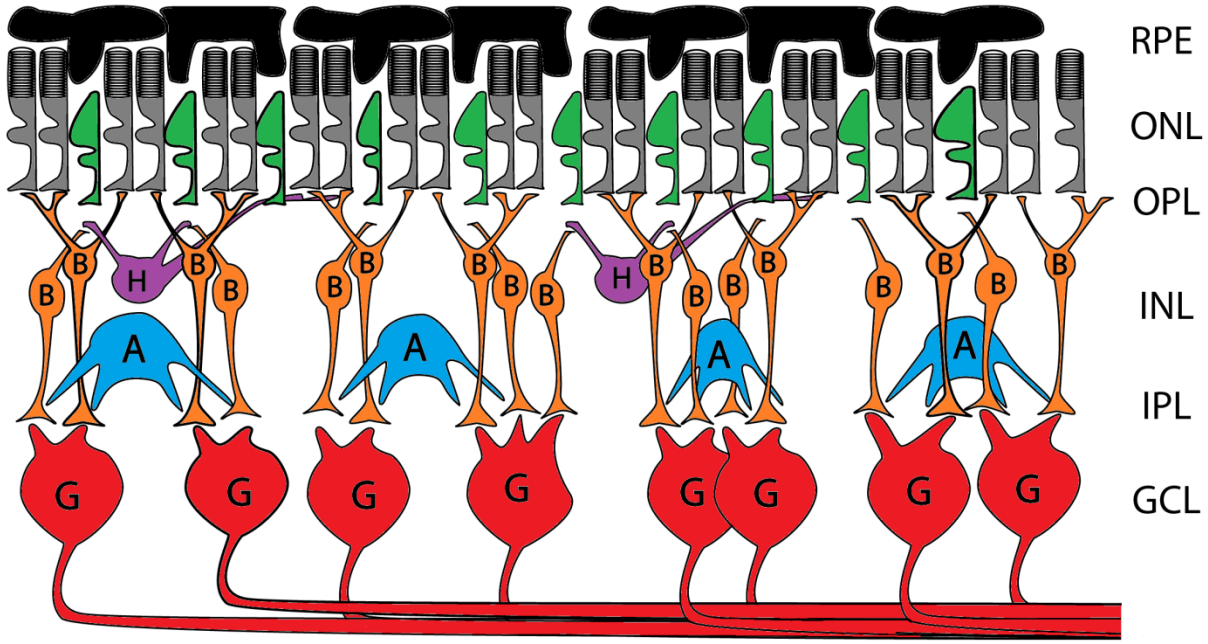

Schematic demonstrating the laminar structure of the neurosensory retina and the opposing retinal pigment epithelium
The neurosensory retina is comprised of several layers containing multiple cell types. The innermost layer, adjacent to the vitreous, is the ganglion cell layer (GCL) which is composed of retinal ganglion cells (G, red). Retinal ganglion cells project axons to the brain via the optic nerve and form synapses with cells of the inner nuclear layer (INL) at the inner plexiform layer (IPL). Several cell types make up the INL, including bipolar cells (B, orange), amacrine cells (A, blue) and horizontal cells (H, purple). Bipolar and horizontal cells form synapses with cells of the outer nuclear layer (ONL) at the outer plexiform layer (OPL). The outer nuclear layer consists of rod (grey) and cone (green) photoreceptors, and is directly opposed to the retinal pigment epithelium (RPE, black). For clarity Müller glia cells, which span the full retinal thickness, are not shown. Müller cells contribute significantly to the inner limiting membrane, which partially separates the neural retina from the vitreous, and the outer limiting membrane, located at the junction of the photoreceptor inner and outer segments.

Sensitivity and Distribution of Cone Photoreceptors in Mice and Humans

The spectral sensitivity and distribution of cone photoreceptors differs dramatically across vertebrate species. The retina of mice is comprised predominantly of rod photoreceptors, with approximately 400,000/mm^{2}making up 97-99% of the outer nuclear layer (ONL) (Ahnelt and Kolb, 2000). Murine cone photoreceptors correspondingly comprise 1-3% of the ONL and can be broadly divided into two classes: M-cones and S-cones (Carter-Dawson and LaVail, 1979; Jeon et al., 1998). The former express medium wavelength sensitive (MWS) opsin which has a maximal absorbance (λ_{max}) of 508nm (blue/green) (Sun et

al., 1997), and the later express short wavelength sensitive (SWS) opsin with a λ_{max} of 359nm (ultraviolet) (Yokoyama et al., 1998).Whilst the human retina is also comprised predominantly of rods (78-110 million per retina), cones contribute a greater percentage of the ONL than in mice, with approximately 4-6 million cones per retina, or ~5%. Cone photoreceptors in humans can be divided into three classes: L-cones, M-cones and S-cones. L-cones express long wavelength (LWS) opsin with λ_{max} of 560nm (yellow/red), M-cones express an MWS opsin with λ_{max} of 530nm (green), and S-cones express an SWS opsin with λ_{max} of 420nm (blue) (Deeb, 2006).

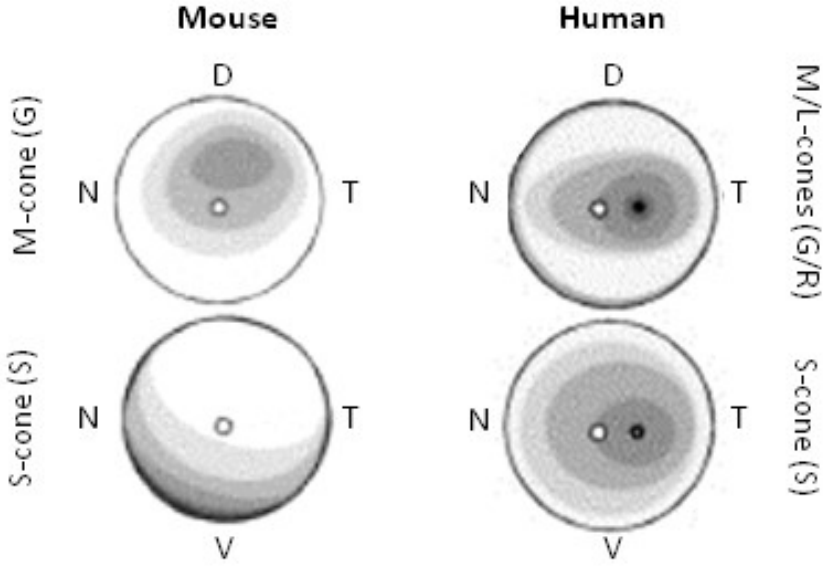

Schematic demonstrating the spatial distribution of cone photoreceptors in mice and humans by spectral cone class
Cone distribution of each cone class is shown as a greyscale image where white represents areas in which cone photoreceptors of a given class are absent, and black represents areas in which cones of a given class are most dense. Note the high foveal density of L- and M- class cones, and the peri-foveal ring of S-cones in the human eye. Human M- and L-cones are difficult to resolve anatomically and so are grouped together. Images are illustrative and not to any scale. White circle (central all images) = optic nerve head. N = nasal; T = temporal; D = dorsal; V = ventral. Figure adapted from Ahnelt & Kolb, 2000.

Cone photoreceptor distribution is not even across the retina in either mice or humans and is dependent on class. In mice the greatest density of M-cones is found dorso-temporally, immediately superior to the optic nerve head (average cone-to-cone spacing of 6.46±1.34μm), and decreases concentrically towards the peripheral retina (8.97±2.53μm cone-to-cone distance) (Ahnelt and Kolb, 2000; Fei, 2003). M-cones are largely absent from the ventral retina in the far periphery. Contrastingly, the greatest density of S-cones is located naso-ventrally in the far peripheral retina. An oblique ventral-dorsal gradient of S-cones

is observed, with S-cone numbers decreasing towards the dorso-temporal aspect, and very few S-cones observed superior of the optic nerve head. Consequently, the gradients of MWS opsin and SWS-opsin expression largely overlap in the mouse retina, somewhat blurring the distinction between M-cones and S-cones, with many cone photoreceptors expressing both opsins. However, the extent to which cone photoreceptors co-express MWS and SWS opsins is not clear. One study using northern blot analysis to assess mRNA levels of the two opsins demonstrated that only cones in the peripheral dorsal retina expressed a single photopigment, with all others expressing both opsins to a certain degree (Applebury et al., 2000). A more recent study using antibody double labelling demonstrated that the majority of cones in the dorsal retina express only MWS opsin, with just 3-5% co-expressing SWS opsin, and that a population of cones (8-20%) in the ventral retina express only SWS opsin (Haverkamp et al., 2005). Single cell patch recordings have shown that many cones have spectral sensitivities consistent with the presence of dual opsins, but that some cones elicit responses indicative of only one opsin being present (Jacobs and Williams, 2007; Nikonov et al., 2006).

In humans the distribution of cone photoreceptors is somewhat more complex. The maximum density of cones is found in the fovea, a 0.35mm wide depression surrounded by slightly thickened margins located 3mm temporal to the optic nerve head (Forrester et al., 2008). The fovea comprises almost exclusively L- and M-class cones to the total exclusion of rods. The spectral sensitivity of each cone opsin is best described as a probability that it will absorb a photon of a given wavelength, and whilst each human cone photoreceptor expresses a different opsin, the activation of a photoreceptor following the absorption of a photon by the chromophore is identical regardless of which opsin is expressed. The identity of a photon is lost once it is absorbed regardless of the energy it possessed before absorption, and it is therefore not possible for a single photoreceptor to distinguish a change in the wavelength of a light stimulus from a change in intensity - a principal termed univariance. Consequently, colour discrimination in humans relies on the comparison of activity from multiple cone photoreceptors with different spectral sensitivities (Solomon and Lennie, 2007). Given that colour vision is a composite function arising from

the activation of from multiple cones, for the greatest colour resolution one might expect the distribution of L- and M-cones within the fovea to be a regular lattice, with cones arranged alternately by class. However, whilst cones are broadly arranged in a regular hexagonal lattice, the patterning of the cones within that lattice is seemingly random, with clusters of each cone class unevenly distributed across the fovea (Solomon and Lennie, 2007). Furthermore, the ratio of L- to M-cones within the fovea differs markedly between individuals, with the proportion of L-cone ranging from 27% to 71% (Deeb, 2006). The developmental mechanisms underlying cone photoreceptor differentiation and migration in the fovea are poorly understood, and so it is unclear why there are such differences between individuals, or why the cone photoreceptor mosaic is arranged so that it must limit the acuity of colour vision.

S-cones are almost totally absent from the fovea, comprise just 5-10% of human cones, and are arranged randomly across the human retina except in the area immediately proximal to the fovea, where S-cone density peaks (3000 S-cones/mm^2) leading to the formation of a peri-foveal ring surrounding the fovea (Solomon and Lennie, 2007). Cone photoreceptor density remains high for all cone classes in the macular, a 1.5mm wide area containing the fovea, but decrease peripherally in an oblique concentric pattern (Ahnelt and Kolb, 2000). Opsin co-expression does not exist in human cone photoreceptors, with each cone expressing a single visual pigment, although chimeric opsins with unique absorbance characteristics caused by hybrid rearrangements of the LMW and MWS opsin genes, do exist.

The phenotype of many human retinal diseases is closely related to photoreceptor distribution. In particular, the fovea is often preserved until the late stages of disease in disorders where the genetic abnormality is manifest only in rod photoreceptors, such as rhodopsin mutations in retinitis pigmentosa. Conversely, conditions where the genetic deficit primarily affects cone photoreceptors often lead to cone-rod dystrophies, where bilateral systemic cone loss occurs with associated reduction in colour perception and visual acuity before peripheral vision loss or changes in dark adaptation - a rod driven response – are manifest.

Differences in photoreceptor distribution likely contribute to the observed lack of phenotypic correlation with regard to diseases progression in a human patient compared to the respective mouse model of that disease. A striking example is that of Stargardt's disease, an autosomal recessive form of juvenile macular degeneration caused by mutations of the ABCA4 gene. Humans present with bilateral loss of central photoreceptors and RPE with an associated reduction visual acuity, and increased autofluorescence and retinal flecking due to lipofuscin deposition. Contrastingly, ABCA4 knockout mice show only limited electrophysiological deficits, if any, and no evidence of retinal degeneration or loss of visual function. Although ABCA4 knockout mice do develop increased levels of autofluorescence from a young age, they are a poor model of the human disease. As in this instance, the absence of a macular and fovea in mice greatly complicates the use of murine disease models to assess the likely clinical outcome of a treatment in human patients.

Retinitis Pigmentosa

Retinitis pigmentosa (RP) describes a genetically and phenotypically heterogeneous disorder, with mutations collectively affecting between 1 in 2,500 and 1 in 4,000 individuals worldwide (Haim, 2002; Pagon and Daiger, 2005). RP is characterized by the progressive loss of photoreceptors, most commonly presenting as a rod-cone dystrophy, where rod loss occurs early – usually within the first two decades of life – and is followed by a secondary loss of cone photoreceptors. In principal, the treatment of RP using gene therapy should be relatively straightforward. The disease is typically diagnosed early and central cone-mediated vision is often preserved until late stages of the disease, giving a wide window within which to intervene. The majority of RP arises as a result of single gene defects affecting either the photoreceptors or RPE, both of which are can be targeted relatively efficiently using recombinant adeno-associated virus (rAAV) vectors delivered to the subretinal space, an anatomically constrained potential space interposed between the two tissue layers. Furthermore, 50-60% of RP is recessively inherited, and so in many cases direct gene replacement might be expected to significantly ameliorate the disease

phenotype and potentially halt progression of the degeneration. However, the clinical reality is somewhat more complex. The window for preservation of rod function is narrow, with significant rod degeneration usually evident by the time patients present to the clinic. The mechanism underlying the secondary loss of cone photoreceptors in poorly understood, particularly in those cases of RP in which the genetic defect is manifest only in rod photoreceptors (e.g. *RHO*, *NRL*, *PDE6β*), and the cones may not express any of the abnormal gene product. Furthermore, the genetic heterogeneity of RP may make the development of gene specific therapies impractical for all but the most prevalent alleles. And lastly, the genetic etiology underlying many cases of RP has not been elucidated, with approximately 50% of dominant RP and 30% of recessive non-syndromic RP having no identified genetic case, precluding a gene replacement approach.

Therapeutic Strategies for Cone Preservation

With a significant proportion of RP having no know genetic cause, and the mechanisms underlying secondary cone degeneration poorly understood, one must look to alternative therapeutic options. Arguably, any therapeutic intervention for the treatment of RP should focus on the preservation of cone photoreceptors, where these cells are critical for execution of routine daily tasks, being responsible for colour and deep perception, and detailed vision. There are several avenues of research by which cone photoreceptors might be preserved in RP.

i) Cell replacement therapy

The clinical reality is that patients typically present to the clinic only once rod degeneration is significantly advanced, and cone loss has commenced. The mechanism underlying secondary cone loss is poorly understood, but it is likely that the absence of rods results in a reduction of trophic support and an increase in physical stress on the remaining cones, such as compression between the inner nuclear layer and RPE as the outer nuclear layer collapses. One option for the preservation of remaining cones would,

therefore, be the reintroduction of rod photoreceptors into the subretinal niche. Rod transplantation has been shown to be feasible in animal models with a relatively intact outer nuclear layer (MacLaren et al., 2006b; Pearson et al., 2012), and more recently in mice whose retina are totally degenerate (Singh et al., 2013). Whilst the latter closely mimics the clinical situation, several questions remain before the transplantation of photoreceptors might become a clinical reality. Foremost, how to produce photoreceptor cells for engraftment? Embryonic stem (ES) cells, derived from the inner cell mass of blastocyte-stage embryos, have been demonstrated repeatedly to maintain potency and are able to be differentiated into mature cell types, such as photoreceptors (Haruta, 2005). However, despite the eye being relatively immune privileged ES cells are still immunogenic as they are non-autologous. Additionally, as the name suggests, ES cells are foetal in origin and not present in adult humans. Consequently, their sourcing, usually from cultures of pre-implantation embryos, remains ethically problematic and practically difficult (Evans, 2005). Induced pluripotent stem (iPS) cells, where fully differentiated postmitotic cells such as fibroblasts undergo reprogramming to revert them to a stem-like state of potency, represent an alternative to the use of ES cells. iPS cells have already been derived from patients with various degenerative diseases, including Parkinson's and Amyotrophic lateral sclerosis (Dimos et al., 2008; Park et al., 2008) and have been successfully differentiated into photoreceptor cells (Hirami et al., 2009). However, given that differentiation is less efficient for iPS cells than ES cells, the question remains can iPS cell be generated in sufficient number for ONL repopulation to be practicable in humans? Additionally, the use of autologously derived iPS cells is likely to raise certain regulatory issues, where currently drugs or treatments destined for clinical use require extensive trials prior to their licensing. It is unclear how cell based therapies, where each is uniquely derived from a single patient for one-time use might be subject to approval prior to being used. This is of particular importance in terms of ensuring the purity of iPS derived cell populations, where the exclusion of potentially tumourogenic undifferentiated cells needs to be guaranteed. Finally, would ex vivo correction prior to transplantation of rod precursors be required to prevent degeneration of the transplanted cells? And would cell replacement

still be a viable treatment option when the gene defect is not known, and the transplanted cells would likely degenerate also? Consequently, whilst the field is rapidly progressing, at this stage, photoreceptor transplantation, either for the restoration of sight in totally blind patients, or to provide trophic support to residual cone photoreceptors, is unlikely to be a viable option for some time (Singh & MacLaren (2011).

ii) Anti-apoptotic therapy

Anti-apoptotic therapies focus not on the correction of a specific deficit in gene function, but on prolonging the lifespan of cells in spite of their genetic abnormality. The functional mechanism of anti-apoptotic proteins require that they are expressed intracellularly and so, in contrast to neuroprotection (see below), the therapeutic gene must be delivered directly to the cone photoreceptors.

X-linked inhibitor of apoptosis (XIAP) has shown considerable promise in attenuating the degeneration of photoreceptors in models of ischemic injury and in models of retinitis pigmentosa (Chen et al., 1996; Leonard et al., 2007; Renwick et al., 2006; Shan et al., 2011; Zadro-Lamoureux et al., 2009). Similarly, delivery of BiP/Grp78, a molecular chaperone, has proved effective in suppression of apoptosis in mis-sense mutations where activation of the unfolded protein response (UPR) is triggered. UPR activation occurs when the accumulation of incorrectly folded protein is detected by a transmembrane kinase (IRE1) present in the endoplasmic reticulum (ER) (Shamu, 1997). Subsequently, translational attenuation is triggered by phosphorylation of the α-subunit of elF2 resulting in the non-specific down regulation of translation, and ultimately to apoptosis. Expression of Bip/Grp78 delivered subretinally in rAAV resulted in photoreceptor preservation in animals with dominant P23H rhodopsin mutations (Gorbatyuk et al., 2010). These studies demonstrate that anti-apoptotic therapies have the potential to preserve photoreceptors which are genetically abnormal and subsequently degenerate; however, it is unclear to what extent expression of anti-apoptotic proteins might have in genetically healthy yet stressed residual cone photoreceptors - it is conceivable that delivery and expression of a transgene might increase cellular stress and expedite cell death. Additionally, whilst anti-apoptotic factors are promising, their

inherent mechanism of action - preventing cells from undergoing programmed cell death – gives rise to concerns relating to the potential for oncogenesis, where control of apoptosis is deregulated in many cancers and malignancies. However, this may be a lesser concern in the retina, where the cells targeted are post-mitotic and fully differentiated.

iii) Neuroprotection

Similarly to anti-apoptotic therapies, neuroprotection aims not to correct a deficit in function, but to prevent cell death regardless of the mechanism by which degeneration occurs. This is typically accomplished through the expression of naturally occurring low molecular weight 'growth factors', which when present at high concentration elicit a neuroprotective effect. A distinct advantage of this approach is that growth factors are typically highly diffusible, and so the therapeutic gene can be delivered to any tissue, often the RPE (via subretinal injection) or ganglion cell layer (via intravitreal injection), from where the factor is secreted resulting in a paracrine effect. Several neurotrophic factors have been demonstrated the have efficacy in the treatment dominant RP arising from rhodopsin mutations, including ciliary neurotrohic factor (CNTF) (Liang et al., 2001), brain-derived neurotrophic factor (BDNF) (Okoye et al., 2003) and glial-cell derived neurotrophic factor (GDNF) (McGee Sanftner et al., 2001). The neuroprotective approaches utilized in these studies were dependent on rhodopsin mutation class (all class-I, in which mutant rhodopsin protein accumulates in the cell membrane), which implies that neuroprotection could be a strategy that in many dominant conditions is dependent on the nature of the disease mechanism. However, neuroprotective approaches have also been used successfully in models of recessive retinal disease both *in vitro* and *in vivo*, and present one of the only approaches for the preservation of cone photoreceptors in RP (Buch et al., 2006; Lipinski et al., 2011a; Schlichtenbrede et al., 2003a).

CNTF is a particularly promising neuroprotective candidate, being a low molecular weight (22kDa) polypeptide type I cytokine that binds a specific CNTF receptor alpha (CNTFRα) and two

general receptors, LIFRβ and gp130, resulting in activation of Jak/STAT and MAPK pathways (Kassen et al., 2009). Activation of STAT3 and ras-MAPK by CNTF (Peterson et al., 2000) has been associated with neuroprotection of ganglion cells in response to a wide variety of stress stimuli, including ocular hypotension, autoimmune optic neuritis, oxidative stress and experimental glaucoma (Ji et al., 2004; Leaver et al., 2006; MacLaren et al., 2006a; Maier et al., 2004; Pease et al., 2009), and of photoreceptors in models of RP (Kassen et al., 2009; Liang et al., 2001; Lipinski et al., 2011a). Neuroprotection represents one of the most straightforward strategies by which cone photoreceptors might be preserved in RP.

The Eye and Gene Delivery

The success of a therapeutic intervention, such as the expression of a neuroprotective protein, is dependent upon the efficiency with which the therapeutic transgene can be delivered to the appropriate cell type. For ocular gene therapy, the most commonly used method of delivery is to use a recombinant adeno-associated virus (rAAV). Based on adeno-associated virus (AAV), a non-pathogenic dependovirus (subfamily: *Parvovirinae*) that is unable to replicate in the absence of an active synergistic virus infection, typically of adenovirus or herpes simplex virus (Berns, 1996), rAAV virions are approximately 25nm in diameter, non-enveloped and package a single stranded DNA (ssDNA) genome (Baltimore class II) with a maximum length of 5.1kb (Arsuaga et al., 2002; Berns, 1996; Srivastava et al., 1983). The wild-type AAV genome has two open reading frames (ORF) each containing a single gene. ORF-1 contains *rep,* which encodes four proteins (Rep40, Rep52, Rep68 and Rep78) required for virus replication, and ORF-2 contains *cap*, which encodes the three structural proteins (VP1, VP2 and VP3) that comprise the icosahedral capsid. The coding sequence is flanked by two inverted terminal repeats (ITRs), palindromic sequences 145bp in length which form hairpin-loop secondary structures at the strand termini (Spear et al., 1977). ITRs are critical components, facilitating genome packaging, which occurs from the 3’

terminal ITR. Additionally, ITRs prevents recognition of the ssDNA genome by host cell immunity and forms a template from which to initiate second strand synthesis (Hauswirth and Berns, 1977).

There are presently at least 11 naturally occurring AAV serotypes which are well characterised (AAV1 – 11), though over one hundred non-redundant species of proviral sequence have been recovered, with sequence identity of *cap* ranging from 45% to 99% (Gao et al., 2005; Mori et al., 2004). The polymorphic nature of *cap* gives rise to capsid proteins with affinities for different cell surface receptors. The primary receptor mediating cell binding of AAV serotype 2 (AAV2) is heparan sulphate (Summerford and Samulski, 1998), with $\alpha_v\beta5$ integrin (Summerford et al., 1999), fibroblast growth factor-1 (Qing et al., 1999), hepatocyte growth factor (Kashiwakura et al., 2005) and laminin all implicated as co-receptors (Akache et al., 2006). By contrast, AAV4 and AAV5 bind preferentially to α2,3 sialic acid or platelet-derived growth factor (Di Pasquale et al., 2003; Kaludov et al., 2002), while AAV3, AAV8 and AAV9 bind laminin (Akache et al., 2006). Differential binding significantly affects the natural tropism of each AAV serotype, an aspect which can be exploited to direct cell-specific targeting when using AAV derived vectors (Wang et al., 2011).

rAAV vector construction requires modification of a wild-type virus genome, usually that of AAV2. ORF-1 and ORF-2, containing the *rep* and *cap* genes, are deleted, and replaced with a transgene cassette which minimally consists of a promoter, therapeutic cDNA and poly-adenylation (poly-a) signal. The ITRs are retained, and are the only viral sequence required for cis-packaging of a recombinant vector genome (McLaughlin et al., 1988). The necessary inclusion of ITRs reduces the total coding capacity of AAV vectors to approximately 4.7kb, and limits the size of the therapeutic gene that can be delivered.

The cellular tropism of AAV is conferred predominantly by the capsid, which harbours receptor binding domains with affinity for specific cell-surface residues (summarized above), such as the heparin binding domain located on the externalized loop-domain of AAV2 VP3 protein (Wu et al., 2000). It is possible to utilize this differential tropism through production of recombinant AAV (rAAV) vectors, formed by the process of 'pseudotyping', where an AAV2 based expression cassette is packaged into a

capsid originating from a different serotype. Using recombinant vectors gene delivery to RPE has been effectively shown with several pseudotypes, particularly rAAV2/1 (AAV2-based genome in AAV1 capsid), rAAV2/2 and rAAV2/4 following delivery into the subretinal space (Ali et al., 1996; Le Meur et al., 2007; Lebherz et al., 2008). rAAV2/2 also exhibits photoreceptor transduction, but to a lesser degree than either rAAV2/5 or rAAV2/8 when delivered subretinally (Bennett et al., 1999; Flannery et al., 1997; Mussolino et al., 2011; Vandenberghe et al., 2011), but uniquely demonstrates transduction of ganglion cells and Müller glia following intravitreal administration (Ali et al., 1998; Yin et al., 2011). It is not known if any rAAV can transduce the choroid effectively, although various serotypes are known to transduce vascular endothelial cells and muscle (Kilian et al., 2008; Zincarelli et al., 2008).

Consequently, selection of capsid serotype depends predominantly on the tissue type to which the therapeutic gene is to be delivered. For this reason, rAAV2/2 has been used extensively in the current ongoing LCA trials, and would be an ideal choice for targeting ganglion cells from which to secrete a neuroprotective protein, such as CNTF.

Clinical utility of rAAV vectors

Recombinant AAV vectors have been shown to be effective vehicles for therapeutic gene delivery in numerous pre-clinical and clinical studies of retinal disease, and that gene expression is maintained long term. Probably the most widely studied models of retinal disease are those with mutations affecting RPE65. The Rpe65/Rd12 mouse model has RPE dysfunction resulting in degeneration of rod photoreceptors with preservation of cones, and as such accurately reflects the human disease phenotype (Pang et al., 2005; Redmond et al., 1998). Additionally, a subset of Briard dogs has a natural 4bp deletion in the RPE65 gene which results in the introduction of a premature stop codon. Dogs have RPE inclusions and rod photoreceptor with abnormal morphology (shortened inner segments) which progressively degenerate, leading to reduction in ERG amplitude with age (Aguirre et al., 1998). The Briard dog model represents an excellent model for human RPE65-LCA as it has both a similar phenotype in addition to

having eyes of similar size and structure, despite the absence of a macula. Acland et al (2001) first demonstrated subretinal administration of RPE65 cDNA could significantly improve dark-adapted ERG and blue flicker response. Additionally, performance of visually guided tasks improved significantly to wild-type levels, reflecting that visual evoked cortical potentials (VEPs) from treated eyes, which were significantly higher than untreated eyes, were being transduced into useful visual input (Acland et al., 2001). Following demonstration of therapeutic efficacy in Briard dogs, safety studies were conducted in both Briards and non-human primates which demonstrated that there was no systemic toxicity in response to either the vector or transgene, though moderate inflammation and localized retinal thinning at high doses was observed (Jacobson et al., 2006a; Jacobson et al., 2006b). Human and canine RPE65 expression when delivered by AAV vectors has since been shown to be consistent and long-lived, with ERG response stable for over three years (Acland et al., 2005; Bennicelli et al., 2008).

Similar results have been observed in pre-clinical studies developed for the treatment of achromatopsia, a condition in which photoreceptors are dysfunctional but not degenerate, resulting in extreme photophobia, poor daytime visual acuity and nystagmus. Several well established naturally occurring or transgenic animal models of achromatopsia exist on which to evaluate therapeutics, including *Gnat2*, *Cnga3* and *Cngb3* deficient mouse strains, all of which have absent ERG responses. Recent studies have demonstrated that re-expression of murine *Cnga3* protein using a rAAV vector leads to restoration of a recordable light-adapted ERG which was maintained for at least 2 months (Michalakis et al., 2010; Pang et al., 2009; Pang et al., 2010). *Gnat2*$^{-/-}$ (*cpfl3*) mice have a recessive mutation affecting exon 6 of the cone α-transducin subunit, which results in progressive loss of light-adapted ERG response over 9 months and secondary loss of rod function (Chang et al., 2006).

Recombinant AAV vectors, therefore, are likely to be ideal vehicles from which to express a therapeutic transgene, such as a secretable neuroprotective compound, with a realistic prospect that the intervention will be a one-time occurrence and that the resultant treatment effect will be long-term.

Aims and Outline

In the long term, the elucidation of the mechanisms underlying photoreceptor degeneration in RP, particularly with regard to secondary cone loss, is critical for the development of future treatments. Only by understanding the root causes of secondary cone loss – what makes genetically healthy cells degenerate – can we effectively prevent their loss. Consequently, in chapter 1 (Lipinski et al., 2011b) we examine a mouse model which was reported to have an RP-like degeneration featuring cone loss, characterizing the disease progression and probing the underlying genetic etiology. We revealed a dominant cone dystrophy which is potentially orthologous to two retinal degenerations observed clinically in humans, North Carolina macular dystrophy (NCMD), and progressive bifocal choreoretinal atrophy (PBCRA).

Currently, ocular gene delivery focuses almost exclusively on the use of rAAV to deliver therapeutic transgenes. Whilst rAAV is capable of being targeted towards specific cell types, and gene delivery is highly efficient, the coding capacity is limited. Despite recent advances in vector technology, including attempts to artificially expand the coding capacity through use of recombining or trans-splicing vectors, delivery of large genes to photoreceptors remains inefficient (Lipinski et al., 2012). It is likely as further loci associated with RP are identified the number of genes which are unable to be packaged in to an rAAV vector will increase beyond the current few. Consequently, in chapter 2 we examine the ability of two differently pseudotyped lentivirus vectors, which have significantly greater coding capacity than rAAV, to transduce the retina.

In the short term, whilst the clinical situation remains that the process of degeneration is incompletely understood in many forms of RP, and the economic and administrative burden of conducting gene therapy trials remain high, it is important to focus on the development of a broadly applicable therapy which might prevent further cone photoreceptor degeneration regardless of genetic cause - neuroprotection is an attractive approach to fulfil this aim. A neuroprotective therapy would likely involve the delivery of the therapeutic transgene to a non-cone cell type – such as ganglion cells which do

not typically degenerate in RP – from where the trophic factor can be secreted. Ideally, neuroprotection should occur for the life time of the patient following a single minimally invasive intervention, e.g. an intravitreal injection such as carried out routinely for the management of neovascular age related macular degeneration (AMD). The latter part of this thesis deals with two of these questions – firstly, the identification of an appropriate neuroprotective compound which preserves cone photoreceptors when advanced rod loss has already occurred. In chapter 3 (Lipinski et al., 2011a) we explore how secondary cone loss can be reduced using a novel ex vivo model of RP to precisely quantify cone survival longitudinally in responses to dose, allowing accurate comparison as to the likely effectiveness of several compounds to prevent cone loss. Secondly, in chapter 4, we examine if the most promising neuroprotective molecule identified using ex vivo screening (previous chapter) can maintain cone photoreceptors long term when administered to a mouse model of RP exhibiting secondary cone loss using an rAAV2/2 vector to target ganglion cells.

Finally, in the general discussion the work presented herein is place in context within the wider field of ocular gene therapy.

General Materials and Methods

Mice

All animal experiments were performed in compliance with the ARVO statement for the Use of Animals in Ophthalmic and Vision Research under a current UK Home Office project licence. Mice were housed under standard 12:12 light/dark cycle with food and water available *ad libitum*.

C57Bl/6J: Purchased from Harlan Laboratories (Oxford, UK) as required and hereafter described as wild type mice.

B6.Cg-Tg(OPN1LW-EGFP): A transgenic strain which has been described previously (Fei and Hughes, 2001). Briefly, mice express enhanced green fluorescent protein (EGFP) from the human long-wave cone opsin promoter (OPN1LW), resulting in a subset of cone photoreceptors being fluorescent. Mice homozygous for the transgenic insertion are referred to throughout as $B6^{TgOPN1LW\text{-}EGFP+/+}$, and mice heterozygous for the transgenic insertion referred to as $B6^{TgOPN1LW\text{-}EGFP+/-}$, where B6 is reference to the congenic strain. Founders of the colony were a kind gift from Dr Rachel Pearson, UCL Institute of Ophthalmology (UK) (Originally obtained under MTA from Mutant Mouse Regional Resources Centre (MMRRC: 000043-MU Opn1.gfp). F1 heterozygote mice were created by crossing $B6^{TgOPN1LW\text{-}EGFP+/+}$mice with wild type C57Bl/6J mice. Genotype was determined by PCR using sense (5'-CAATTAAGAGATCAGGTAGTGT-3') and antisense (5'-AGTTCACCTTGATGCCGTTCTT-3') primers to amplify a 641bp product specific to the transgenic insertion (Fei and Hughes, 2001). PCR was performed using ImmoMix Red (Bioline Reagents Ltd, London, UK) as follows: 1 cycle of 10 min at 95^{O}C, 30 cycles of 15 sec at 95 ^{O}C, 15 sec at 55 ^{O}C and 30 sec at 72 ^{O}C, 1 cycle of 10 min at 72 ^{O}C. PCR products were analysed by electrophoresis on a 1% TAE gel with band sizes identified using 1kb marker (New England Biolabs, Hichin, UK).

C57B/6.129 Rho^{tm1Phm}: Transgenic knockout described previously (Humphries et al., 1997). Briefly, mice have a targeted knockout of the rhodopsin gene within exon II leading to retinopathy characterized by the absence of rod photoreceptor function from birth, and a degeneration of rod photoreceptors over a 12 week period. C57B/6.129 Rho^{tm1Phm} mice, referred to throughout as $Rho^{-/-}$, were a kind gift obtained under MTA from Jane Farrar, Trinity College Dublin, Ireland. The transgenic insertion was maintained in a

homozygous state ($Rho^{-/-}$) and genotype assessed by duplex PCR, using one sense primer (5'-AGGTTAGAGCTGGAGGACTG-3') specific to the 5' of exon II, and two antisense primers (5'-TAAGACTGATTGGACCATTC-3' and 5'-TTCAAGCCCAAGCTTTCGCG-3') where the former binds to the wild-type exon II allele, and the later to the pol2:neo insertion designed to disrupt exon II. PCR was performed using ImmoMix Red (Bioline Reagents Ltd, London, UK) as follows: 1 cycle of 10 min at 95^{O}C, 30 cycles of 15 sec at 95 ^{O}C, 15 sec at 55 ^{O}C and 30 sec at 72 ^{O}C, 1 cycle of 10 min at 72 ^{O}C. Products were analysed by electrophoresis on a 1% TAE gel with band sizes identified relative to a 1kb marker (New England Biolabs, Hichin, UK). Fragments of 139bp and 394bp were diagnostic of the knockout and wild-type alleles, respectively (Humphries et al., 1997).

Anaesthesia

General anaesthesia was induced by a single intraperitoneal injection of Dormitor (medetomidine hydrochloride, 1mg/kg body weight) and ketamine (60mg/kg body weight), and where appropriate, anaesthesia was reversed by intraperitoneal injection of antisedan (atipamezole, 5mg/kg body weight) and the mice placed in a heated chamber for the duration of the recovery period. For long-term procedures (>15 min) body temperature was monitored throughout using rectal thermometry and regulated with a feedback heat block.

Fundus imaging using a confocal scanning laser ophthalmosope (cSLO)

The ocular fundi of each mouse were imaged using a confocal scanning laser ophthalmoscope (cSLO; Spectralis HRA, Heidelberg Engineering, Heidelberg, Germany) as previously described (Charbel Issa et al., 2011). Briefly, following dilation a contact lens (PMMA mouse lens, Cantor and Nissel, Brackley, UK) was placed on the cornea using a viscous coupling gel (0.3% w/v hypromellose, Viscotears, Novartis, Frimley, UK)to prevent cataract formation and to improve and standardize image quality. The mouse was placed on a raised imaging platform and the near-infrared (NIR) reflectance mode (820nm laser) used to achieve camera alignment at the confocal plane of the neural retina. EGFP expression in the

retina or RPE was evaluated using the autofluorescence (AF) imaging mode (480nm excitation) and high resolution images (1536 x 1536) recorded at a range of standardized sensitivities using automated real-time (ART) averaging.

Chapter 1

Characterization of a dominant cone degeneration in a GFP-reporter mouse with disruption of loci associated with human dominant retinal dystrophy

INTRODUCTION

The degeneration of photoreceptors in RP typically results in severe visual impairment that carries with it a high economic and social cost. In many cases, the molecular mechanisms that cause photoreceptor degeneration are unknown, however, the use of animal models, specifically transgenic reporter lines, have led to major advances to understanding the genetic mechanisms that mediate retinal disease.

Due to its short half-life enhanced green fluorescent protein (EGFP) is observed only in living cells where protein production is maintained at a constant level, making it a commonly used reporter for the study of tissue development and cell survival (Chalfie et al., 1994; Corish and Tyler-Smith, 1999; Megason et al., 2006). Transgenic lines expressing GFP in retinal cell types (e.g. (Akimoto et al., 2006)) have proved invaluable for the study of photoreceptor survival *in vivo*, where the unique properties of the eye allow for repetitive autofluorescence imaging (Beck et al., 2010), as well as for examinations of donor cell engraftment in models of photoreceptor transplantation (MacLaren et al., 2006b). In addition to a rod pigment (encoded by the *Rho* gene), mice possess two cone subpopulations that express *SWS* (S-cone) and *MWS* (M-cone) photopigments, encoded by *Opn1sw* and *Opn1mw* genes, respectively. A mouse model expressing EGFP driven by the human OPN1LW promoter was described previously, where EGFP expression is present in cone photoreceptors expressing *MWS* opsin (Fei and Hughes, 2001). Although *MWS* opsin protein can be detected to some extent in the majority of cone photoreceptors across the mouse retina (Applebury et al., 2000), in the human OPN1LW-EGFP reporter mouse, greater numbers of EGFP-expressing cells are observed in the dorsal retina than the ventral retina (Fei and Hughes, 2001). Over time, a gradual loss of EGFP-expressing cells has been observed in OPN1LW-EGFP mice *in vivo* (Beck et al., 2010). This cone degeneration has been attributed to EGFP-mediated toxicity as observed in other tissues (Huang et al., 2000). However, EGFP expression has not previously been associated with toxicity in the rodent retina (Daniels et al., 2003; Dreyer et al., 1999) raising the question of whether EGFP expression is the direct cause of the observed cone loss.

Accordingly, we set out to investigate the contribution of EGFP toxicity to cone degeneration through anatomical and functional characterization of the OPN1LW-EGFP transgenic mouse. An anatomical quantification of cone survival over nine months was performed. Light- and dark-adapted electroretinography (ERG) was employed to examine cone function in OPN1LW-EGFP animals compared to wild-type controls, including an LED-based approach using short wave-length flicker stimulus to preferentially activate cones in the ventral retina (S-cones).

An alternative cause for the observed cone degeneration was also explored. Fluorescence *in situ* hybridization (FISH) was employed to locate the chromosomal position of the transgenic insertion, and to examine the potential disruption of a cone-specific locus as an underlying cause of the observed degeneration.

CHAPTER SPECIFIC MATERIALS AND METHODS

Morphological studies

In order to perform a morphological characterization of cone survival, eyes from transgenic($B6^{TgOPN1LW-EGFP+/-}$ and $B6^{TgOPN1LW-EGFP+/+}$) and wild type (C57Bl/6j)mice were harvested at P80, P140 and P245 time points(n=3 mice of each genotype per time point). Eyes were enucleated and fixed in 4% paraformaldehyde (PFA) for 30 minutes during which time the anterior segment and lens were removed. The posterior segment was cryoprotected overnight at 4°C in 30% sucrose and embedded in OCT. 16µm Cryosections were taken sagittally through the optic disc and immunostained for either SWS opsin (1:1500 dilution; Santa Cruz, SC-14363) or MWS opsin (1:1000 dilution; Millipore, AB5405). Flat-mounted eyes were fixed as above and the retina detached; immunostaining was performed free floating and the primary antibody incubation period extended to 4 days. Cone number was quantified on flat-mounted retinas (n=3 mice per group) by analysis of multiple non-overlapping fields (x20 objective) covering ventral/dorsal and temporal/nasal opsin gradients. Automated quantification of cone number was

carried out using ImageJ software (Abramoff et al., 2004). Automated counts were validated and found to be highly consistent with manual counts.

Electroretinography (ERG)

ERG recording was carried out using an Espion E2 system (Diagnosys LLC, Cambridge, UK). Prior to testing mice were dark adapted for 4 hours. All animal preparation and set-up were conducted under dim red illumination. Mice were anesthetized and their pupils dilated (see general materials and methods) prior to being placed on a heated platform, maintained at 37^{o}C by a circulating pump-water bath. A custom-made silver-coated nylon contact lens active electrode was manually positioned on the study eye using hypromellose eye drops (0.5% methylcellulose) to maintain electrical conductivity and prevent corneal desiccation. Subdermal platinum needle electrodes were placed in the scruff (reference) and at the base of the tail (ground). Prepared animals were positioned inside the Ganzfeld dome of the Espion E2 system. Stimulus timing, duration and intensity were all controlled by the Espion software (except for the UV-LED intensity, which was controlled manually by a potentiometer). Stimuli were rendered full field through reflection in the Ganzfeld dome or, in the case of the UV-LED array, by proximity of an extended source close to the test eye. All recordings were made in a custom-made, light-tight Faraday cage. ERG signals were differentially amplified and digitized at a rate of 5 KHz (bandpass filtered 0-100Hz) using the Espion E2 system. Recording sessions began with the dark-adapted flash ERG intensity series, progressed to dark-adapted flicker ERG recording, and concluded with light-adapted flash ERG testing (after at least 10 min exposure to the rod-saturating background). Animals with late stage degeneration (P245) were used to establish the correlation between anatomical cone loss and retinal function. For dark-adapted responses, brief (4 ms) white flash stimuli were delivered over a six-log intensity series (-4 to 1 log cd.s/m^2). For dim stimuli (-4 to -3 log cd.s/m^2) 10 responses were averaged with an interstimulus internal (ISI) of 5 s, for all other stimuli (-2 to 1 log cd.s/m^2) 5 responses were averaged with an ISI of 10 s or 20 s. Dark-adapted flicker ERGs were carried out using 513nm and 365nm stimuli. Continuous 15Hz

and 30Hz stimuli were delivered and 20 response epochs (500 ms) averaged for each condition. The 513nm (green) flicker stimulus intensity was 3 cd.s/m^2. Photometric units are inappropriate for quantification of the 365nm (UV) flicker stimulus (as luminosity functions used do not extend below 400nm). However, during preliminary testing the forward voltage of the LED-array was altered so the UV flicker output evoked response amplitude similar to the green flicker stimulus. For light-adapted responses, white flash stimuli of 3, 10 and 25cd.s/m^2were superimposed on a 30 cd/m^2 white background with 20 responses averaged using an ISI of 1 s. a- and b- wave amplitudes (flash stimuli) and trough-to-peak amplitudes (flicker stimuli) were quantified with the Espion software (Diagnosys LLC, Cambridge, UK).

Fluorescent *In Situ* Hybridization (FISH)

Chromosome slides for metaphase FISH analysis and high resolution mapping on DNA fibres were obtained from short term fibroblast cell cultures established from ear explants as previously described (Jefferson and Volpi, 2010). Briefly, Cells were cultured in Dulbecco's Modified Eagles Medium (DMEM) supplemented with 10% foetal bovine serum (FBS) and 1% L-Glutamine at 37°C in a 5 % CO_2 incubator. Three hours before harvesting they were treated with Colcemid (Gibco BRL) at a final concentration of 0.2 µg/ml. They were then resuspended in hypotonic solution (0.034 M KCl/ 0.017 M TriSodium Citrate) at 37°for 5 minutes and fixed in three changes of 3:1 methanol: acetic acid. For FibreFISH analysis the cells were grown until confluent, then centrifuged at 195*g* for 5 minutes and resuspended to a density of 2 x 10^6 cells/ ml in 1 X PBS. 10µl of this solution was dried on a microscope slide. The slides were assembled in a cover-plate holder (Shandon), and the cells were lysed using a Sodium Hydroxide solution (5 volumes 0.07M NaOH with 2 volumes ethanol) and then fixed with methanol. To identify the chromosome(s) holding the transgenic insertion , a ~39Kb clone (G248P88405H3) for the OPN1LW gene and its upstream region from a human fosmid library was labelled by nick-translation (Abbott Molecular) with Biotin-16-dUTP (Roche) and detected with Texas

Red-conjugated Streptavidin (Molecular Probes), and initially co-hybridised with a panel of FITC-labelled mouse chromosome-specific probes (Cambio or Metasystems). Once the chromosome holding the transgenic insertion was identified, the OPN1LW probe was co-hybridised with a number of clones from mouse fosmid and BAC libraries mapping on the sub-chromosomal region of interest. Clones were selected for their potential interest on the basis of both their cytogenetic band location and gene content. They were labelled by nick-translation (Abbott Molecular) with Digoxigenin-11-dUTP (Roche) and detected using a Rhodamin anti-Digoxigenin antibody (Roche), while in this instance the biotin-labelled transgene was detected with FITC-conjugated Streptavidin (Molecular Probes). The hybridization procedure followed a standard protocol. Briefly, the genomic probes were ethanol precipitated in a mix of Salmon testis DNA (Gibco BRL), Escherichia coli tRNA (Boehringer) and 3M sodium acetate. They were then dried on a heating block at 60^{o}C with a 50X excess of either Human or Mouse Cot-1 DNA (Gibco BRL) and resuspended at 20 ng/µl in hybridisation solution (50% formamide, 10% dextran sulphate, 2x SSC). The probes were denatured at 72^{o}C for 5 minutes and pre-annealed at 37^{o}C for 30 minutes, before being applied to the denatured slides. The slides were denatured in 70% formamide at 70^{o}C for 2 minutes, quenched in 2xSSC at 4^{o}C and then dehydrated in an ethanol series. Following hybridisation, the slides were washed in 50% formamide at 42^{o}C for 10 minutes and 2 X SSC at 42^{o}C for 5 minutes. The FITC directly labelled mouse chromosome-specific probes (or “paints”) were obtained commercially and hybridized following the manufacturer’s instructions. The slides were mounted with Vectashield (Vector Laboratories) containing 4', 6-diamidino-2-phenylindole (DAPI) for chromosome counterstaining. Image capture and analysis were carried out on a CytoVysion system (Genetix) consisting of an Olympus BX-51 epifluorescence microscope coupled to a JAI CVM4+ CCD camera.

Statistics

Anderson-Darling test for normality on full data sets for anatomical quantification of cone photoreceptors revealed that the data was not normally distributed (A^2 = 1.04; p=0.0094). Due to low sample size (n=3)

plotting of residuals versus fitted means to determine variance could not be accomplished. Non-parametric tests, specifically one-tailed Mann-Whitney U tests, were employed to assess differences in population mean throughout, with significance (p) set at 0.05.

RESULTS

The extent of cone loss is identical in dorsal and ventral cone populations

Initially we confirmed previous reports that GFP expression is observed in a greater number of cones in the dorsal retina compared to the ventral. Immunostaining on flat mounted retinas of young (<2 month) $B6^{TgOPN1LW\text{-}EGFP+/+}$ mice for the presence of *MWS* and *SWS* opsin allowed the quantification of total cone numbers across the retina regardless of cone class. The number of GFP expressing cones was found to be significantly higher in the dorsal retina (50±5%) than in the ventral retina (9±3%) (P=0.05, one-tailed Mann-Whitney U, n=3 eyes/group) (Fig. 1.1 A-C).

The number of cone photoreceptors in the dorsal and ventral retina of wild type (WT) and$B6^{TgOPN1LW\text{-}EGFP+/+}$ mice was compared at three ages (P80, P140 and P245) by immunostaining for cone both SWS and MWS cone opsins. WT mice showed no significant (ns) reduction in the number of cone photoreceptors in either the dorsal or ventral retina over the time period, indicating an absence of cone loss in WT mice up to 9 months of age (p=0.35, one-tailed Mann Whitney U, n=3 eyes/group) (Fig. 1.1D-E). In contrast, a significant reduction in total cone number was observed in the ventral(p=0.05) and dorsal(p=0.05) retina of $B6^{TgOPN1LW\text{-}EGFP+/+}$ mice over the same time period (both one-tailed Mann-Whitney U, n=3 eyes/group) (Fig. 1.1 D-E). There was no significant difference between the number of cone photoreceptors remaining in the dorsal and ventral retinas of $B6^{TgOPN1LW\text{-}EGFP+/+}$ mice at P245 (p=0.50, one-tailed Mann-Whitney U, n=3 eyes/group). Additionally, the ratio of EGFP to non-EGFP expressing cone photoreceptors remained consistent throughout the time course in both the dorsal and ventral retina (Fig. 1.1 D-E), indicating that cone degeneration occurs independently of EGFP expression.

The uniformity of loss across the retina strongly contraindicates the role of EGFP-toxicity in cone degeneration, where significantly fewer cones express EGFP in the ventral than dorsal retina. Rod

photoreceptors were not quantified in this study. However, the gross retinal morphology of $B6^{TgOPN1LW-EGFP+/+}$ mice revealed no appreciable thinning of the outer nuclear layer compared to WT controls (data not shown), indicating that the observed cone degeneration is not secondary to the loss of rod photoreceptors.

Dark- and light-adapted flash electroretinography reveals significant deficits in cone function in OPN1LW-EGFP mice

We sought to correlate the observed anatomical loss of cone photoreceptors in OPN1LW-EGFP transgenic mice with functional response. WT, $B6^{TgOPN1LW-EGFP+/-,}$ and $B6^{TgOPN1LW-EGFP+/+}$ mice, were examined at P245, the time point at which the anatomical degeneration was most pronounced and functional deficits had previously been reported (Beck et al., 2010).

The dark-adapted flash series revealed no significant difference in a-wave amplitude across all intensities (-4 to 1 log cd.s/m^2) between WT and transgenic animals ($p>0.05$, all tests one-tailed Mann-Whitney U; WT n=3 eyes; EGFP+/- n=6 eyes, EGFP+/+ n=3 eyes) (Fig. 1.3 A-B). As the murine retina is rod-dominated (97% rods vs 3% cones)the a-wave is primarily a rod-driven response (Brown, 1968). Therefore, the absence of any differences in the a-wave amplitudes between WT and OPN1-EGFP transgenic mice strongly supports the morphological evidence that there is no detectable degeneration of rod photoreceptors. Dark-adapted b-waves showed a small but statistically significant reduction in amplitude in both $B6^{TgOPN1LW-EGFP+/-}$ and$B6^{TgOPN1LW-EGFP+/+}$ mice compared to WT mice at 0 log Cd.S/m^2 ($p=0.05$) and 1 log Cd.S/m2 ($p=0.05$, both one-tailed Mann-Whitney U; WT n=3 eyes; EGFP+/- n=6 eyes, EGFP+/+ n=3 eyes) (Fig. 1.3 A, C). This might be expected due to an increasing contribution from cone pathways at higher light intensities (Biel et al., 1999). No significant difference in b-wave amplitude was observed between $B6^{TgOPN1LW-EGFP+/-}$ and $B6^{TgOPN1LW-EGFP+/+}$ mice at any light intensity ($p>0.05$, all tests one-tailed Mann-Whitney U; WT n=3 eyes; EGFP+/- n=6 eyes, EGFP+/+ n=3 eyes) (Fig 1.3 A, C).

The light-adapted b-wave, which primarily reflects cone pathway activation, showed a large reduction in amplitude in $B6^{TgOPN1LW-EGFP+/-}$($p=0.0119$)and $B6^{TgOPN1LW-EGFP+/+}$($p=0.05$) mice compared to

WT mice at all intensities (all tests one-tailed Mann-Whitney U; WT n=3 eyes; EGFP+/- n=6 eyes, EGFP+/+ n=3 eyes). Amplitudes in heterozygous and homozygous mice were reduced to a similar extent indicating that the degeneration follows a dominant inheritance pattern (Fig. 1.3 D-E).

UV flicker electroretinography reveals a functional loss of *SWS* opsin expressing photoreceptors

Cone opsins are spectrally tuned to maximally absorb different wavelengths of light, with *MWS* and *SWS* photopigments exhibiting a spectral peak of absorbance (λ_{max}) of approximately 508nm (Sun et al., 1997) and 359nm (Yokoyama et al., 1998), respectively (Fig. 1.2). Stimulating at the λ_{max} of the *MWS* photopigment is likely to evoke some degree of response from cones throughout the retina, where *MWS* opsin is expressed to a certain extent in cones in both dorsally and ventrally. By contrast, expression of *SWS* opsin is predominantly restricted to cones in the ventral retina, and stimulation at the λ_{max} of the *SWS* photopigment is likely to elicit a response from cones of the ventral retina only (Jacobs et al., 1991; Lyubarsky et al., 1999).

It has previously been shown that a relatively small population of SWS-opsin expressing cone photoreceptors can elicit reliable cone-based ERGs in response to a UV flicker stimulus (Williams et al., 2005). Consequently, we aimed to utilize UV flicker photometry to determine the survival of SWS-opsin expressing cones in the ventral retina, where a significant reduction in ERG response in a non-EGFP expressing cone population would provide strong evidence that cone photoreceptor loss was not linked to toxicity of the fluorescent reporter. Although the spectral peaks of the SWS and MWS opsins are separated by ~149nm, attempts to isolate responses from the two photopigments have proven difficult. The use of a double-flash technique, where a high intensity 530nm orange conditioning flash was given to saturate rod and green cone function followed by a UV test flash (330nm) resulted in the suppression of both the MWS and SWS opsin driven responses (Lyubarsky et al., 1999). However, the use of dim monochromatic flash stimuli at 340nm (UV) or 500nm (green) have been shown to isolate responses from individual cone populations, with each noted to have unique oscillatory potentials (Lyubarsky et al.,

1999). The use of a saturating background (25 Cd/m^2) to reduce rod photoreceptor contribution in conjunction with monochromatic flash stimuli affects the amplitude of the cone driven response observed, with a yellow background (>490nm bandpass), significantly reducing the sensitivity of cone response to a 520nm flash stimulus compared to a polychromatic white background (Ekesten et al., 2001).

The use of flicker stimuli with a frequency above the temporal resolution of rod photoreceptors (see discussion) can be used in conjunction or in isolation of a rod-saturating background to separate cone driven responses. Consequently, we resolved to use dark-adapted flicker photometry with dim light stimuli close to the respective λ_{max} of each opsin to isolate the responses from each cone population.

A custom array of TTL controlled UV LEDs with a narrow emission peak of 365±3nm was constructed to stimulate SWS-opsin expressing cones. MWS-opsin expressing cones were stimulated using the 513nm LED stimulus present in the Espion E2 system. The spectral absorption curves of mouse opsins (Fig 1.2) show that each responds with varying sensitivity to a broad range of wavelengths, and that MWS opsin has a slight peak of absorbance in the range of 350nm (Jacobs and Williams, 2007). However, sensitivity is significantly lower in response to wavelengths outside the respective opsins λ_{max}, with SWS opsin being ~100,000-fold less sensitive at 500nm than at its λ_{max} (Naarendorp et al., 2010). Consequently, herein we used relatively dim stimuli (3 $Cd.S/m^2$) to reduce the activation of the opsins at wavelengths other than at their spectral peak.

Flicker stimuli (15Hz and 30Hz) were utilized to minimize contributions from rod pathways. Responses were quantified by measurement of trough-to-peak amplitude, as a- and b-waves of 'traditional' appearance are not observed in response to flicker stimuli.

Photometric units (e.g. candela) are inappropriate for quantifying the intensity of a stimulus with a wavelength below 400nm, where such units are standardized to the luminosity function (e.g. the average range of human spectral perception). The intensity of the 365nm flicker stimulus delivered by our LED array was set by adjustment of the forward voltage until it elicited a similar amplitude trough-to-peak flicker ERG response as the 3 $cd.s/m^2$ 513nm stimulus in WT mice.

The modification of the forward voltage to alter the output of the 365nm UV light source so that the amplitudes of the ERG flicker response was equal to that elicited from the 513nm green light source, rather than matching the light output quantitatively using radiometric measurments (e.g. $W.Sr/m^2$), was carried out to take into account the relative spectral sensitivities of the MWS and SWS opsins. A series of elegant experiments conducted by Naarendorp et al (2010) in functionally rodless Gnat1-/- mice demonstrated that dark-adapted cones are more sensitive to a 365nm monochromatic light stimulus than a 500nm stimulus of equal intensity, indicating that the cone response at threshold is driven by SWS opsin ventral cones (Naarendorp et al., 2010). In wild type mice where rods were present the dark adapted threshold sensitivity was approximately three-fold higher at 500nm than at 365nm, as expected where rhodopsin governs the threshold response. From these experiments we can draw that SWS opsin is more sensitive than MWS opsin in dark-adapted conditions, having a lower sensitivity threshold, and that rhodopsin driven responses are more sensitive than those of both cone opsins. In a cone isolating situation, such as when using flicker photometry, one would expect cone sensitivities to more closely reflect that of the Gnat1-/- mouse than the wild type as rod function is saturated. It follows that one therefore requires a comparatively less intense UV stimulus to elicit ERG amplitudes of similar magnitude compared to those elicited from a 513nm stimulus. Given the small peak in sensitivity of MWS opsin at ~350nm (Fig. 1.2) it was elected to normalize the amplitude of the ERG responses, by use of a relatively less intense UV stimulus, in order to minimize cross activation of the MWS opsin, rather than to match the radiance of the two light sources, which would likely have resulted in larger ERG responses from the UV stimulus, but potentially cross activation of the MWS opsin.

The trough-to-peak amplitude in response to the 15Hz and 30Hz 513nm stimuli was significantly reduced in $B6^{TgOPN1LW\text{-}EGFP+/-}$ and $B6^{TgOPN1LW\text{-}EGFP+/+}$ mice compared to wild type mice at P245 (Fig. 1.3 F, H), indicating a loss of cones across the whole retina ($p=0.0011$ all comparisons, all one-tailed Mann-Whitney U tests, n=6 eyes/group in all tests). Trough-to-peak amplitude in response to the 15Hz and 30Hz 365nm stimulus was similarly reduced in both heterozygote and homozygote transgenic mice

compared to WT (p=0.0011 all comparisons, all one-tailed Mann-Whitney U tests, n=6 eyes/group in all tests) (Fig 1.3 F-G). Whilst the reduction in the flicker ERG amplitude in response to a 513nm stimulus likely reflects a global loss of cone photoreceptors, where the majority of cones express MWS opsin and are, therefore, likely to respond, the reduction in ERG response to a 365nm stimulus strongly indicates that there is a significant loss of cones in the ventral retina, where few cones express EGFP. Collectively, the flicker ERG results confirm the anatomical observations that cones of the ventral retina degenerate to a similar extent to those of the dorsal retina in OPN1LW-EGFP mice. This strongly contraindicates the role of EGFP-mediated toxicity as a causal mechanism of retinal degeneration in this mice model. Furthermore, the observation of a similar reduction in cone function in heterozygous and homozygous mice confirms that cone loss in transgenic mice is dominantly inherited.

Fluorescence *In Situ* Hybridization (FISH) localizes the transgenic insertion to chromosome 10

The creation of transgenic animal strains necessitates the integration of an expression cassette, or transgene, within the host genome. The site of integration is often random and therefore the potential exists for insertional mutagenesis, where normal host genetic function is subverted by the introduction of the transgene into the genome. The possibility of insertional mutagenesis resulting in the disruption of a cone specific locus was examined.

The primary strategy applied for localization of the OPN1LW-EGFP expression cassette was chromosomal mapping by FISH analysis. Initially, we obtained a probe for the human OPN1LW promoter sequence which drives expression of EGFP in this transgenic strain. The OPN1LW sequence has no direct homolog in the mouse genome. The probe was validated on metaphase chromosome spreads from a human female and found to map to chromosome X, as expected (Fig. 1.4A). The probe hybridized specifically to metaphase chromosome spreads from several OPN1LW-EGFP transgenic mice (Fig. 1.4 B). Co-hybridization of OPN1LW probe with various differently labelled chromosome-specific probes or

'chromosome paints' was used to unequivocally map the transgenic insertion to a specific sub-chromosomal region of mouse chromosome 10 (Fig. 1.4 C).

Having determined the insertion site was on chromosome 10, probes were obtained for several genes in that sub-chromosomal region, including *Nr2e1*, *Grik2*, *Ascc3*, *Mdm-1* (Fig. 1.4 D-G), *CDH23*, *BVES*, and *Gja1* (data not shown)and co-hybridized with the transgene specific probe on metaphase spreads. Co-hybridization allows the position of the transgene insertion to be determined relative to known landmarks. The transgene is clearly proximal to the *Mdm-1* gene (Fig. 1.4 G) and distal to *Nr2e1* (Fig. 1.4 D). Overlapping signals in metaphase were observed with both *Grik2* and *Ascc3* probes (Fig. 1.4 E-F).Higher resolution mapping was carried by Fibre-FISH, which is a technique whereby individual genomic sequences can be visualized on DNA fibres. DNA strands are obtained by deproteination of nuclear chromatin in a high salt environment, or through use of detergents, resulting in the dissociation of the bound histones and unwinding of the genomic DNA. Localization of the transgene to the region containing *Ascc3* and *Sim-1* was carried out through co-hybridization with pairs of genomic probes (Fig. 1.4 H-I).This region is located close to the macular dystrophy retinal 1 (MCDR1) locus, associated with North Carolina macular dystrophy in humans, and within the PBCRA locus, associated with progressive bifocal chorioretinal atrophy (Gehrig et al., 1998; Small, 1998) (Fig. 1.4J).

DISCUSSION

The aim of this chapter was to characterize anatomically and functionally the cone degeneration previously observed in the B6.Cg-Tg(OPN1LW-EGFP) mouse model (Beck et al., 2010). A UV-LED array was used to deliver a flicker stimulus, allowing isolation of the response from S-cones in the ventral retina, where significantly fewer cones express EGFP in comparison to the dorsal retina. Here, we show that cone degeneration affects cones of the dorsal and ventral retina alike. The degeneration follows a dominant pattern of inheritance and is independent of EGFP expression. With the likelihood that an underlying genetic cause for this degeneration is common to both cone subpopulations, multiple probe

Fibre-FISH was employed to map the insertion site of the OPN1LW-EGFP transgene. The transgene was mapped to chromosome 10 and the insertion site located to an intergenic region situated between *Ascc3* and *Sim1*.

Cone degeneration in the OPN1LW-EGFP transgenic mouse strain has previously been attributed to EGFP toxicity (Beck et al., 2010). While expression of various fluorescent proteins results in light-induced cytotoxicity (Strack et al., 2008), there are few reports of EGFP induced cytotoxicity either *in vitro* (Liu et al., 1999) or *in vivo* (Huang et al., 2000). Indeed, EGFP has previously been described as being nontoxic in the rodent retina (Daniels et al., 2003; Dreyer et al., 1999; Nour et al., 2004), where its lack of cytotoxicity compared to other fluorescent proteins is most likely due to a limited production of damaging reactive oxygen species (ROS) upon photoactivation (Bulina et al., 2006; Tour et al., 2003; Wiedenmann et al., 2009).

Herein, cone survival was quantified by direct immunolabelling of the cone opsins on post-mortem tissue. Given that significantly fewer cones in the ventral retina express EGFP than in the dorsal retina, one would expect to observe a greater reduction in cone number in the dorsal retina if cone loss was caused by EGFP toxicity. We found that the rate and extent of cone loss was similar in the dorsal and ventral retina, and that the ratio of GFP to non-GFP expressing cones remained consistent over the time course, strongly indicating that cone loss is independent of the presence of EGFP. Gross retinal morphology showed that the observed degeneration was not secondary to a primary cause of rod degeneration, as is been observed in animal models (Punzo et al., 2009) and human patients with RP (Hartong et al., 2006). Additionally, the absence of significant cone loss in WT mice of the same background (C57Bl/6) excludes the possibility that slow cone degeneration might be a feature of the background mouse strain.

The anatomical loss of photoreceptors corresponded to a functional deficit. Electroretinography with a 365nm flicker stimulus delivered using high-powered LEDs, indicated the presence of a functional loss of *SWS* opsin expressing cones. This deficit was equally as profound as the impairment in responses

to a green (513nm peak) flicker stimulus, likely to activate a far larger population of cones based on the more widespread expression of *MWS* opsin.

Cone isolation is generally achieved by one of two methods. One can use a double-flash technique, whereby an initial conditioning flash of sufficient intensity to saturate rod photoreceptors is administered followed rapidly by a test flash (Lyubarsky et al., 2000; Lyubarsky et al., 1999; Lyubarsky et al., 2002). Alternatively, one can use a rod-desensitizing background over which the test stimuli are superimposed, with a background intensity of 1.3 Log Cd/m2 considered to be cone isolating (Peachey and Ball, 2003; Peachey et al., 1993). Flicker stimuli can also be used to isolate cone populations, often in conjunction with a rod de-sensitizing background. Clinical electroretinography predominantly focuses on the use of a 30Hz flicker stimulus, where this frequency is above the temporal resolution of the human rod pathway, and is thus cone isolating (Fishman and American Academy of Ophthalmology., 2001; Odom et al., 1992; Peachey and Ball, 2003). Rod photoreceptors were initially proposed to responds to a maximum flicker rate of approximately 20Hz under dark adapted conditions (Dodt, 1951), however more recent ERG recordings under certain conditions have shown rod based responses up to 28Hz (Stockman et al., 1995). However, under conditions of light adaptation, 20-25Hz has been described in humans as sufficient to effectively isolate a cone-only response (Jacobs et al., 1996).

The recovery time of rod photoreceptors in mice has been shown to be similar to that of humans, at approximately 200ms, and consequently a 30Hz flicker stimulus could be considered as cone isolating, even in the absence of a saturating background. However, here we observed that the amplitude of flicker responses to a 30Hz stimulus were small, in line with previous studies (Peachey and Ball, 2003). As the amplitude of flicker responses is also related to the speed of stimulation, with amplitude increasing with decreasing stimulation rate, a 15Hz flicker stimulus was also included. The greater amplitude observed using the 15Hz stimulus was critical to measuring the responses of MWS and SWS cones in B6TgOPN1LW-EGFP mice, where based on data from the light adapted flash series, we expected cone function in response to our 513nm and 365nm monochromatic stimuli to be significantly reduced.

The equivalence of the deficits strongly suggests that all cones are affected and supports the conclusion that the degeneration is independent of EGFP expression. The data supports that cone degeneration follows a dominant inheritance pattern. Similar to another recently described mouse model of dominant cone dystrophy (COD3) (Buch et al., 2011), a slightly more severe cone dysfunction is observed in $B6^{TgOPN1LW\text{-}EGFP+/+}$ mice than heterozygote mice. That the presence of a wild-type allele confers little phenotypic compensation suggests that the degeneration is likely dominant negative (antimorphic).

Through the use of Fibre-FISH, a 40 kb intergenic region situated between *Ascc3* and *Sim1* was identified as the likely location of the transgenic insertion. The insertion site falls within the locus associated with PBCRA and close to the currently defined MCDR1 locus. NCMD is a congenital maculopathy resulting in the degeneration of cone photoreceptors (Small, 1998), while PBCRA is characterised by progressive atrophy of the nasal retina and diffuse abnormalities of both rod and cone function (Godley et al., 1996). Both NCMD and PBCRA are dominantly inherited and affect cone function; however, whilst the OPN1LW-EGFP mouse has a retinal phenotype, one must be cautious when correlating phenotypic observations in mice, which have no macula, to human macular dystrophies.

In the OPN1-EGFP transgenic mouse line, disruption of the *Ascc3* gene is most likely, due to the close proximity of the transgene, although neither the function nor the expression profile of this gene are well understood. Disruption of *Sim1* is highly unlikely, where homozygous knockout of this gene results in perinatal lethality (Michaud et al., 2001). Alternatively, the OPN1LW-EGFP transgene insertion may not directly be the cause of the observed cone degeneration, but may segregate with the locus responsible, in this instance, PBCRA or MCDR1.

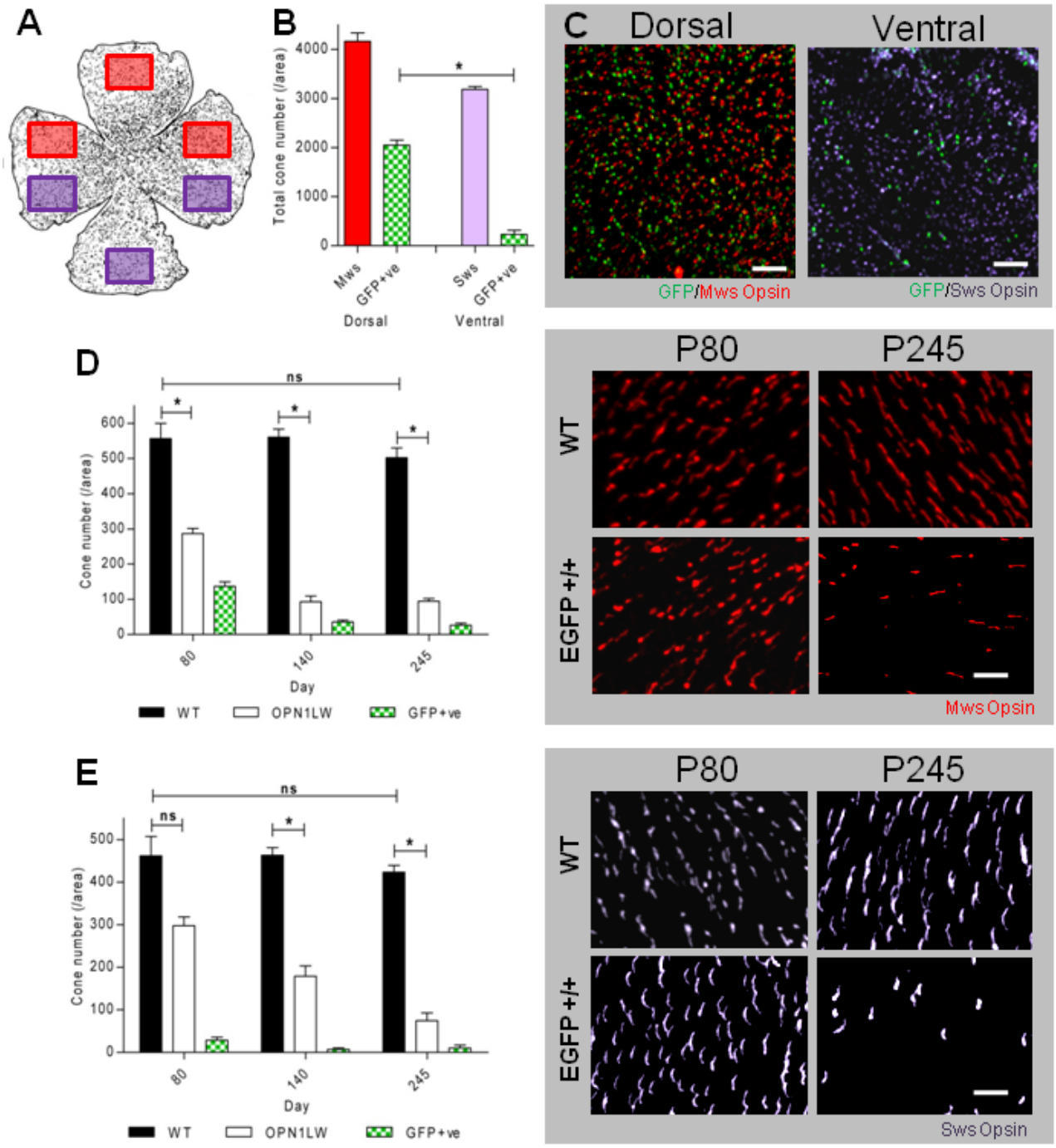

Figure 1.1 – Anatomical characterization of cone numbers in the B6TgOPN1LW-EGFP+/+ mouse
Immunohistochemistry double labelling for *MWS* and *SWS* opsin was performed on flatmounted retinas from B6TgOPN1LW-EGFP+/+ (n=3) and wild-type (C57Bl/6j) mice (n=3) and cone numbers quantified by microscopy on non-overlapping fields in the superior and inferior retina (6 fields per retina) **(A)**. Significantly higher numbers of EGFP expressing cells were observed in the dorsal retina compared to the ventral **(B)**(n=3, * p=0.05, one-tailed Mann-Whitney U test; error bars = s.d.). **(C)** Example fields from the dorsal and ventral retina of a B6TgOPN1LW-EGFP+/+ mouse showing fewer EGFP positive cells in the ventral retina. A significant reduction in cone numbers was observed in both the dorsal**(D)** and ventral**(E)** retina of B6TgOPN1LW-EGFP mice (n=3) compared to wild-type C57Bl/6j mice (n=3) at all time points examined (postnatal day 80, 140 and 245) (n=3, * p=0.05, one-tailed Mann-Whitney U test; error bars = s.d.). A slight but not significant decline in photoreceptor numbers was observed in wild-type (C57Bl/6j) mice (n=3) over the time course in the dorsal (n=3, p=0.35, one-tailed Mann-Whitney U test; error bars = s.d.) and ventral (n=3, p=0.35, one-tailed Mann-Whitney U test; error bars = s.d.) retina. Scale bars = 50µm **(C)** and 100µm **(D-E)**.

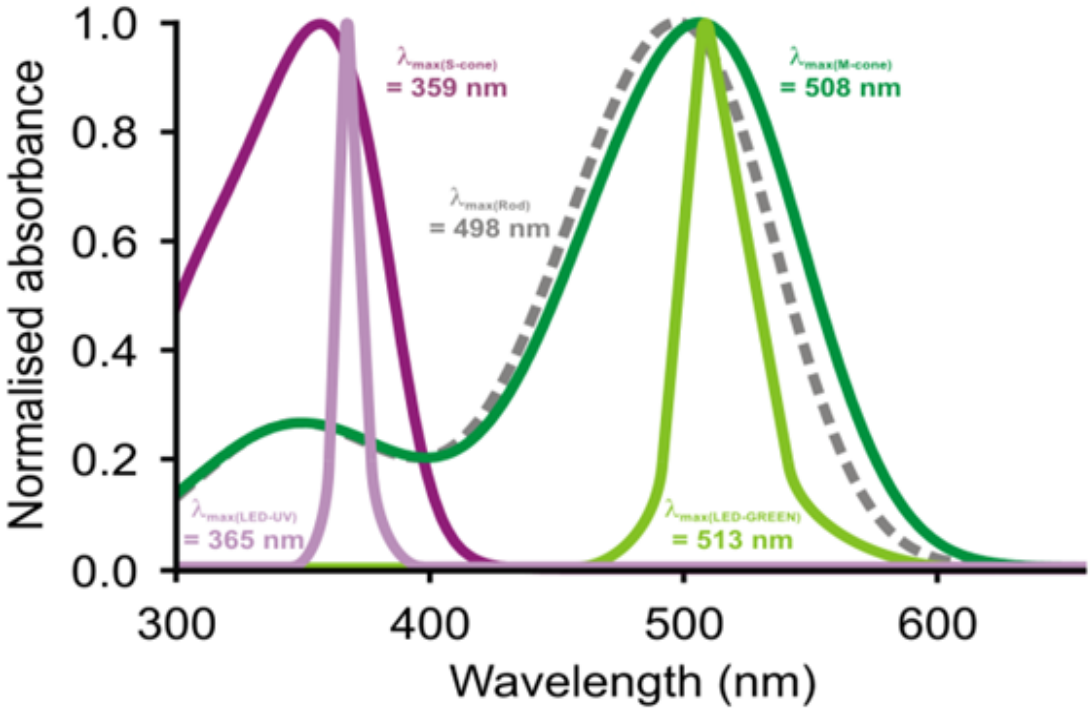

Figure 1.2 – Spectral sensitivities of mouse opsins and emission wavelengths of the LED stimuli used for cone isolation
Murine opsins are spectrally tuned to absorb at specific wavelengths of light. The short wavelength (*SWS*) opsin (light purple) has a maximum peak of absorbance (λ_{max}) at 359nm. The medium wavelength (*MWS*) opsin (dark green) has a maximum peak of absorbance (λ_{max})at 508nm. Murine rhodopsin (grey dotted) has a peak absorbance λ_{max} of 498nm. There is minimal overlap in the spectral sensitivities of *SWS* and *MWS* opsins, and so a light source with peak emission close to the λ_{max} of an opsin can be used to isolate an electrophysiological response from cells expressing that opsin.LED light sources, which typically have a narrow emission peak, were used to isolate cells expressing each opsin. A stimulus with λ_{max} of 365nm (dark purple) was used to isolate *SWS* opsin expressing cells, and a stimulus with λ_{max} of 513nm (light green) used to isolate *MWS* opsin expressing cells.

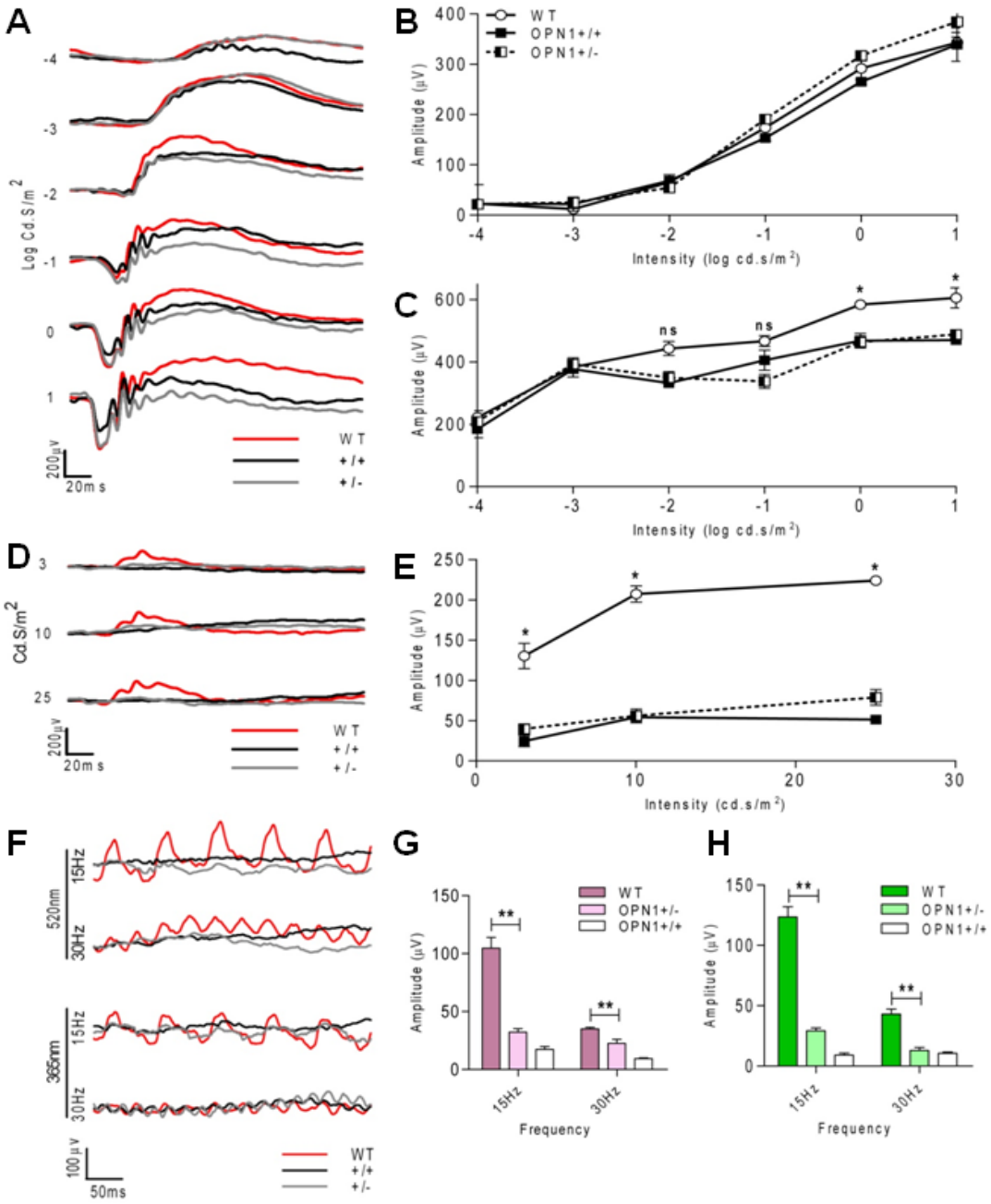

Figure 1.3 –Electroretinography reveals specific deficits in cone function in the B6TgOPN1LW-EGFP mouse
Scotopic (dark adapted) and photopic (light adapted) electroretinography (ERG) was used to assess the function of rod and cone photoreceptors in B6TgOPN1LW-EGFP+/- and B6TgOPN1LW-EGFP +/+ mice compared to wild-type C57Bl/6j mice. A scotopic flash series using low light intensity polychromatic white light (-4 log Cd.S/m^2 to 1 log Cd.S/m^2) over a dark background was used to isolate the contribution of rod photoreceptors**(A)**. The amplitude of the scotopic a-wave was not significantly reduced in B6TgOPN1LW-EGFP+/- (n=6) and B6TgOPN1LW-EGFP +/+ (n=3) mice compared to wild-type C57Bl/6j (n=3) mice (all intensities p=>0.05; one-tailed Mann-Whitney U)**(B)**. The amplitude of the scotopic b-wave was significantly reduced at the highest light intensities in B6TgOPN1LW-EGFP+/- (n=6) and B6TgOPN1LW-EGFP +/+ (n=3) mice compared to wild-type C57Bl/6j (n=3) mice (0 log Cd.S/m^2, p=0.119 (+/-) and 0.05 (+/+); 1 log Cd.S/m2, p=0.119 (+/-) and 0.05 (+/+), one-tailed Mann-Whitney U)**(C)**. A light adapted flash series using high intensity polychromatic white light (3 – 25 Cd.S/m^2) over a bright white background (30 Cd/m^2) was used to isolate cone driven responses **(D)**. The amplitude of the photopic b-wave was significantly reduced in B6TgOPN1LW-EGFP+/- (n=6) and B6TgOPN1LW-EGFP +/+ (n=3) mice compared to wild-type C57Bl/6j (n=3) mice (all intensities p=>0.05; one-tailed Mann-Whitney U) **(E)**. Responses of *SWS* or *MWS* opsin expressing cones were isolated using photopic flicker stimuli with monochromatic 365nm or 513nm light, respectively. Significant reductions were observed in the responses of both cone populations at 15Hz and 30Hz flicker reduced in B6TgOPN1LW-EGFP+/- (n=6) and B6TgOPN1LW-EGFP +/+ (n=6) mice compared to wild-type C57Bl/6j (n=6) mice (** p=0.0011 all comparisons, one-tailed Mann-Whitney U). All error bars = s.d.

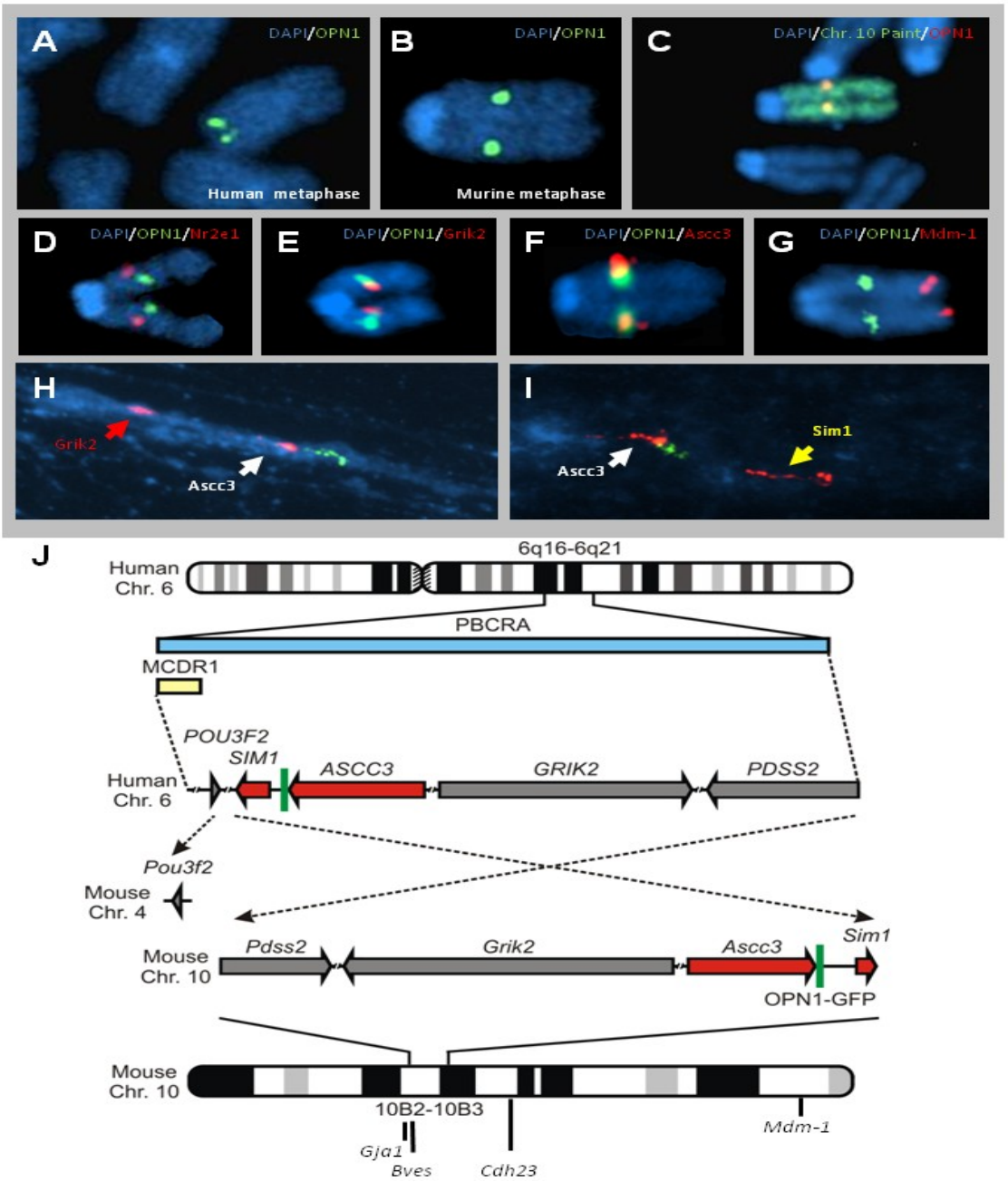

Figure 1.4 – FISH shows the transgenic insertion to be in a region homologously associated with retinal disease in humans The OPN1 probe bind specifically to human **(A)** and transgenic **(B)** metaphase chromosomes and is localized to chromosome 10 in the OPN1LW-EGFP mouse **(C)**. Various genes (red and yellow), such as nuclear receptor subfamily 2 group E member 1 (*Nr2e1*) **(D)**, glutamate receptor ionotropic, kainate 2 (*Grik2*) **(E, H)**, activating signal cointegrator 1 complex subunit 3 (*Ascc3*) **(F, H, I)**, transformed mouse 3T3 cell double minute 1 (*Mdm1*) (G), and single-minded homolog 1 (*Sim1*) (I), were used as chromosomal landmarks to map the location of the OPN1-EGFP transgene (green) **(B-I)** through co-hybridization. Fibre-FISH with multiple probes (labelled) refines the likely insertion point to a 40 kb region intergenic of *Ascc3* (white) and *Sim1* (yellow) **(H-I)**. Analysis of the syntenic relationship between the chromosomal insertion point of the OPN1-EGFP transgene (green) on murine chromosome 10 and human chromosome 6 shows that the transgene has been inserted into a highly conserved region containing both *Sim1* and *Ascc3* genes (red) **(J)**. Closer inspection demonstrates that this region in the mouse is orthologous to the progressive bifocal chorioretinal atrophy PBCRA (blue), flanked by prenyl (decaprenyl) diphosphate synthase subunit 2 (*PDSS2*) and POU class 3 homeobox 2 (*POU3F2*) genes, and the macular dystrophy retinal 1 (MCDR1; North Carolina macular dystrophy, NCMD) (yellow) loci in humans. Chromosomal location of probes which are not illustrated (gap junction protein alpha 1, Gja1; blood vessel epicardial substance, BVES; Cadhedrin 23, CDH23; mouse double minute 1, mdm-1) are shown **(J)**. FISH experiments were kindly performed as part of collaboration with the Wellcome Trust Centre for Human genetics, University of Oxford, UK by Drs Emanuella Volpi and Mohamed Yusuf.

Chapter 2

The ocular tropism of Venezuelan equine encephalitis virus pseudotyped lentivirus vector in mice and humans

INTRODUCTION

In the past decade, several clinical trials have successfully demonstrated that a therapeutic transgene may be delivered efficiently to the human retinal pigment epithelium (RPE) using recombinant adeno-associated virus (rAAV) vectors (Lipinski et al., 2012). Whilst numerous studies have also shown effective serotype-dependent targeting of photoreceptors in animal models of retinal disease, the delivery of large genes to the neural retina using rAAV has thus far proven problematic, in spite of recent efforts to artificially increase the coding capacity through packaging of recombining or transplicing genomes split across multiple rAAV virions (Duan et al., 2003; Lai et al., 2005; Yan et al., 2000).

Lentivirus vectors, typically based on either human immunodeficiency virus (HIV) or equine infectious anaemia virus (EIAV), are a viable alternative, having a comparatively large coding capacity and the ability to be pseudotyped, a process whereby the native viral surface glycoproteins are exchanged for those of another enveloped virus, thus altering the tropism. The most commonly employed pseudotype, derived from vesicular stomatitis virus glycoprotein (VSV-G), has broad cellular tropism due to an affinity for binding to ubiquitously expressed surface residues, most likely negatively charged lipids (Lyles and Rupprecht, 2006).

Lentivirus vectors have been used to target gene delivery towards numerous cells types, including hepatocytes, dedritic cells, myocytes, haematopoietic stem cells and neurons (Demaison et al., 2002; Naldini et al., 1996; Poeschla et al., 1998; Sakuma et al., 2012; Zufferey et al., 1998) and have been shown to correct genetic deficits in disease models of sickle-cell anaemia, haemophillia B and β-thalassaemia (Brown et al., 2007; Malik et al., 2005; May et al., 2000; Pawliuk et al., 2001). Additionally, lentiviral vectors have been used to significantly ameliorate models of other major genetic disorders, including cystic fibrosis and spinal muscular atrophy (Azzouz et al., 2004; Wang et al., 1999), and are currently being used in phase I/II clinical trials for the treatment of Parkinson's disease.

In the eye VSV-G pseudotyped vectors have demonstrated efficient transduction of RPE *in vivo* following delivery to the subretinal space, yet have thus far proven ineffective at targeting photoreceptors

in rodent (Auricchio et al., 2001; Ikeda et al., 2003) and primate models (Ikeda et al., 2009), limiting their utility for delivering large genes necessary for the treatment of several retinal diseases, such as Stargardt's disease or Usher syndrome Type Ib. Attempts to improve neuronal targeting by employing pseudotypes derived from neurotropic viruses, such as rabies-G (Balaggan et al., 2006) or mokola (Bemelmans et al., 2005), have met with little success. Similarly, whilst photoreceptor specific promoters have been successfully incorporated into both HIV and EIAV vectors, they effectively limit ectopic expression of the transgene but do not significantly increase the levels of photoreceptor transduction in the adult retina (Miyoshi et al., 1997; Nicoud et al., 2007). Herein, we employ longitudinal *in vivo* fluorescence imaging to examine the tropism of a further pseudotype derived from Venezuelan equine encephalitis virus (VEEV-G), a zoonotic virus which causes encephalopathy in various equine species and humans. VEEV has single amino acid substitutions in the E2 region of the surface glycoprotein which facilitate attachment of wild-type virus to multiple neuronally expressed surface markers - a property which may give increased tropism for photoreceptors. In addition to evaluating retinal tropism following subretinal administration, we also examine the tropism of the VEEV-G pseudotype in the anterior chamber, an ocular niche where VSV-G pseudotyped vectors have previously been shown to effectively transduce the corneal endothelium and trabecular meshwork (Balaggan et al., 2006).

Given the lack of successful retinal transduction observed in previous studies using pseudotyped lentivirus vectors, we hypothesized successful photoreceptor transduction may be inhibited not by the receptor binding of a given pseudotype, but by the presence of physical barriers, such as the outer limiting membrane (OLM), outer segment (OS) disc shedding, or the accumulation of cellular debris in the sub-retinal space, which may impede virion access to the photoreceptor cell bodies. To examine this clinically important question we utilized a modified explant culture system to maintain degenerate human retina biopsied from patients undergoing surgery for retinal detachment.

Retinal detachments in humans fall broadly into three categories: rhegmatogenous, traction, and exudative. Rhegmatogenous retinal detachments (RRD) occur when liquefied vitreous passes through a

tear or hole in the retina into the subretinal space, resulting in a fluid build up which separates the neural retina from the RPE. Retinal tears or holes in such cases are typically caused by vitreous detachment, where changes in the fibrillar structure of the vitreous lead to localized dissociation of the vitreous from the retina, with traction and subsequently tearing of the surrounding retina where the vitreous is more firmly attached. Changes in vitreoretinal attachment and fibrilar structure, and the posterior migration of the vitreous base, are associated with aging, though the cellular and molecular processes underlying vitreous liquefaction and the alteration of collagen composition with aging, are poorly understood (Mitry et al., 2010b). Non-aging risk factors for the development of RRD include cataract surgery, with pseudophakic RRDs accounting for an estimated 40% of retinal detachments presenting to the clinic (Haimann et al., 1982; Lois and Wong, 2003), and trauma, which accounts for approximately 10% of RRDs, mainly amongst males under 50 years old (Mitry et al., 2010a). As expected, the photoreceptor/RPE interface is the most affected by RRDs, where detachment leads to degeneration of the outer segments OS. OS regenerate subsequent to reattachment, and despite heterogeneity in terms of OS length and orientation, vision largely returns to its pre-detachment levels (Kroll and Machemer, 1969a, b; Lewis et al., 2002). Long-term detachment results in photoreceptor cell death by apoptosis with associated decline in ONL thickness which is halted by reattachment (Anderson et al., 1983; Cook et al., 1995; Erickson et al., 1983).

Traction retinal detachments (TRD) occur primarily in fibrocontractive retinal disorders such as proliferative vitreoretinopathy (PVR) or proliferative diabetic retinopathy (PDR), where either scar-like tissue forms on the retinal surface, producing tractional forces that distort the shape or position of the retina in relation to the RPE, or cells proliferate, causing distortion of the established cellular matrix (Guidry, 2005). In TRDs no hole or tear is present, the detachment instead being caused by contractile forces within the retina itself.

Exudative retinal detachment (ERD) is a serious complication of several retinal and systemic diseases, and occurs when blood or fluid, primarily from the chorioretinal vasculature, leaks into the

subretinal space. ERD is associated with inflammatory disorders, such as Vogt-Koyanagi-Harada (VKH) disease, in addition to severe hypertension, kidney failure, or as a rare complication of pregnancy. However, ERD is most commonly associated with neovascular age related macular degeneration (NV-AMD) as a direct result of blood vessel leakage during angiogenesis.

Minor retinal detachments often resolve without intervention; however, in cases of major or chronic retinal detachments surgery to reattach the retina is commonly performed. During surgery it is routine to remove small fragments of the retina, which depending on the cause underlying the retinal detachment, are often viable and can be cultured. Herein we utilized tissue biopsied from patients undergoing retinal detachment surgery to explore the ex vivo transduction of differentially pseudotyped lentivirus vectors, where in such an *ex vivo* environment physical barriers to transduction are likely to be either compromised or absent, and so the effect of pseudotype on retinal transduction can be isolated.

CHAPTER SPECIFIC MATERIALS AND METHODS

Viral vectors

Recombinant non-replicative HIV-1 based lentiviral vectors were produced in the Laboratory of Nicholas D. Mazarakis, Imperial College London, UK, using a modified transient calcium phosphate transfection protocol based on the standard four plasmid transfection of 293T cells. Briefly 12 x 150mm tissue culture dishes were seeded with 1.4 - 1.6x10^7 293T cells per dish. The next day cells were transfected with 15 μg vector plasmid (*pRRLsincppt-CMV-eGFP-WPRE* expressing GFP from the CMV promoter), 15 μg of plasmid expressing the HIV-1 gag/pol gene (*pMD2-LgpRRE*), 3 μg of plasmid expressing HIV-1 Rev (*pRSV-Rev*) and 5.1 μg of the plasmid expressing the appropriate envelope GP *pMD2-VSVg (*this and other HIV1 vector plasmids were obtained from Professor James Uney, University of Bristol, UK*)* or *pcDNA3-VEEV.3908* (obtained from Dr Robert A. Davey, University of Texas) following the addition of 1M $CaCl_2$. 16 hours post transfection media were replaced with fresh media supplemented with 10mM

sodium butyrate. 36 hours after sodium butyrate induction, vector containing media were harvested and filtered through a 45 μm filter.

Large scale preparations were concentrated by centrifugation at 6000 RPM for 12-16 hours at 4^{o}C (Beckman Coulter Avanti J-E, F500 rotor). The pellet was then resuspended in ice cold PBS and was further concentrated by ultracentrifugation for 90 minutes at 20,000 RPM, 10^{o}C (Beckamn Coulter Optima L-80XP). The pellet was resuspended in 50μl ice-cold TSSM formulation buffer (20 mM Tromethamine, 100 mM NaCl, 10 mg/ml sucrose and 10 mg/ml mannitol) every 15 minutes for 3 hours and then centrifuged at 13.000 RPM for 30 seconds. The supernatant was stored overnight at 4^{o}C along with the pellet which was resuspended with a further 50μl ice cold TSSM. The resuspended pellet was centrifuged at 13.000 RPM for 30 seconds and the two supernatants were pooled giving a final volume of 100μl (2000 fold concentration). Vector preparations were stored at -80^{o}C.

Biological activity of lentiviral vectors carrying the GFP reporter gene was determined by flow cytometry (Becton Dickinson LSR Benchtop Flow Cytometer). Briefly, HEK 293T cells were seeded in 12-well plates at 5x10^{5} cells per well. 18 hours after seeding the cells in a single well were quantified using a haemocytometer. Cells were transduced for 6 hours with a serial dilution of the vector to be quantified in the presence of 8 μg/ml polybrene. 72 hours post transduction the percentage of GFP positive cells was determined by flow cytometry. The number of physical lentiviral particles present in a preparation was estimated using a HIV-1 p24 Antigen ELISA (RETROtek from ZeptoMetrix).

Intraocular injection

Juvenile (6-8 week old) C57Bl/6J 'wild-type' mice (n=19) were purchased from Harlan Laboratories (Hillcrest, UK) and housed under standard 12:12 light/dark cycle with food and water available *ad libitum*. Anesthesia was induced as described in 'General Methods and Materials' section. Following pupil dilation, a gel lubricant (Viscotears, Novartis, Frimley, UK) was used to position a 6mm circular cover slip over the cornea, allowing good visualization of the retina when viewed under a surgical

microscope (M620 F20, Leica, Wetzlar, Germany). Injections were performed by advancing a Hamilton syringe with attached 10mm 34-guage needle (Hamilton 65N, Hamilton AG) trans-sclerally either into the subretinal space (subretinal injection) or further, through the neural retina, into the vitreous chamber (intravitreal injection), or into the anterior chamber (intracamerally). Reflux of vector suspension was limited by allowing the intraocular pressure to normalize for 20-30 seconds prior to rapid removal of the needle. Orientation and stabilization of the eye was maintained throughout by holding the superior or inferior rectus muscle with notched forceps. Separate syringes were used for each vector pseudotype to avoid contamination and the needles flushed with sterile saline between injections.

Autofluorescence imaging using a confocal scanning laser ophthalmoscope

The ocular fundi of each mouse were imaged using a confocal scanning laser ophthalmoscope (cSLO; Spectralis HRA, Heidelberg Engineering, Heidelberg, Germany) 1, 2, 7, 14 and 21 days (D) post injection, as previously described (Charbel Issa et al., 2011). Briefly, following dilation a contact lens was placed on the cornea using a viscous coupling gel (0.3% w/v hypromellose) to prevent cataract formation and to improve and standardize image quality. Each mouse was placed on a raised imaging platform and the near-infrared (NIR) reflectance mode (820nm laser) used to achieve camera alignment at the confocal plane of the RPE. Onset of EGFP transgene expression was evaluated using the autofluorescence (AF) imaging mode (480nm excitation) and high resolution images (1536 x 1536) recorded at a range of standardized sensitivities using automated real-time (ART) averaging.

Tissue processing and histology

Eyes were enucleated and fixed in 4% paraformaldehyde (PFA) for 30 minutes, during which time the anterior segment and lens were removed. The posterior eye cup was cryoprotected for 48 hours at 4^{o}C in 30% (w/v) sucrose and embedded in optimum cutting temperature (OCT) media. 18µm cryosections were taken coronally from the optic disc towards the iris. Sections were immunostained for either RPE65

(1:1000 dilution; antibody a kind gift from Rosalie Crouch, Medical University of South Carolina, USA) or cone arrestin (1:1000; Millipore AB15282, Watford, UK), prior to being counter stained with Hoechst 33342 and mounted with ProLong Gold antifade reagent (both Invitrogen, Paisley, UK).

***Ex vivo* culture of human retinal explants**

Retinal explant samples were obtained from a 32 year old male patient undergoing retinectomy as part of surgery for a complex chronic rhegmetogenous retinal detachment with associated proliferative vitroretinopathy. Surgery was carried out with approval from the UK Research Ethics Committee (REC 10/H0505). In accordance with the Declaration of Helsinki, patients gave written, informed consent prior to the start of the procedure. A routine 23 gauge pars plana vitrectomy was performed for retinal detachment surgery. Discs of the peripheral retina were cut with a vitrectomy system (Ocutome; Alcon Surgical, Irvine, TX), refluxed into the eye, aspirated with a flute needle and placed in balanced salt solution. Within 30 minutes retinal samples were transferred into organotypic culture, as describe previously (Lipinski et al., 2011a). Briefly, retinal tissue was transferred using a cut-off 3ml Pasteur pipette (to reduce crush injury) into 24-well tissue culture inserts containing 700µl complete culture media (Johnson and Martin, 2008) consisting of NeurobasalA, L-glutamine (0.08mM), penicillin (100 U/ml), streptomycin (100 U/ml), Amphotericin B (0.25ug/ml), B27 supplement (2%) and N2 supplement (1%, all Invitrogen Ltd, Paisley, UK). One day (D1) post explantation media was replaced and supplemented with 10µl virus vector suspension (VEEV-G = $1.7x10^7$TU; VSV-G = $2.6x10^8$TU); media was changed every third day thereafter. Transparency of the tissue culture inserts (cat. 353095; BD Falcon, Bedford, MA) allowed explants to be monitored for onset of transgene expression in culture using an inverted epi-fluorescent microscope (DMIL, Leica, Wetzlar, Germany). At D14 explants were fixed in 4% PFA for 24 hours at 4^oC, during which time both outer and inner retinal aspects were imaged. Fixation time was extended from 30 minutes in this instance for a two reasons. Firstly, after several days in culture retinal samples lose a degree of structural integrity, making them particularly susceptible to

tearing or stretching; a longer fixation time ensured that the retinal explants remained in a good condition for subsequent histology. Secondly, tissue samples from human retina were deemed valuable due to their limited availability, and so a longer fixation time was used to ensure that minimal EGFP signal was lost during tissue processing. The effects of long fixation time on subsequent immunohistochemistry, where long fixation times can lead to extensive protein cross-linking that inhibits antibody binding, were considered to be secondary to the acquisition of good primary histology, where cellular tropism could likely be determined by anatomical location. For example, EGFP expression localized to the outer nuclear layer would provide strong evidence of photoreceptor transduction without necessarily requiring co-labelling of a photoreceptor specific gene target. Subsequent to fixation, explants were cryoprotected for 48 hours in 30% (w/v) sucrose, embedded in OCT and 18μm cryosections cut.

RESULTS

Autofluorescence imaging reveals rapid onset of transgene expression in the RPE following subretinal administration

Confocal scanning laser ophthalmoscope (cSLO) imaging is employed clinically to non-invasively assess retinal pathology, where the retina can be visualized through the pupil aperture. Observations can be used to inform diagnosis, guide treatment, and allow monitoring of disease progression. AF imaging using a 488 nm laser for excitation can also be used to examine the ocular fundus in mice (Charbel Issa et al., 2011), and may visualize retinal expression of fluorescent reporter proteins, particularly enhanced green fluorescent protein (EGFP), which has an excitation maximum close to that of the AF laser stimulus (Beck et al., 2010). Pseudotyped VSV-G (high titre = 5.20×10^7 TU in 2μl; low titre = 5.20×10^6 TU in 2μl) or VEEV-G (high titre = 3.40×10^6 TU in 2μl; low titre = 3.40×10^5 TU in 2μl) lentiviral vectors carrying an EGFP transgene (Fig. 2.1A-B) were injected into the subretinal space of six C57Bl/6j mice (n = 6 eyes per pseudotype). Three further C57Bl/6j mice acted as injection controls receiving 2μl TSSM injection in one eye, with the contralateral remaining uninjected. AF fundus imaging was performed at 1, 2, 7, 14

and 21 days (D) post injection to track the onset and distribution of transgene expression (Fig 2.2). AF fundus imaging revealed a 'cobble-stone' pattern of fluorescence, indicating transduction of the RPE, a monolayer of hexagonally arranged cuboidal or low-columnar epithelial cells underlying the photoreceptors (Fig. 2.3 A). Quantitative grey level (q-GL) values within the area of injection were measured from non-normalized fundus AF images recorded using a standardized non-saturating detector setting (90AU), allowing comparison of the relative intensity of EGFP expression between mice injected with different vector titres (Fig. 2.2 and Fig. 2.3 B). EGFP expression was visible one day (D1) post injection, although q-GL values did not show a large increase in fluorescence within the injected area compared to the surrounding uninjected retina. Fluorescence intensity continued to increase rapidly in all groups, with fold changes in fluorescence intensity at D2 of between 6.6±0.1 (VEEV-G high titre) and 7.0±1.0 (VSV-G high titre) compared to uninjected baseline (Fig 2.3 B). EGFP transgene expression in high titre groups reached peak fluorescence intensity at D7 (Fig. 2.3 B), with fold-changes in q-GL of 9.9±0.1 (VEEV-G) and 8.3±1.9 (VSV-G) above baseline. The peak of fluorescence intensity was reached later(D14) in both low titre groups (Fig. 2.3 B), though the fold-change in q-GL compared to baseline (VEEV-G = 8.2±0.3; VSV-G = 8.7±0.8) was not substantially different to that of the high titre groups at their peak (D7). Assuming that fold-change increases in q-GL are proportional to EGFP protein levels, and that fluorescence intensity can therefore be used as a measure of relative transgene expression, these data indicate that vector titre does not significantly impact the level of transgene expression, but the speed at which expression occurs. Interestingly, a decrease in overall fluorescence intensity was observed in both high titre groups from D7 onwards, with patches of geographic fluorescence loss apparent by D14 (Fig. 2.2). A reduction in fluorescence intensity on AF imaging strongly indicates either attenuation of EGFP protein levels within a tissue, suggestive of promoter silencing or down regulation, or tissue death. The overall reduction in fluorescence levels was comparable in extent and pattern between VSV-G and VEEV-G treatment groups, indicating that the effect is unlikely to be pseudotype-dependent. We hypothesised that over expression of the transgene might be leading to toxicity, where EGFP has

previously been demonstrated to be well tolerated in photoreceptors (Daniels et al., 2003; Lipinski et al., 2011b; Nour et al., 2004), but high level expression of EGFP in the RPE has been linked to cell death (Doi et al., 2002).

Robust transgene expression in corneal endothelium and the trabecular meshwork following intracameral injection of pseudotyped lentivirus

Whilst the main focus herein is whether lentivirus vectors can be used to successfully deliver large genes to the neural retina, it has previously been noted that VSV-G pseudotyped vectors can transduce cells of the anterior segment, in particular the corneal endothelium and trabecular meshwork (Balaggan et al., 2006). Consequently, given the robust RPE expression of the VEEV-G pseudotype observed following subretinal administration, we examined the whether VEEV-G might also successfully transduce other endothelial cells, such as those on the posterior surface of the cornea, which are susceptible to various dystrophies with underlying genetic etiology. VSV-G (high titre = $5.20x10^7$ TU in 2µl) or VEEV-G high titre = $3.40x10^6$ TU in 2µl) vector was injected intracamerally in six C57Bl6/j mice (n = 6 per pseudotype) through a self-sealing corneal tunnel made at the surgical limbus. Three further C57Bl/6j mice acted as injection controls receiving 2µl TSSM injection in one eye, with the contralateral remaining uninjected. The virus suspension was delivered to the centre of the anterior chamber, where aqueous convection is most likely to drive virions towards the inner corneal surface, and aqueous outflow to drive virions radially towards the iridocorneal angle (Fig. 2.5 A). Near infra-red (NIR) imaging was used to obtain a centred image of the anterior chamber; reflectance artefacts (white glare spots) were observed on the corneal surface only in NIR mode (Fig. 2.4 A, B). AF imaging revealed expression of EGFP from both pseudotypes by D7 which was maintained until D21(Fig 2.4 A-B). Fluorescence was predominantly observed centrally at the confocal plane of the cornea with both pseudotypes (Fig. 2.4 A-B), indicating robust expression of EGFP in the corneal endothelium, which was later confirmed by histology (Fig. 2.5 B iv). The pattern of fluorescence was in an atypical ‘Krukenberg spindle’ distribution, a phenomenon

observed whereby aqueous convection drives free floating particles in the anterior chamber (classically, pigmented iris cells) towards the interior corneal surface, leading to their deposition in a central, vertically orientated oval/stripe (Krukenberg, 1899). Fluorescence was observed to have radial symmetry (e.g. Fig. 3A vi), being most intense centrally and less intense peripherally (Fig 2.4 A-B). The absence of a 'classic' Krukenberg spindle pattern (vertically orientated ovoid) likely results from differences in the size and shape of the mouse lens relative to the cornea (Heys and Barocas, 2002). AF imaging focusing at the plane of the limbus revealed a ring of fluorescence at the irido-corneal angle with both pseudotypes (Fig 2.4 A-B), which on histology correlated to EGFP expression in the anatomical area of the trabecular meshwork (Fig. 2.5B i-iii), a structure which regulates aqueous outflow and is critical to maintaining proper intraocular pressure.

VEEV-G Pseudotyped lentiviral vector exhibits toxicity in the outer retina

Following fixation and embedding at D21 (Fig 2.1C) injected eyes were sectioned for histology and immunohistochemistry to determine the cellular tropism. In all groups robust EGFP expression was observed to co-localize with areas of heavy pigmentation (Figs. 2.6, 2.7, 2.8 and 2.9), strongly indicating transduction of the RPE within the area of injection. EGFP expression was observed to co-localize with RPE65, an RPE specific retinal isomerase, following injection of VSV-G (Fig. 2.6) or VEEV-G (Fig. 2.8).RPE65 levels appeared to be reduced in areas of greatest EGFP expression - down regulation of RPE65 has previously been observed to result from cellular stress potentially preceding apoptosis (Alge et al., 2003; Alizadeh et al., 2001; Lee et al., 2010). However, no morphological evidence of RPE thinning, cell migration or death was observed compared to surrounding uninjected areas with either vector. EGFP expression was not observed in the outer nuclear layer (ONL) following injection with either pseudotype, in accordance with findings described previously (Auricchio et al., 2001; Bainbridge et al., 2006; Balaggan et al., 2006). Immunohistochemistry with a marker of cone photoreceptor (c-arrestin) revealed no co-localization with either VSV-G (Fig. 2.7) or VEEV-G (Fig. 2.9) pseudotype, strongly indicating

that neither successfully targets murine photoreceptors *in vivo*. Thinning of the ONL within the area of injection was observed in eyes administered the VEEV-G pseudotyped vector at both high (Fig 2.8) and low (Fig. 2.9) doses. No retinal thinning was observed at either high (Fig 2.6) or low (Fig. 2.7) VSV-G titre, or in TSSM injected control eyes(data not shown). Disruptions in cellular pathology and decreased electrophysiological responses have previously been noted in rodents following administration of high titre lentivirus vector suspensions, and are likely caused by a sustained inflammatory reaction (Ikeda et al., 2009). Areas where EGFP expression was absent were visible within the area of injection, particularly at high virus titre (e.g. Fig 2.7 i), which may correspond to areas of decreased AF observed *in vivo* (Fig 2.2). However, the RPE appeared normal in morphology with no evidence of cellular infiltration into the subretinal space (Doi et al., 2002), limited RPE migration (Fig. 2.6 iii) and no depigmentation, which would indicate significant cellular pathology.

To address the issue of toxicity associated with vector production (e.g. residual chemical contaminants) injections were repeated with multiple vector preparations and ONL thinning was observed in each instance with the VEEV-G pseudotype, but not with concurrently produced VSV-G vector batches of comparable titre, indicating a pseudotype specific effect. TSSM injected eyes additionally showed no indicators of toxicity. While expression of various fluorescent proteins has been shown to result in cytotoxicity both in vitro (Liu et al., 1999) and in vivo (Huang et al., 2000), photoreceptor toxicity arising from intracellular expression of EGFP is unlikely, given the lack of observed ONL transduction. Furthermore, EGFP has been shown to be well tolerated in the retina, with no significant cell death observed when EGFP is expressed following transduction of photoreceptors using alternative vectors (e.g. rAAV), or when EGFP is expressed intrinsically, as in various transgenic mouse models (Daniels et al., 2003; Dreyer et al., 1999; Lipinski et al., 2011b; Nour et al., 2004).

***Ex vivo* transduction of human retinal explants reveals transduction of photoreceptors and Müller glia**

To explore whether photoreceptor transduction *in vivo* is inhibited by the presence of physical barriers, we modified a previously described explant culture system to maintain small samples (2-3mm^2) of human retinal tissue obtained from patients undergoing retinectomy surgery to treat complex retinal detachment (Lipinski et al., 2011a).The retina in such patients is often diseased and the OLM compromised, potentially allowing virions greater access to the photoreceptor cell bodies. Additionally, the RPE is absent from the culture environment, and the rate of OS disc shedding is greatly reduced, removing further impediments to virion access. One day post explantation, retinal samples taken from a single patient with a retinal detachment were transduced *ex vivo* by the addition of 1.7x10^{7}TU (VEEV-G) or 2.6x10^{8}TU (VSV-G) diluted in 700µl culture medium. Imaging of the retinal explants in culture showed EGFP expression by D3 (both pseudotypes; data not shown) which increased in intensity until D14, at which time the tissue was fixed. Examination of the retinal tissue whilst still in culture following delivery of VEEV-G pseudotyped vector revealed transduction of cells with long axonal projections that were visible from the inner retinal aspect only, indicating targeting of ganglion cells or activated microglia (Fig. 2.10 B i). Transduction of Müller cells could also be observed *in vitro*, particularly at the edge of the tissue, where folding of the retina allowed a cross sectional view of heavily stratified cells spanning the full retinal thickness (Fig. 2.10 B i). Histology confirmed the presence of heavily stratified expressing EGFP cells which co-localized with GFAP (Fig. 2.10 B ii-iii), a marker of activated astrocytes that is expressed by Müller cells and activated microglia. By contrast, the VSV-G vector resulted in a punctuate pattern of EGFP expression visible in culture only when viewed from the outer retinal aspect (Fig. 2.10 A i). That the observed 'dot-like' pattern was not clearly visible from the inner retinal aspect indicates that the transduced cells were located in the outer nuclear layer (ONL). Histology showed widespread transduction of cells throughout the ONL which co-localized with recoverin, a photoreceptor specific inhibitor of rhodopsin kinase, confirming transduction of photoreceptors (Fig. 2.10 A ii-iii). Limited numbers of EGFP expressing cells with long processes were additionally observed located within the ganglion cell layer.

DISCUSSION

Herein, we evaluated the ocular tropism of a lentivirus vector pseudotyped with Venezuelan equine encephalitis virus glycoprotein (VEEV-G), the neurotropic nature of which we hypothesized would increase levels of photoreceptor transduction compared to VSV-G pseudotyped vector. The VEEV-G pseudotyped vector was found to transduce RPE with similar efficiency to that of VSV-G pseudotyped vector, but was observed to have deleterious effects on the overlying neural retina, indicating that this pseudotype is poorly tolerated when injected subretinally and is not a good candidate for photoreceptor gene delivery. In contrast, both vectors were well tolerated in the anterior chamber, leading to robust transduction of the corneal endothelium and trabecular meshwork that could be clearly observed *in vivo* using AF imaging. The lack of successful photoreceptor targeting *in vivo* with either pseudotype led us to theorize that physical barriers contribute significantly to the inhibition of transduction. Using a modified explant culture system to maintain *ex vivo* retina removed from patients with retinal disease, we observed significant levels of retinal transduction with both pseudotypes, in particular VSV-G which successfully transduced photoreceptors.

To our knowledge this represents the first time that a lentivirus vector has been demonstrated successfully to transduce human photoreceptors. The observation that photoreceptor transduction is observed *ex vivo* indicates that VSV-G is able to bind photoreceptors and trigger virion internalization resulting in expression, and that this is not the limiting step to photoreceptor gene delivery with this pseudotype. By contrast, VEEV-G pseudotyped vector did not target photoreceptors in the *ex vivo* model, instead targeting Müller glia or activated astrocytes. With cellular tropism mediated predominantly by the interactions of a virion's surface glycoproteins with cellular receptors, it is likely that differences in receptor substrate distribution across the retina are responsible for the observed difference. In particular, cellular attachment of VSV-G occurs via non-specific hydrophobic/electrostatic interactions, potentially mediated by ubiquitously expressed phosphatidylserine (PS), conferring it broad tropism, whereas VEEV-

G cell attachment is thought to involve laminin binding receptors (Ludwig et al., 1996; Malygin et al., 2009) with heparin sulphate (HS) as a secondary receptor.

The absence of significant photoreceptor transduction *in vivo* with either pseudotype indicates that gene delivery to the photoreceptors *in vivo* is instead impeded by physical barriers which are not present in tissue culture. A probable factor *in vivo* is the presence of the RPE, a monolayer of highly phagocytotic cells that is closely associated with the neural retina, and which likely internalizes the majority of enveloped virions following subretinal injection. Additionally, the presence of an outer limiting membrane (OLM), interposed between the photoreceptor inner and outer segments, and the movement of the outer segments themselves towards the RPE as a result of disc shedding, is likely to further impede virion transport to the cell body *in vivo*. In our tissue culture environment the RPE is absent, the OLM is likely to be disrupted, and disc shedding is unlikely to occur at a normal rate, factors which when combined may allow for effective retinal transduction. In contrast rAAV vectors appear to be minimally affected by these impediments, likely due to their small size (~20nm diameter compared to ~120nm for lentiviruses) and absence of a surrounding lipid envelope, which likely promotes lentivirus fusion with the membrane of the OS discs. So, whilst our *ex vivo* culture clearly demonstrates that lentivirus vectors can effectively transduce human photoreceptors, *in vivo* administration of identical vector batches in mice resulted in no significant transduction. This implies either that efficient gene transfer *in vivo* is likely to require the circumvention of various physical barriers or that cellular tropism may differ between species, as observed with rAAV vectors (Boye et al., 2012; Calame et al., 2011; Yin et al., 2011). However, the ability of VSV-G pseudotyped vectors to transduce photoreceptors *ex vivo* may make them suitable in the context of developing future photoreceptor replacement therapies for the treatment of end stage retinal disease, where any autologously generated photoreceptor cells would require correction of the underlying genetic defect prior to transplantation.

The VEEV-G pseudotyped vector was not observed to have a transduction profile more favourable to that of VSV-G. Widespread cell death was observed in the neural retina with two separately

manufactured batches of VEEV-G vector, but not with concurrently produced VSV-G vectors, suggestive of a pseudotype specific effect. Whilst this finding contraindicates the use of VEEV-G pseudotyped vector for gene delivery to photoreceptors, it highlights the requirement for novel vector technologies to be rigorously evaluated in a laboratory environment prior to clinical application, particularly with respect to toxicity. The observation that RPE65 expression is apparently down regulated following lentivirus transduction of the RPE regardless of titre or pseudotype, most likely as part of a stress response, is particularly troubling given the recent progression of several lentivirus therapies into phase I/II clinical trials. Furthermore, RPE disregulation is likely to limit the effectiveness of RPE cell-specific promoters, a key method of providing spatial regulation and improving vector safety, where one might expect transgene expression levels when using such promoters to be similarly suppressed.

Vector administration into the anterior chamber demonstrated that both lentiviral vectors were well tolerated and led to widespread transduction of the corneal endothelium and the trabecular meshwork. The extent of transduction using VEEV-G was comparable to that of VSV-G, indicating that either might be used successfully to deliver large or multiple gene expression cassettes to these tissues, potentially for the treatment of glaucoma and corneal endothelial dystrophies. Interestingly, AF imaging revealed that transduction of the corneal endothelium is not uniform, and is likely linked to the dynamics of aqueous flow within the anterior chamber. In humans, aqueous flow is driven by a number of complex factors (Heys and Barocas, 2002), and is likely to greatly complicate the ability to uniformly transduce the corneal endothelium, thus possibly limiting the effectiveness of therapies for diseases such as endothelial dystrophies. Furthermore, these experiments demonstrate that aqueous flow will direct virions released into the anterior chamber towards both the corneal endothelium and the trabecular meshwork, potentially necessitating the use of promoters to limit ectopic gene expression.

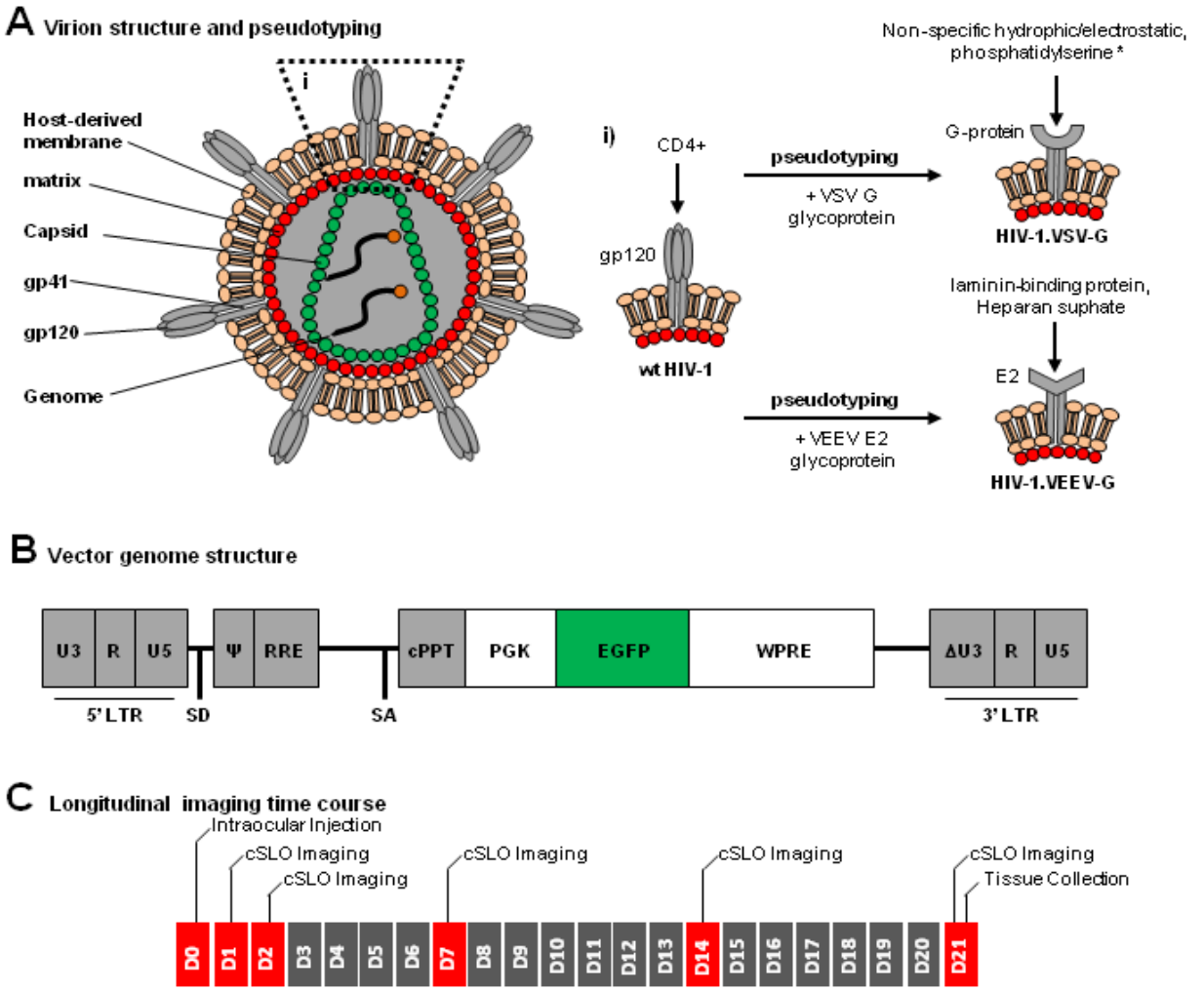

Figure 2.1 – Diagrammatic representation of lentivirus structure, pseudotyping, vector genome and experimental design. Lentivirus virions have a complex structure where multiple single stranded RNA genomes are enclosed in an enveloped nucleocapsid expressing viral surface glycoproteins gp41 and gp120 **(A)**. Virions can be pseudotyped – the process where the native surface glycoproteins are substituted with those of an alternative virus – to alter tropism. Note that unless chimeric glycoproteins are constructed, the transmembrane region must be compatible with the host derived lipid membrane and able to interact with the underlying virion matrix. **(B)** Structure of the third generation self inactivating (SIN) transgene expression cassette packaged into the pseudotyped viruses. Minimal virus sequences are shaded grey. LTR = long terminal repeat; SD = splice donor; ψ = packaging signal; RRE = Rev response element; PGK = phosphoglycerate kinase promoter; EGFP = enhanced green fluorescent protein; WPRE = woodchuck posttranscriptional regulatory element. **(C)** Schematic detailing the imaging time course. * phosphatidylserine was thought to be the primary cellular receptor, but is now known to be a secondary receptor.

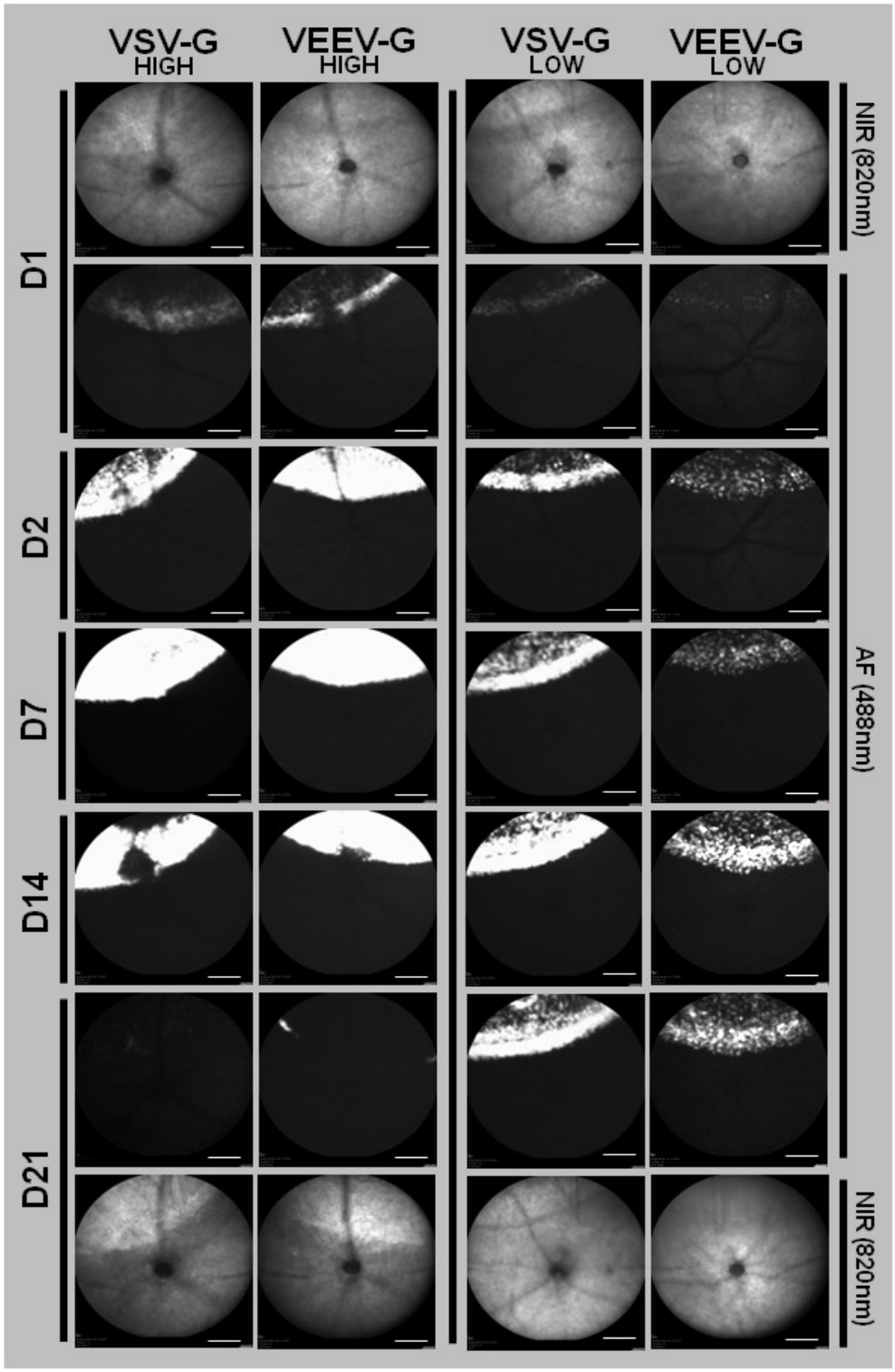

Figure 2.2 – In vivo fluorescence imaging of the mouse fundus following subretinal injection of pseudotyped vectors
EGFP fluorescence (white signal on autofluorescence (AF) imaging mode) can be observed 1 day following administration of vectors pseudotyped with VSV-G (high titre = $5.20x10^7$ TU in 2µl; low titre = $5.20x10^6$ TU in 2µl) or VEEV-G (high titre = $3.40x10^6$ TU in 2µl; low titre = $3.40x10^5$ TU in 2µl) envelopes. The signal intensity on AF imaging is correlated to levels of EGFP protein expression. Signal intensity increases in all groups, peaking in high dose groups at postnatal day (D). Patches of decreased signal intensity are observed in high dose groups from D14 onwards, indicative of RPE atrophy. Signal intensity continued to increase in both low dose groups until D21, with no evidence of atrophy apparent. Near infrared reflectance (NIR) mode reveals areas of hyper-reflectivity at D21 in high dose groups. All scale bars = 200µm.

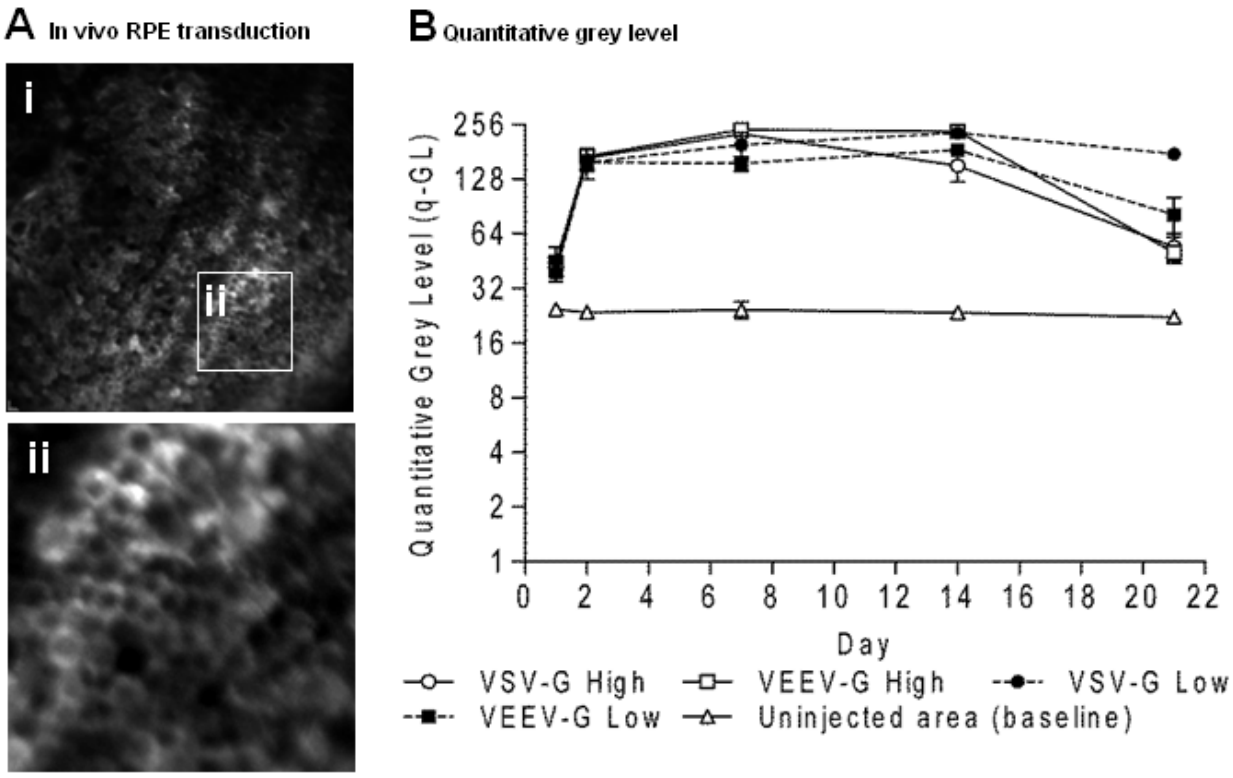

Figure 2.3 –Analysis of fluorescence intensity (grey-level) on AF images allows relative quantification of expression levels
All pseudotyped vectors led to robust transduction of the RPE which was observable by in vivo autofluorescence imaging. Using a 30^{o} lens individual EGFP expressing RPE cells could be resolved, appearing as regularly arranged hexagons **(A i-ii)**. Expression levels of EGFP protein correlate to the intensity of the fluorescence (white) signal observed on in vivo fluorescence imaging. The average grey-value within the area of injection can be quantified on images when taken with standardized detector settings**(B)**. The quantitative grey level (q-GL) can be used to assess the relative strength of EGFP expression between vectors and the dynamics of transgene expression. Time until observed transgene expression was 1 day post injection in all groups. Intensity increased in all groups, peaking at D7 in high dose groups, and day 14 in low dose groups. Peak expression levels were comparable in intensity between vectors and doses. Expression levels were maintained at peak levels only in low dose VSV-G injected eyes, with intensity reducing in all other groups by D21 compared to D14, potentially reflecting loss of fluorescence due to RPE atrophy. D = day post-injection. n = 6 C57Bl/6j animals in each group. Error bars = s.d.

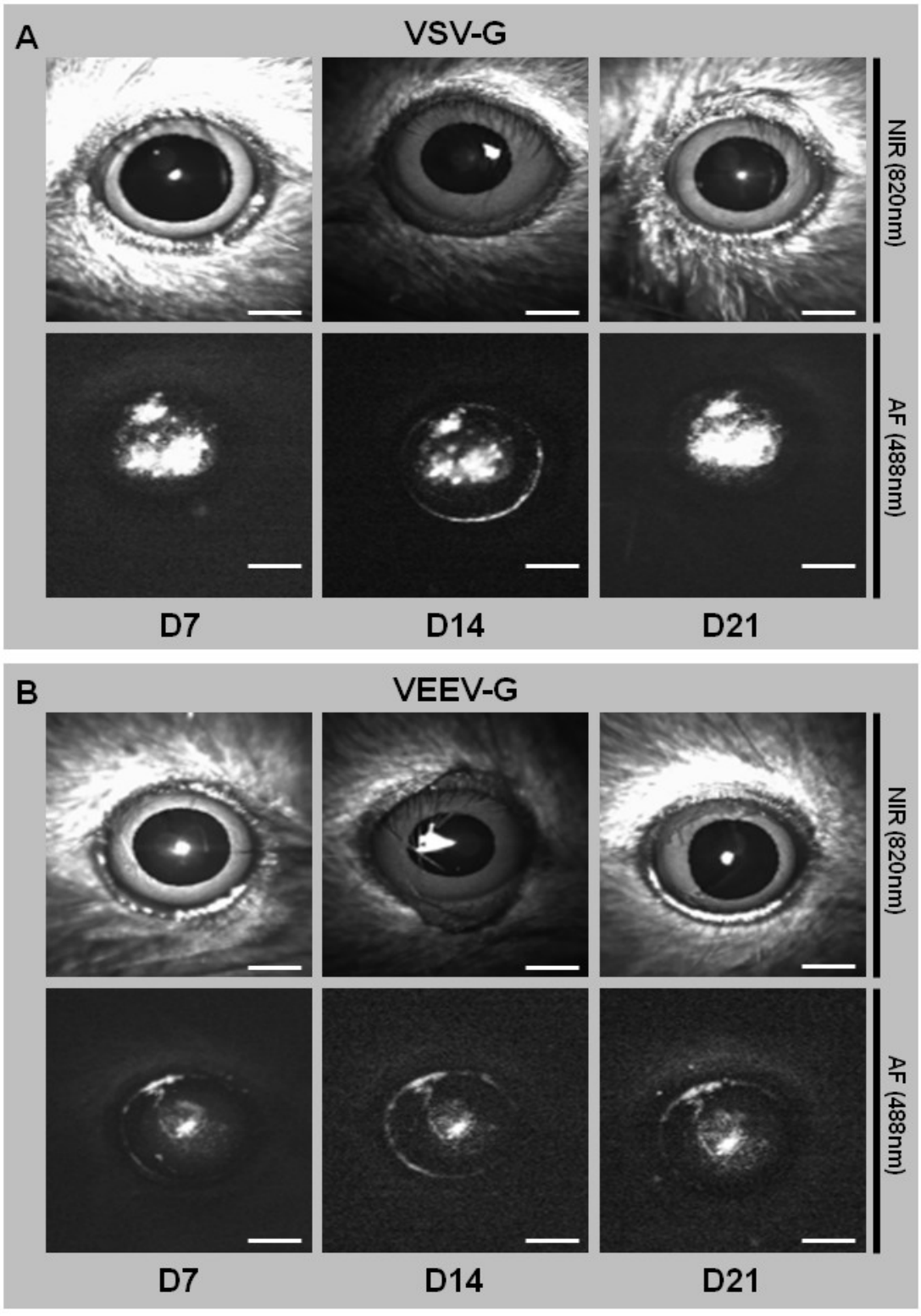

Figure 2.4 – Anterior chamber (intracameral) vector delivery results in transduction of the cornea and trabecular meshwork
In vivo fluorescence imaging of C57Bl/6j mice (n=3 per group) following injection of pseudotyped virus into the anterior chamber revealed observable signal centrally, indicating transduction of the cornea by both VSV-G **(A)** and VEEV-G **(B)** vectors. A ring of fluorescence could also be observed with both vector pseudotypes at the iridocorneal angle, the area where the base of the iris attaches to the peripheral cornea and sclera, indicating transduction of trabecular meshwork. Fluorescence appeared more uniform in distribution across the cornea following VSV-G injection. Fluorescence was stable in intensity and distribution from D7 onwards. AF = autofluorescence; NIR = near infrared; D= post natal day. Scale bars = ~1000µm

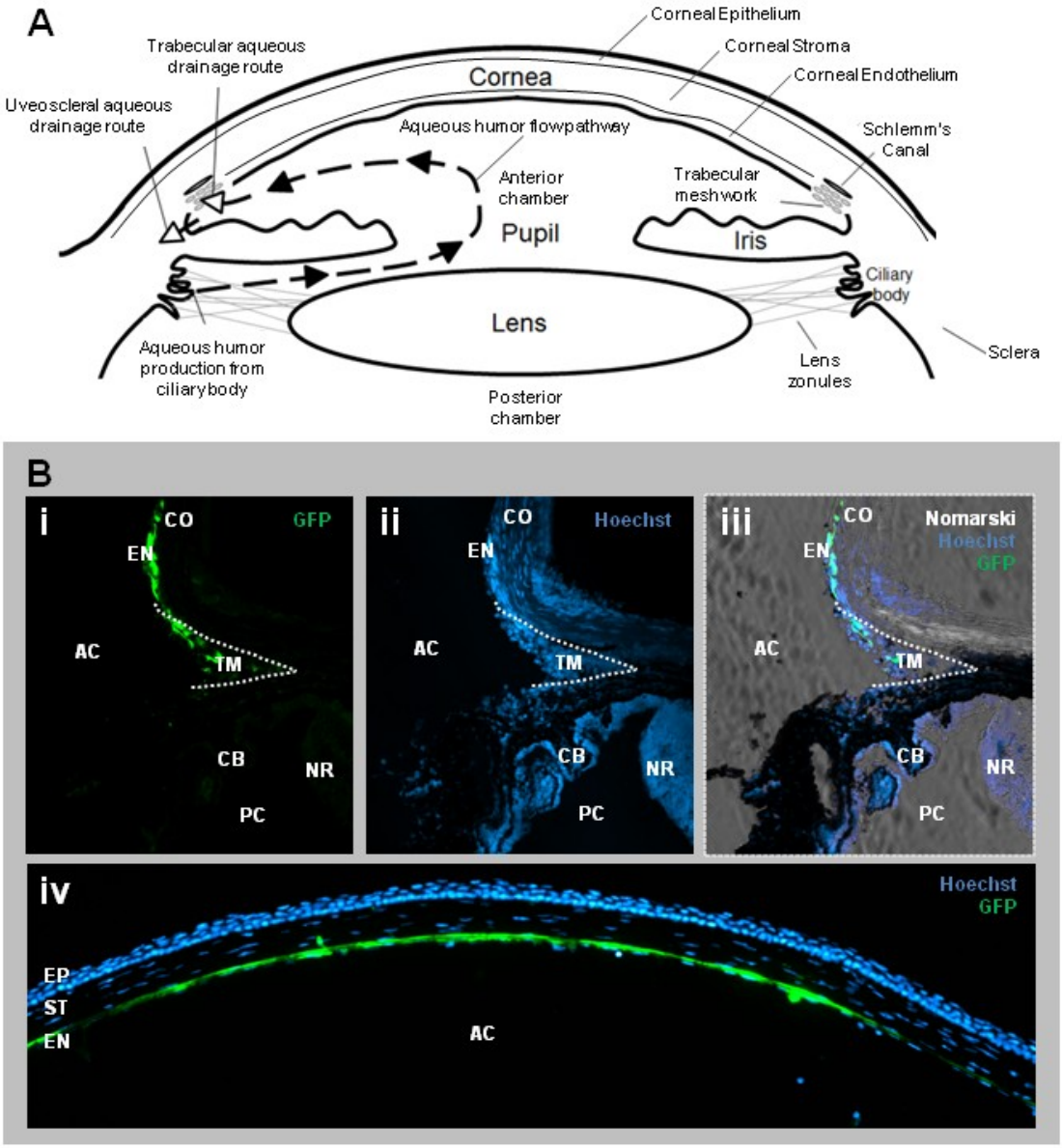

Figure 2.5 - Anterior chamber diagram and representative histology shows corneal and trabecular meshwork transduction
Diagram showing the major anatomical features of the anterior chamber **(A)**.The cornea is comprised of three distinct cell layers of which only the corneal endothelium (innermost layer) is accessible from the anterior chamber. Aqueous humor is produced by ciliary bodies located posterior to the iris and flows round the lens into the anterior chamber. Aqueous flow in the anterior chamber is governed by two forces: 1) convection, which drives the aqueous towards the corneal endothelium, and 2)outflow, which drives the aqueous towards the iridocorneal angle, where it drains primarily through the trabecular meshwork or is absorbed through the iris root. These flow dynamics govern the movement of any particles, such as virions, present in the aqueous. Representative histological sections following VSV-G pseudotyped vector administration into the anterior chamber **(B)** demonstrates EGFP expression in the corneal endothelium and in the trabecular meshwork (inside dotted lines), likely due to aqueous flow driving virions towards these cell types. CO = cornea; EN = corneal endothelium; AC = anterior chamber; PC = posterior chamber; TM = trabecular meshwork; CB = ciliary process; NR = neural retina; posterior chamber. D) Transduction of corneal endothelium following intracameral injection. EP = corneal epithelium; ST = corneal stroma; EN = corneal endothelium; AC = anterior chamber. Panel A was modified from Ito & Walter, 2013.

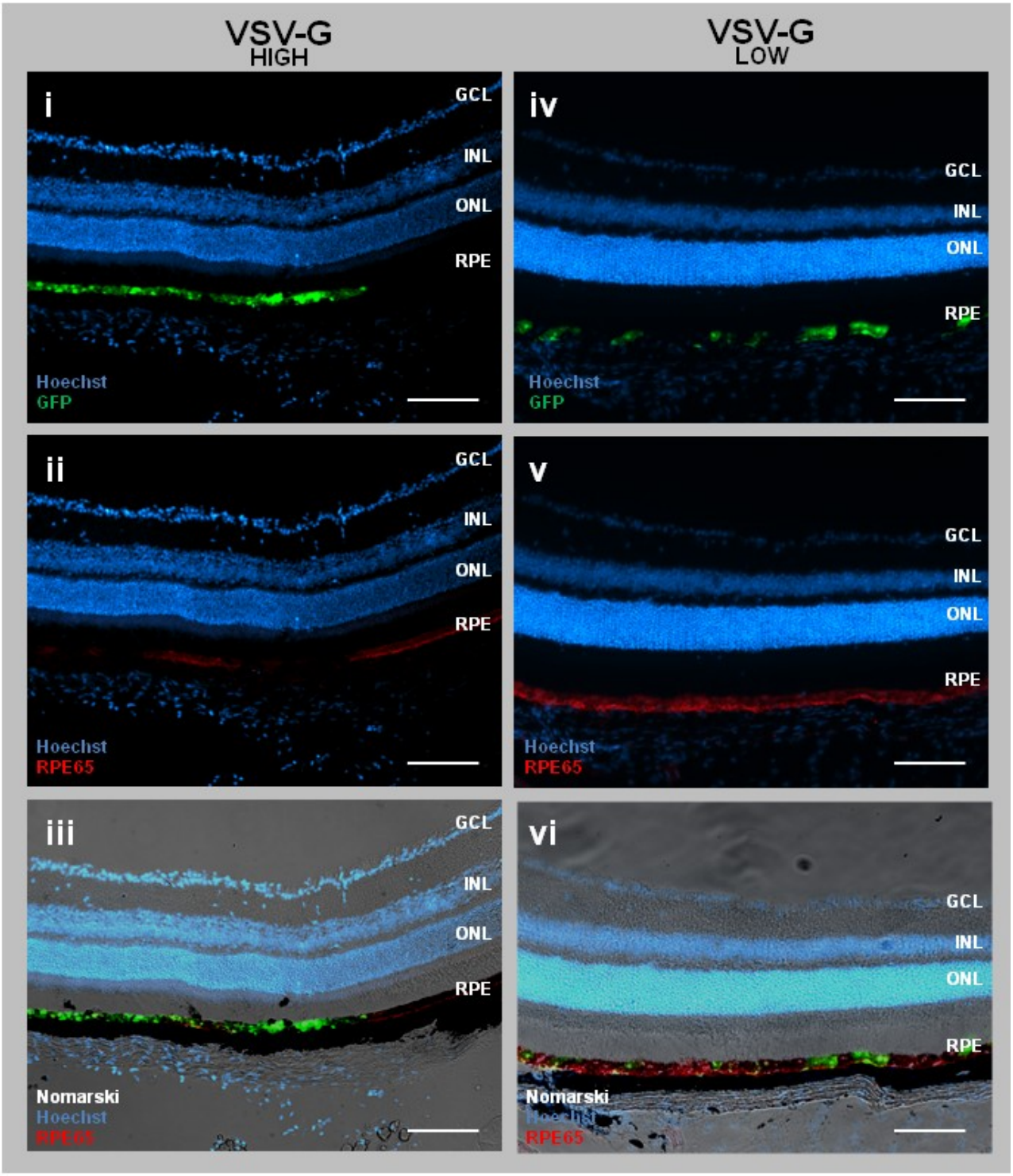

Figure 2.6 – Representative histology showing transduction of the RPE following subretinal VSV-G administration
EGFP expression can clearly be observed in the RPE following subretinal injection of VSV-G pseudotyped vector at both high (I-III) and low (IV-VI) doses. EGFP expression co-localizes with RPE65, a retinal pigment epithelium specific isomerase. No evidence of EGFP expression was observed in the outer nuclear layer (ONL), inner nuclear layer (INL) or ganglion cell layer (GCL). Scale bars = 150μm

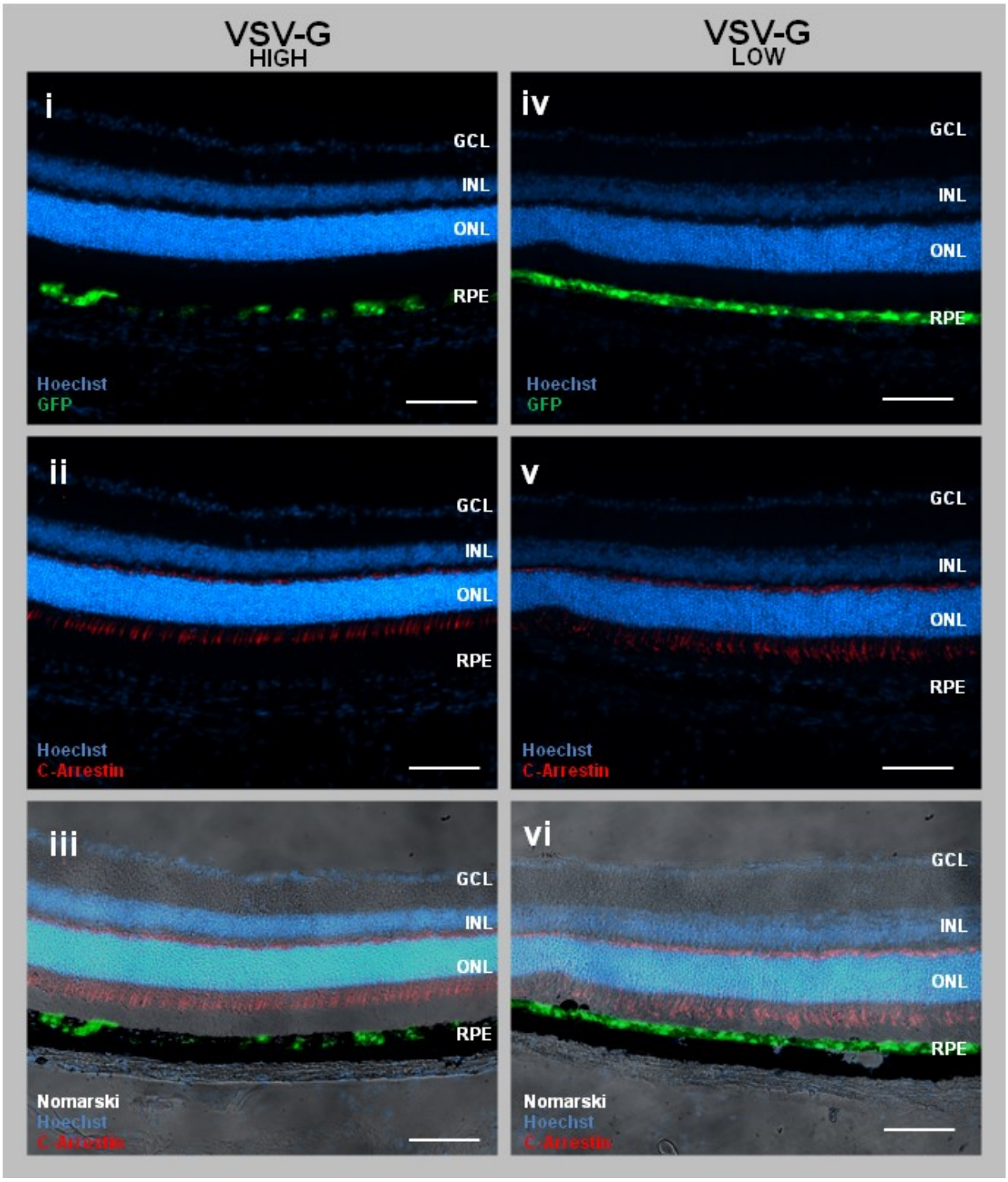

Figure 2.7 - Representative histology showing transduction of the RPE following subretinal VSV-G administration
EGFP expression can clearly be observed in the RPE following subretinal injection of VSV-G pseudotyped vector at both high (I-III) and low (IV-VI) doses. EGFP expression does not co-localize with cone arrestin (C-arrestin), a regulator of G protein-coupled receptors in the visual cycle. No evidence of EGFP expression was observed in the outer nuclear layer (ONL), inner nuclear layer (INL) or ganglion cell layer (GCL). Scale bars = 150μm

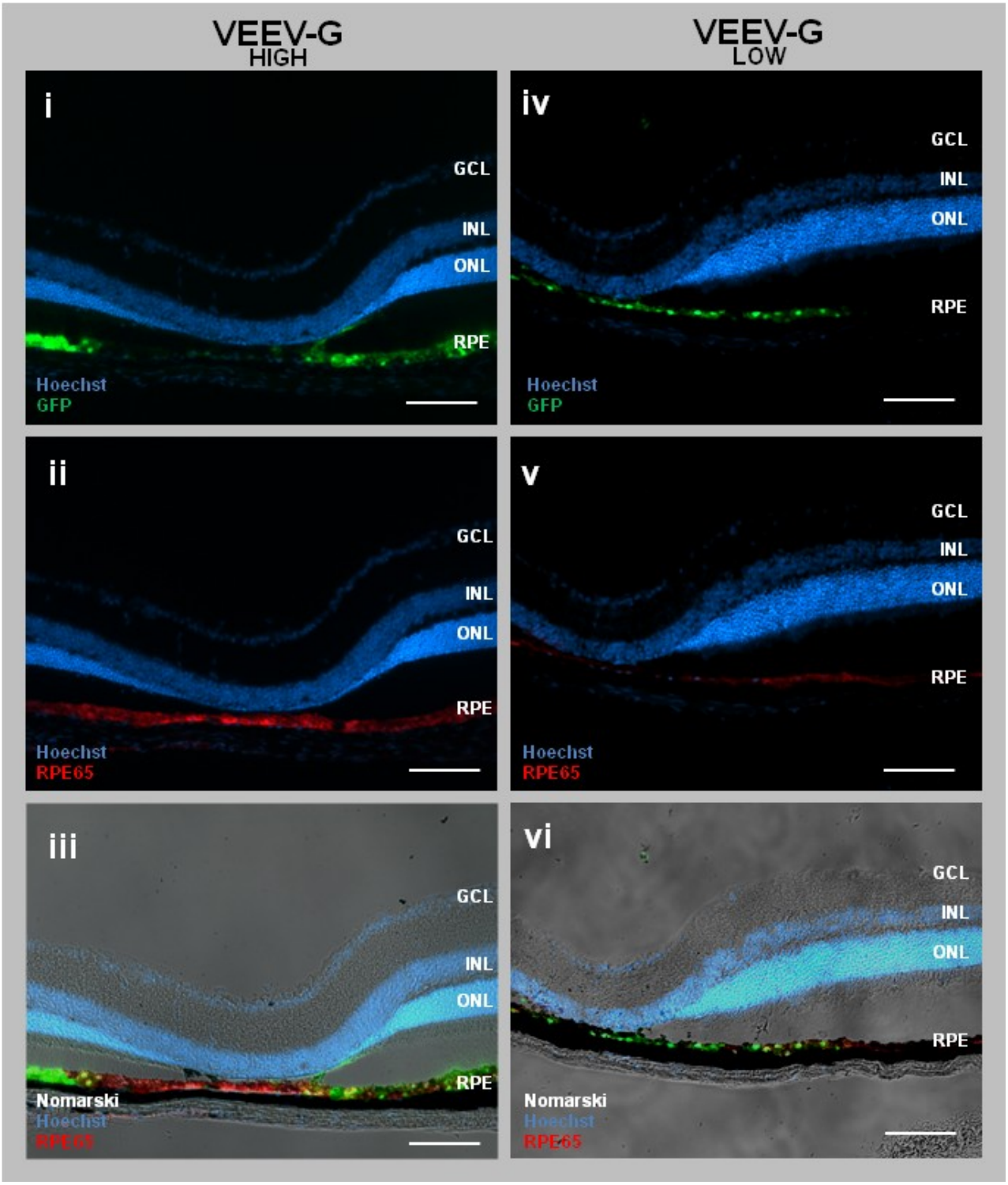

Figure 2.8 - Representative histology showing transduction of the RPE following subretinal VEEV-G administration and outer nuclear layer degeneration
EGFP expression can clearly be observed in the RPE following subretinal injection of VEEV-G pseudotyped vector at both high (I-III) and low (IV-VI) doses. EGFP expression co-localizes with RPE65, a retinal pigment epithelium specific isomerase. No evidence of EGFP expression was observed in the outer nuclear layer (ONL), inner nuclear layer (INL) or ganglion cell layer (GCL). The ONL shows marked thinning in areas overlying transduced RPE, indicating loss of photoreceptors, potentially due to toxicity. Scale bars = 150μm.

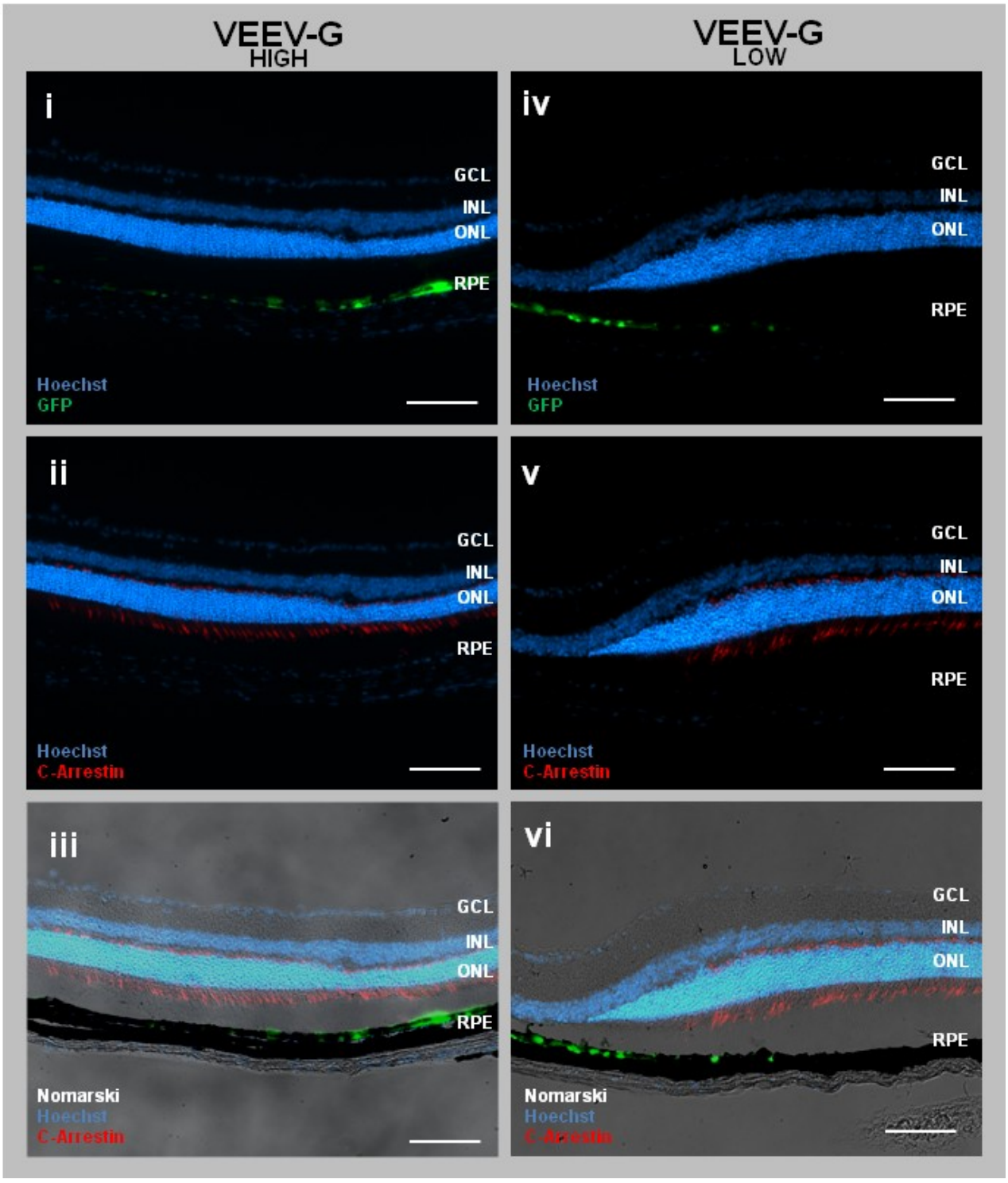

Figure 2.9 - Representative histology showing transduction of the RPE following subretinal VEEV-G administration
EGFP expression can clearly be observed in the RPE following subretinal injection of VEV-G pseudotyped vector at both high (I-III) and low (IV-VI) doses. EGFP expression does not co-localize with cone arrestin (C-arrestin), a regulator of G protein-coupled receptors in the visual cycle. No evidence of EGFP expression was observed in the outer nuclear layer (ONL), inner nuclear layer (INL) or ganglion cell layer (GCL). The ONL shows marked thinning and an absence of C-arrestin staining in areas overlying transduced RPE, indicating loss of photoreceptors, potentially due to toxicity. Scale bars = 150μm.

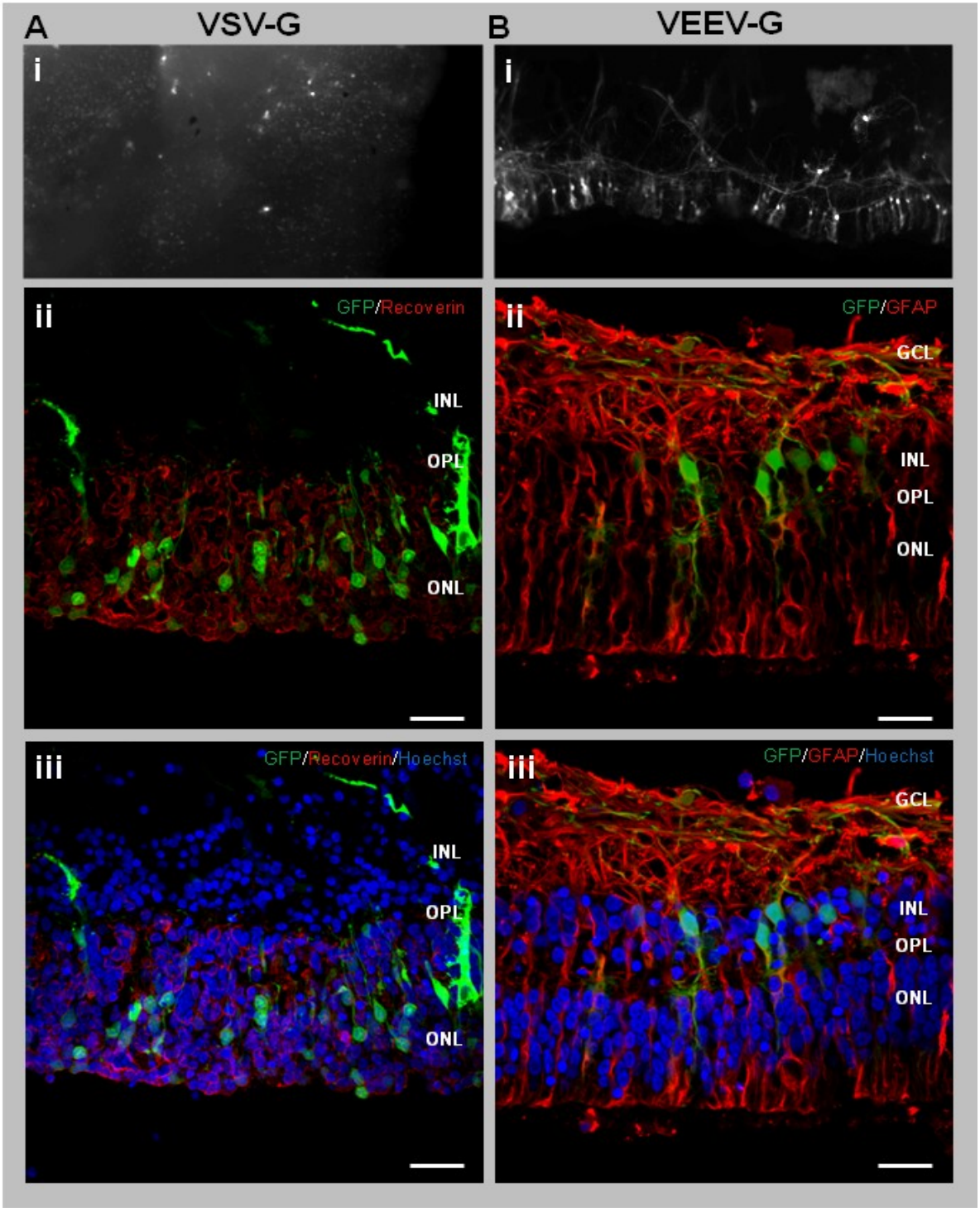

Figure 2.10 – Transduction of human retinal tissue in explants culture shows limited photoreceptor transduction
Transduction of human retinal tissue biopsied from patients undergoing retinectomy as part of detachment surgery using VSV-G (A) or VEEV-G (B) vector. Image taken of the retinal explants whilst in ex vivo culture, showing photoreceptor transduction following VSV-G transduction – photoreceptors appears as punctuate white dots observable from the outer retinal aspect only (A i) – and ganglion cell/Müller cell transduction following VEEV-G transduction (B i). Following VSV-G transduction histology confirms presence of EGFP expressing cells in the ONL which co-localize with recoverin (A ii-iii). In contrast, following VEEV-G transduction widespread co-localisation of EGFP was observed with GFAP (B ii-iii), indicating transduction of Müller cells or astrocytes. ONL = outer nuclear layer; INL = inner nuclear layer; GCL = ganglion cell layer. Scale bars = 50μm.

Chapter 3

Assessment of cone survival in response to CNTF, GDNF, and VEGF165b in a novel ex vivo model of end stage retinitis pigmentosa

INTRODUCTION

In retinitis pigmentosa (RP) the loss of rod photoreceptors is invariably followed by the loss of cones, even when the degeneration is caused by genes that are expressed only in rods. Cone degeneration in such instances is believed to occur due to the loss of sustaining proteins or other factors that are released by rods (Leveillard and Sahel, 2010; Punzo et al., 2009). Identifying a means of sustaining cones in the absence of rods is a critically important strategy in developing treatments for RP because humans are highly dependent on cone mediated visual tasks for activities of daily living. In many cases of RP, patients present to the physician after the majority of their rod photoreceptors have degenerated, which would provide significant challenges for rod gene replacement. Consequently, potential treatment strategies must necessarily focus either on photoreceptor replacement (MacLaren et al., 2006b) or on attenuating the loss of cones at a stage when a reasonable number of cones remain.

Recently, the administration of neuroprotective factors, or 'growth factors', has been described for the preservation of retinal ganglion cells in experimental models of glaucoma (Baltmr et al., 2010) and in human clinical trials for the treatment of geographic atrophy in wet age related macular degeneration (AMD) (Zhang et al., 2011). Consequently, growth factors may provide a viable treatment for the preservation of cone photoreceptors secondary to rod loss in RP (Kassen et al., 2009).

The neuroprotective effects of growth factors are typically determined *in vivo*, where their solubility and low molecular weight allow for intravitreal administration and subsequent diffusion through the vitreous into the neural retina. Testing requires either direct injection of the protein, or expression of the protein from a vector or slow release device. While the former approach is the simpler, the short half-life of many neuroprotective compounds necessitates repetitive protein injections, with potential associated complications, including endophthalmitis. The later approach allows for administration of a single dose, but requires the production of either a viral vector or an encapsulated slow release device, both of which are time consuming and often too expensive to be applied for a high-

throughput screening approach. While rod neuroprotection has previously been examined in vitro using dissociated photoreceptor cultures (Streichert et al., 1999), disruption of the retinal morphology makes such methods unsuitable for studying the neuroprotection of cones secondary to advanced rod degeneration.

Secondary cone loss as seen in RP patients has also been observed in mouse strains with rod degeneration, such as the rhodopsin knockout mouse ($Rho^{-/-}$) (Humphries et al., 1997; Jaissle et al., 2001). Cell loss in mice with retinal degenerations can be examined through use of fluorescent reporter, where intrinsic fluorescence acts as a surrogate marker of cell viability (Beck et al., 2010; Megason et al., 2006). Herein, we utilized the OPN1LW-EGFP reporter mouse, which has fluorescent cone photoreceptors due to expression of enhanced green fluorescent protein (EGFP) under the control of the human OPN1 long wave promoter (OPN1LW), crossed to a rhodopsin knockout mouse, allowing the study of cone photoreceptor survival against a background of progressive rod degeneration.

In the present study we adapted a previously described organotypic retinal culture system (Johnson and Martin, 2008) to maintain retinal explants from rhodopsin knockout OPN1LW-EGFP animals. In this novel *ex vivo* model of RP, cone neuroprotection is assessed longitudinally in through repetitive imaging of retinal explants, with survival of intrinsically fluorescent cones quantified. This model allows dose controlled administration of neuroprotective factors and a robust assessment as to their effect on cone survival without recourse to *in vivo* administration. Herein, we validate our model by evaluating the neuroprotective effects on cone survival of two growth factors, CNTF and glial cell derived neurotrophic factor (GDNF). Additionally, we explore the neuroprotective properties of the vascular endothelial growth factor 165b-isoform ($VEGF_{165b}$). This VEGF isoform has proved to be effective in the treatment of animal models of choroidal neovascularisation (Hua et al., 2010) and may prevent retinal epithelial and endothelial cell death (Magnussen et al., 2010).

CHAPTER SPECIFC MATERIALS AND METHODS

Mice

Mice which express EGFP in cone photoreceptors and have a primary rod specific degeneration ($Rho^{-/-TgOPN1LW\text{-}EGFP+/-}$) were created through crossing of $B6^{TgOPN1LW\text{-}EGFP+/+}$ mice (homozygous for the OPN1LW-EGFP transgene insertion) with $Rho^{-/-}$ (homozygous for targeted rhodopsin knockout), followed by backcrossing of F1 progeny ($Rho^{+/-TgOPN1LW\text{-}EGFP+/-}$) to the parental $Rho^{-/-}$ line. Mice were genotyped at weaning by PCR as described in the general materials and methods section.

Retinal explant culture

Eyes were enucleated from $B6^{TgOPN1LW\text{-}EGFP+/-}$ and $Rho^{-/-TgOPN1LW\text{-}EGFP+/-}$ mice at post-natal day 70 and transferred to room temperature 0.01% phosphate buffered saline (PBS) where the anterior segment and lens were removed. After isolation from the retinal pigment epithelium (RPE) the whole retina was transferred to complete culture media (Johnson and Martin, 2008) consisting of NeurobasalA, L-glutamine (0.08mM), penicillin (100 U/ml), streptomycin (100 U/ml), B27 supplement (2%) and N2 supplement (1%, all Invitrogen Ltd, Paisley, UK). Using an operating microscope and vannas scissors, retinas were divided into several 1-2 mm^2 pieces without bias toward orientation. Using a cut-off 5ml pipette, to eliminate crush injury associated with forcep use, retina pieces were transferred photoreceptor side down into individual 24-wells containing an organotypic culture insert (353095, BD Falcon) and 700µl complete media. Explants from $Rho^{-/-TgOPN1LW\text{-}EGFP+/-}$ mice were randomly assigned to treatment groups (n=5 per group) and cultured at 34°C in a 5% CO_2 environment. Treatment groups received high (200ng/ml), medium (100ng/ml) or low (50ng/ml) doses of CNTF, GDNF (Peprotech, Rocky Hill, NJ) or $VEGF_{165b}$ (R&D systems, Abingdon, UK) resuspended in sterile filtered PBS. Negative controls received an equivalent volume (~7.5µl) of PBS in place of any growth factor. Explants from $B6^{TgOPN1LW\text{-}EGFP+/-}$ mice were used as positive controls showing cone survival in the presence of rods. Treatments were administered daily during a complete media change.

Imaging and quantification

Explants were imaged on days 1, 3, 5, 7, 9 and 12 on an inverted epi-fluorescence microscope (Leica DMIL). Images were acquired after removal of media to ensure that explants rested flat on the membrane and that background autofluorescence due to the presence of media was minimal; fresh media was replaced following imaging. Tissue culture inserts were chosen for their small pore size (0.4μm), transparency and lack of autofluorescence. Multiple overlapping images (x10) covering the whole of each explant were taken; images were subsequently stitched together and the total number of cone photoreceptors per explant manually quantified using imageJ software (Abramoff et al., 2004). Due to the non-standard number of cones per explant, survival is expressed as a percentage of cone number relative to day one, rather than absolute cone number.

Statistics

Anderson-Darling test for normality on full data sets for each experiment revealed that the data was sampled from normally distributed population in each case: Media comparison: A^2=0.218, p=0.8383; CNTF, A^2= 0.539, p=0.166; GDNF, A^2= 0.440, r=0.291; $VEGF_{165b}$, A^2=0.463, r=0.255. Plotting of residuals versus fitted means for each experimental group demonstrated that variance was equal within each test (plots not shown). Repeated measures one-way ANOVA was used to assess longitudinal survival of EGFP-expressing explants in optimal media with time (repeated measure) as the only factor. Repeated measures two-way ANOVAs were used in all other comparisons with treatment (independent variable) and time (repeated measure) as factors. Cone number was the dependent variable in all comparisons. Bonferroni post tests were applied in all instances with a significance (p) level of 0.05.

RESULTS

Retinal explants can be maintained long term in organotypic culture and individual cone photoreceptors visualised

An *ex vivo* organotypic culture system was developed in order to explore the neuroprotection of cone photoreceptors following administration of soluble growth factors. As a model of RP, retinal explants were harvested from $Rho^{-/-TgOPN1LW\text{-}EGFP+/-}$ mice, which express EGFP in cone photoreceptors and have a primary rod degeneration leading to progressive thinning of the outer nuclear layer and the secondary loss of cones (Fig. 3.1 A-B).However, evaluation of cone neuroprotection in such organotypic culture requires first that retinal explants can be maintained over time so that treatment effects might be observed, and second that the ability to identify individual fluorescent cone photoreceptors is maintained throughout, thus enabling quantification at repeated time points.

We initially used explants from $B6^{TgOPN1LW\text{-}EGFP+/-}$ mice to confirm previous reports that retinal explants could be maintained short term (<7 days) in serum free organotypic culture (Johnson and Martin, 2008). A comparison of media constituents revealed that both B27 and N2 supplements were necessary for short term survival of explants, with significantly reduced cone numbers observed by day six in the absence of one or both supplements ($p<0.001$, repeated measures two-way ANOVA with bonferroni post-test, n=5 explants/group) (Fig. 3.2A). Using optimized media in our organotypic culture system it was possible to maintain explants from $B6^{TgOPN1LW\text{-}EGFP+/-}$ mice for over four weeks (Fig. 3.2B). We observed a gradual decline in cone photoreceptor numbers over the time course, with significant reduction by day six ($p=<0.05$). Overall the reduction in photoreceptor numbers was highly significant when compared to day one($p<0.001$, repeated measures one-way ANOVA with bonferroni post-test, n=5 explants). However, despite reduction of ~50% in cone numbers by day 24, the observed explant survival is considerably longer than many other reports in the literature.

Significantly, it was possible to identify individual cone photoreceptors and to follow their survival longitudinally in our culture system. The organotypic culture system provides good oxygenation of layered tissues and the culture inserts used here permitted good visualisation of intrinsically fluorescent cells through the membrane (Fig 3.1 C-E). We were able to identify distinct groups of cones over 12 days in explants from $B6^{TgOPN1LW\text{-}EGFP+/-}$ mice (Fig. 3.2 C). The cells visualized were considered unlikely to be

macrophages due to fluorescence being observed only when stimulated with 488nm light (peak absorption of EGFP), where macrophages typically autofluoresce strongly at a broad range of wavelengths. Cells also lacked motility, where macrophages would be expected to migrate over the imaging time course. Additionally, macrophages do not typically reside permanently in the neural retina in large numbers, instead infiltrating into the neural retina from circulating populations to clear cellular debris when required; in organotypic culture this source of macrophages is absent. Consequently, we consider that the organotypic culture of retinas with intrinsic fluorescence allows for the long term analysis of photoreceptor survival, and provides an ideal *ex vivo* system to evaluate the neuroprotective effects of various soluble compounds.

The distribution of cone photoreceptors in organotypically cultured tissue was not observed to be a regular mosaic pattern (see general introduction) for a number of reasons. Firstly, due to the expression of EGFP from the human OPN1LW promoter, fluorescence is not present in cone photoreceptors that express only *Sws*-opsin, which account for approximately 10% of all cones. Secondly, manipulation of the retina during the process of excision and culturing inevitably leads to distortion of the retina to some extent, leading to alterations in cone spacing. Thirdly, explanted tissue shrinks over the imaging time course; this shrinkage is not necessarily uniform in all directions, further distorting the position of the cone photoreceptors relative to one another. Lastly, the cone photoreceptor mosaic pattern is disrupted by the loss of cone photoreceptors due to the ongoing process of degeneration.

CNTF sustains cone photoreceptors in a dose dependent manner in organotypic culture

Having confirmed that retinal explants can be maintained long term in organotypic culture we examined the neuroprotective effect of CNTF, which has been described previously to protect photoreceptors (Kassen et al., 2009) and ganglion cells (MacLaren et al., 2006a; Pease et al., 2009) *in vivo*.

Explants taken from $B6^{TgOPN1LW\text{-}EGFP+/-}$ animals served as positive controls and showed the survival of cones on a wild type background without rod photoreceptor degeneration. Cone photoreceptor

survival was significantly lower in PBS treated Rho$^{-/-TgOPN1LW-EGFP+/-}$ explants at all time points compared to positive controls ($p<0.001$, repeated measures two-way ANOVA with bonferroni post-test, n=5 explants/group) (Fig. 3.3 B) confirming that the presence of rod photoreceptors is of great importance for the survival of cone photoreceptors. Daily administration of 200ng/ml CNTF to Rho$^{-/-TgOPN1LW-EGFP+/-}$ explants led to significantly higher levels of cone survival from day five onwards compared to the PBS treated group ($p<0.001$, repeated measures two-way ANOVA with bonferroni post-test, n=5 explants/group), though cone survival was still significantly reduced compared to B6$^{TgOPN1LW-EGFP+/-}$ explants at these time points ($p<0.001$, repeated measures two-way ANOVA with bonferroni post-test, n=5 explants/group). In addition to photoreceptor preservation, a reduction in autofluorescence was also observed compared to PBS treated explants (Fig. 3.3 A). In our organiotypic culture system an increase in autofluorescence usually preceded tissue death and rapid cone loss, and served as an indicator of the tissues' general health. Administration of 100ng/ml also led to increased survival of cone photoreceptors in comparison to PBS treated group, with significant preservation apparent by day five ($p<0.01$). Preservation was maintained and was highly significant by day 12 ($p<0.001$) compared to negative controls (repeated measures two-way ANOVA with bonferroni post-test, n=5 explants/group). 50ng/ml CNTF did not have a significant protective effect over PBS treatment (Fig. 3.33B).These results indicate first that CNTF has a dose dependent, neuroprotective effect on cones, supporting the potential use of CNTF for the treatment of secondary cone loss in RP, and second that the effects of neuroprotective compounds can be reliably and quantitatively assessed using our *ex vivo* model.

GDNF is protective to cone photoreceptors only at high dose

Following the successful attenuation of cone degeneration by CNTF, alternative neuroprotective factors were evaluated, in particular GDNF, which has been described previously as having greater neuroprotective effects on photoreceptors compared to CNTF (Buch et al., 2006). Recombinant CNTF and GDNF proteins have similar molecular masses (22.9 kDa and 23.7 KDa, respectively) and

consequently the doses administered here equate to comparable molar concentrations of protein. This allows us to draw direct comparisons as to the neuroprotective effects of these two growth factors.

Administration of 200ng/ml GDNF resulted in observable neuroprotective effects only at late time points (day 9, $p<0.01$; day 12, $p<0.001$) compared to the PBS treated group (repeated measures two-way ANOVA with bonferroni post-test, n=5 explants/group) (Fig. 3.4 A-B). Treatment with 100ng/ml GDNF showed a small but significant preservation of cone photoreceptors compared to PBS treatment at day 12 ($p<0.05$, repeated measures two-way ANOVA with bonferroni post-test, n=5 explants/group), while 50ng/ml appeared to have no impact on cone survival. As with CNTF treatment, all groups had significantly reduced cone photoreceptor numbers compared to $B6^{TgOPN1LW\text{-}EGFP+/-}$ positive controls ($p<0.001$, repeated measures two-way ANOVA with bonferroni post-test, n=5 explants/group) (Fig. 3.4 B). However, autofluorescence was noticeably reduced in the high dose GDNF treatment group compared to PBS treated controls, indicating that GDNF administration does have a positive impact on explant health (Fig. 3.4 A).These results indicate that GDNF has a limited, dose dependent neuroprotective effect, but even when administered at high dose (200ng/ml), GDNF is not as effective at attenuating secondary cone degeneration as CNTF.

$VEGF_{165b}$ isoform does not exhibit a neuroprotective effect *ex vivo*

$VEGF_{165b}$, a C-terminal splice variant of VEGF which has a molecular mass of 19.2 kDa, has previously been demonstrated to reduce neovascularisation in animal models of oxygen induced retinopathy (Konopatskaya et al., 2006) and to have protective effects on retinal epithelial and endothelial cells in culture (Magnussen et al., 2010; Rennel et al., 2008). Our results, however, indicate that $VEGF_{165b}$ does not provide neuroprotection to cone photoreceptors, as there was no attenuation of cone loss at any dose or time point compared to PBS treatment ($p>0.05$, repeated measures two-way ANOVA with bonferroni post-test, n=5 explants/group) (Fig. 3.5 A-B). Additionally, the level of autofluorescence was not

noticeably reduced by the administration of $VEGF_{165b}$ (Fig. 3.5 A). These results do not support the use of $VEGF_{165b}$ as a neuroprotective factor for the treatment of rod-cone dystrophy.

DISCUSSION

Herein, we evaluated the neuroprotective effects of three growth factors on the attenuation of cone loss secondary to rod degeneration. A novel organotypic culture model was developed, wherein cone survival was assessed *ex vivo* through the repetitive imaging of retinal explants with intrinsically fluorescent cone photoreceptors. Our primary finding is that CNTF has potent neuroprotective properties and is a potential compound to be used in the prevention of central vision loss in RP.

The model described is a robust tool for the high-throughput screening of neuroprotective compounds, and provides an alternative to costly *in vivo* assays, where repetitive ocular administration of protein has inherent welfare concerns. The model described potentially has wider applications than the study of photoreceptor survival in RP, and could be adapted to the study of other cell types for which fluorescent reporter lines exist. For example, the study of ganglion cell survival in response to oxidative stress may be conducted using retinal explants from the OPN4-GFP transgenic mouse (Schmidt et al., 2008), in which GFP expression is restricted to retinal ganglion cells under the control of a cell specific promoter. Our results show that CNTF administration leads to a robust dose dependent protection of cone photoreceptors. To a lesser extent GDNF also demonstrated neuroprotective properties, though these were only observed at high dose when administered in our *ex vivo* model. Interestingly, this finding is contradictory to that of a previous study (Buch et al., 2006), which described GDNF as having the greater neuroprotective effect. However, unlike *in vivo* expression of protein, where levels of protein expression can be extremely variable, dosing in the model system we describe is precisely controlled. Consequently, the effects observed here may more faithfully reflect the absolute neuroprotective properties of these two compounds.

Whilst there are many benefits to examining photoreceptor survival in an isolated system, it conversely presents several issues, one in particular being the separation of the retina from the circulating immune system. Since many experiments have shown that subretinal macrophages and other immune cells may have a critical role in regulating apoptosis, the effects of any given neuroprotective compound may be exaggerated in ex vivo culture where those cells are absent. Another drawback to this system is that it is difficult to replicate the increased oxygen levels observed to be present in the subretinal space during end-stage retinal degeneration following photoreceptor loss. Oxidative stress resulting from free radical production is known to be toxic to neurons, and there is a body of evidence that suggests that their accumulation may have a role the progression of inherited retinal diseases. Indeed, antioxidants medications have been marketed as a potential treatment of retinitis pigmentosa despite there being no firm evidence as to their benefit. A final drawback in this system is the fact that there is no light, where light exposure has been demonstrated to increase the rate of retinal degeneration in some disease. Whilst illumination could be applied to the retina in culture, it is unclear whether this would alter the course of photoreceptor degeneration, where the photoreceptors are unlikely to be fully metabolically active in the absence of retinoid cycling and an underlying RPE monolayer.

However, despite a number of short comings, the ability to accurately quantify the effects of a growth factor on cone photoreceptor survival ex vivo potentially allows for the high-throughput screening of neuroprotective compounds whilst reducing animal usage. The results obtained using this ex vivo model are consistent with the previous in vivo observations using CNTF, which has been demonstrated to have strong neuroprotective properties in various models of retinal degeneration, indicating that effects observed in this model are reliable.

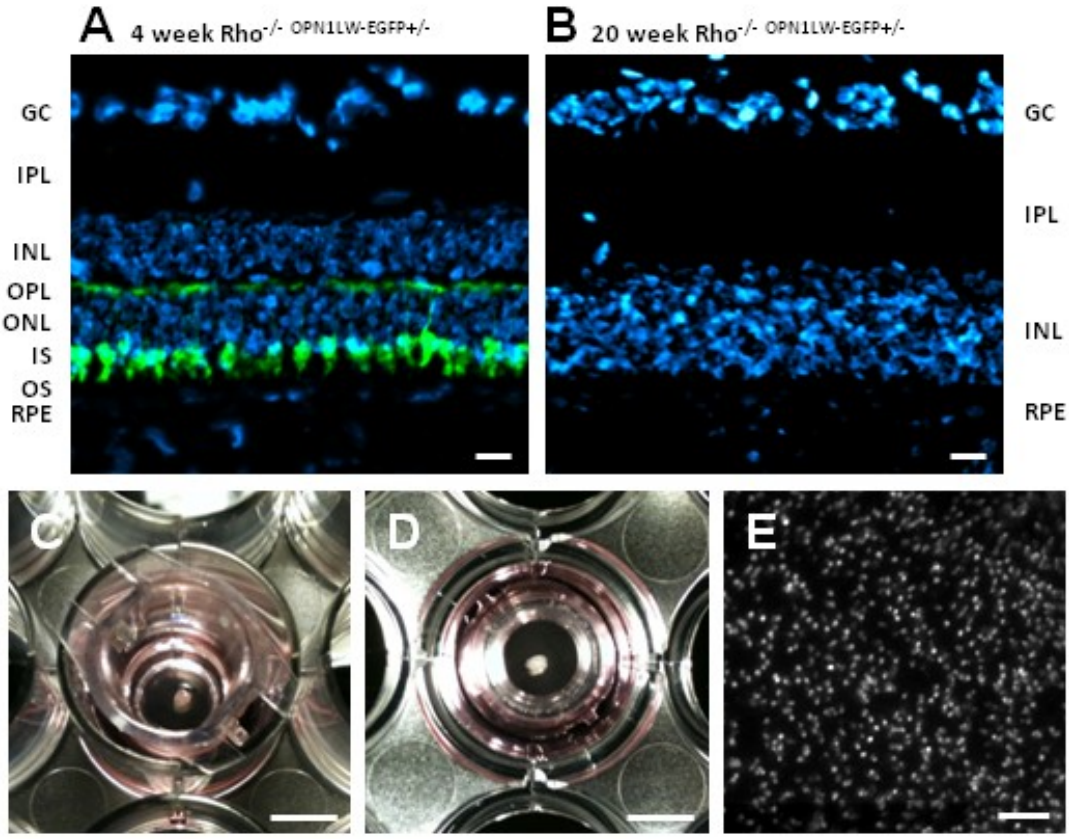

Figure 3.1 – Retinal explants from mice with intrinsically fluorescent cone photoreceptors can be organotypically cultured
Histological section showing intrinsically fluorescent cone photoreceptors in a young (4 week old) Rho-/- TgOPN1LW-EGFP+/- mouse **(A)**.In this model rod photoreceptors degenerate due to the absence of rhodopsin and are largely absent by 12 weeks. Cone photoreceptors degenerate secondary to rod loss mimicking the clinical situation observed in rod-cone dystrophies in retinitis pigmentosa (RP). By week 20 rod and cone photoreceptors are absent, and the outer nuclear layer is totally degenerate **(B)**. Retinal explants taken from Rho-/- TgOPN1LW-EGFP+/- mice can be cultured organotyically in porous tissue culture inserts which allow oxygenation of the retinal tissue from both aspects **(C)**. 6-8 explants can be harvested per eye. The tissue culture membrane is transparent allowing the retinal explants to be viewed in culture from below using an inverted microscope (D). In culture individual intrinsically fluorescent cone photoreceptors can be resolved as punctuate white dots. GC = ganglion cell layer; IPL = inner plexiform layer; INL = inner nuclear layer; OPL = outer plexiform layer; ONL = outer nuclear layer; IS = inner segments; OS = outer segments; RPE = retinal pigment epithelium. A-B scale bars = 50µm; C-D scale bars = 5mm; E scale bar = 100µm.

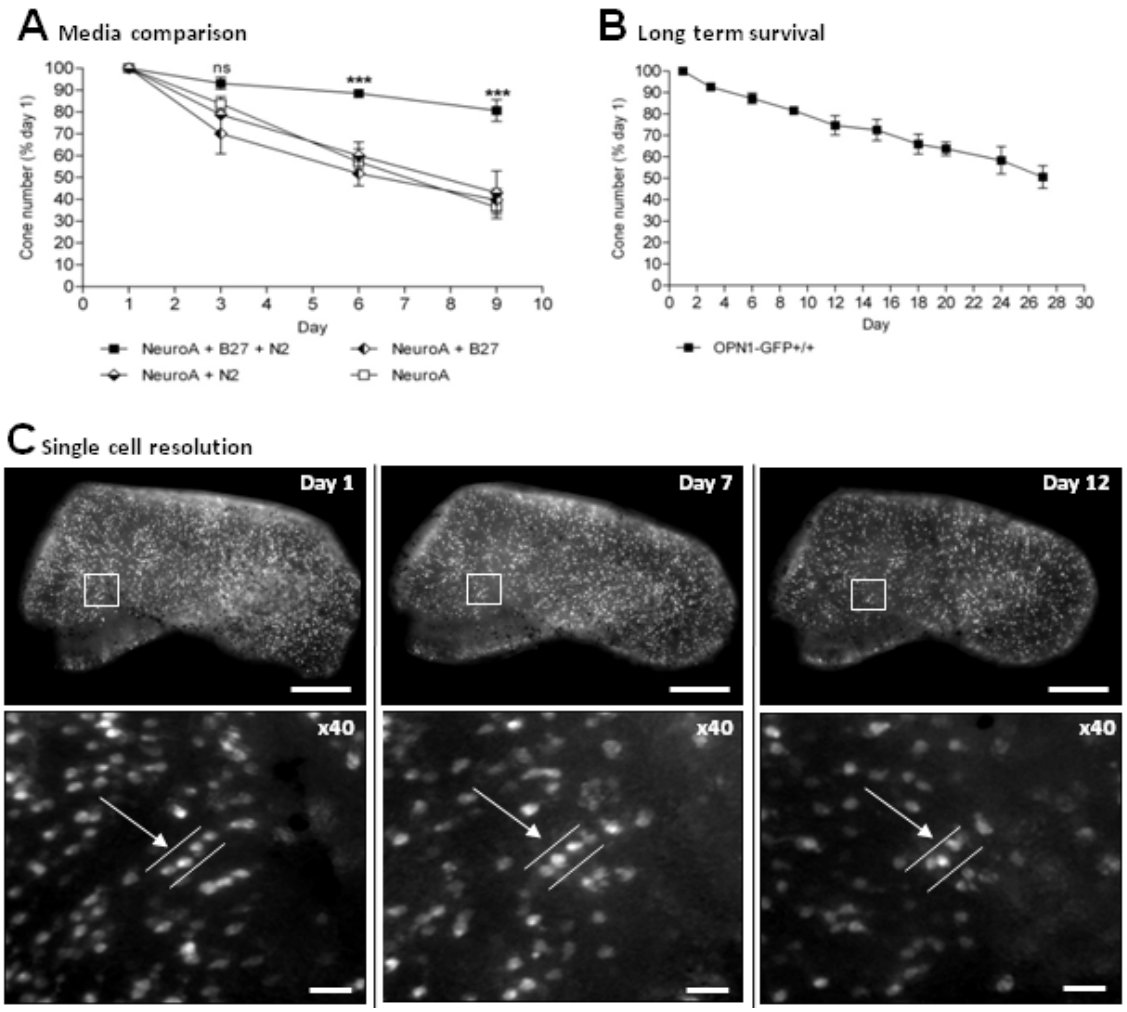

Figure 3.2 – Long term survival of explants in organotypic culture is dependent on media composition
Comparison of media requirements reveals that constituents N2 and B27 (serum free hormonal supplements) are both required for long term survival of organotypically cultured explants (Anderson-Darling test for normality, $A^2 = 0.218$; p=0.83. *** = p<0.001, n = 5 explants per group, two-way repeated measure ANOVA with media composition and age as factors) **(A)**. In complete media (NeuroA + B27 + N2) explants harvested from non-degenerate B6TgOPN1LW-EGFP+/- mice can be cultured for up to 27 days **(B)**. During culture individual cone photoreceptors (white dots) can be identified repeatedly, allowing for accurate repeated quantification of cone photoreceptor survival. All error bars = s.d. Scale bars C upper panels = 200µm, lower panels = 50µm.

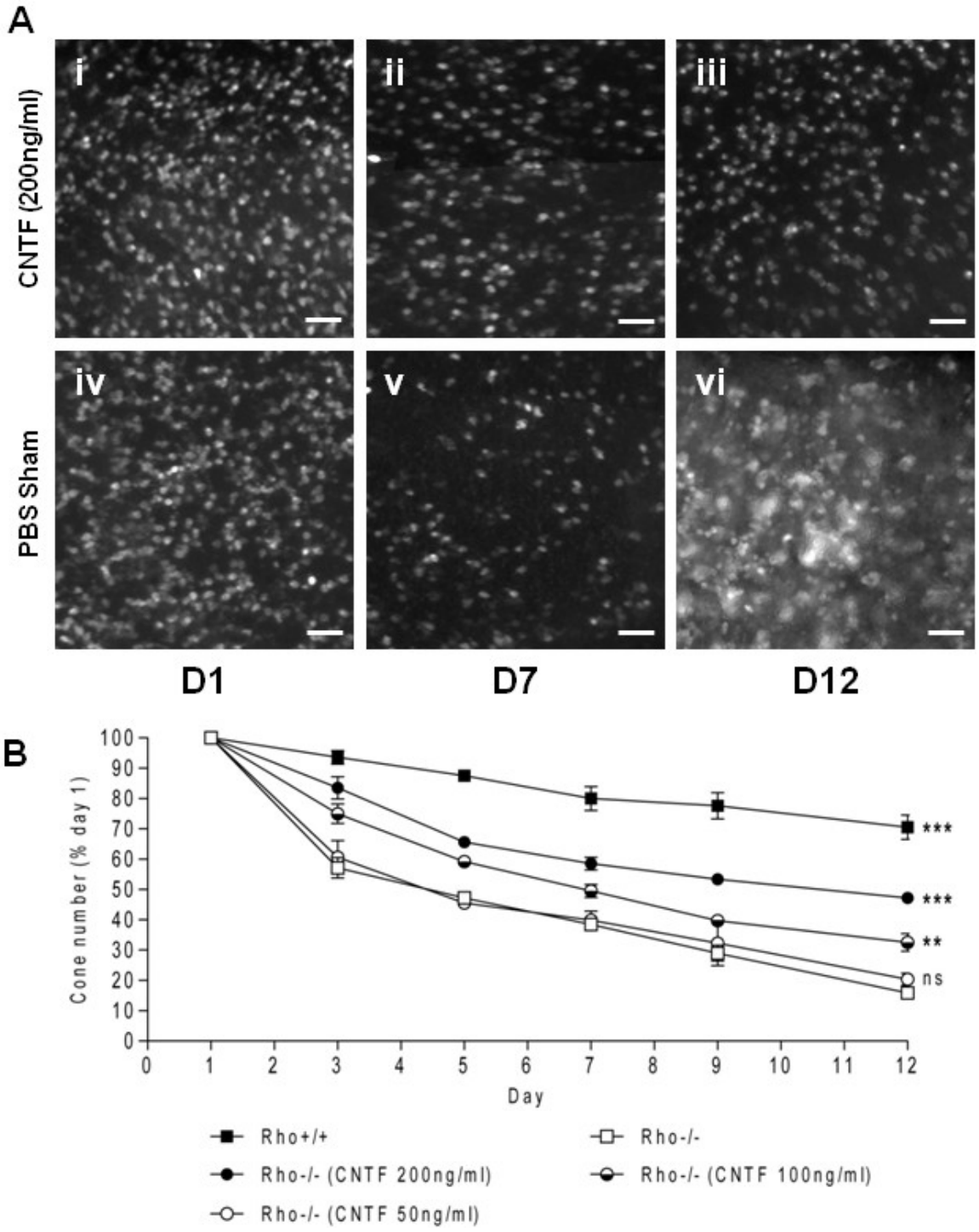

Figure 3.3 – CNTF confers robust protection against secondary cone loss in Rho-/- TgOPN1LW-EGFP+/- explants
CNTF administered to retinal explants (n=6 explants per group) in complete media significantly protects cone photoreceptors from degeneration following advanced rod loss, with individual cone photoreceptors clearly visible 12 days (D) post harvesting **(A I-III)**. In explants treated with an equal volume of PBS cone photoreceptors were largely absent by D12 and tissue had become autofluorescent, an indicator of tissue death in vitro **(A IV-VI)**. Neuroprotection was dose dependent with higher CNTF concentrations resulting in greater neuroprotection **(B)**. Anderson-Darling test for normality, $A^2 = 0.539$; $p=0.166$. ** = $p<0.01$; *** = $p<0.001$, n = 6 explants per group, two-way repeated measure ANOVA with CNTF dose and age as factors. ns = not significant. All scale bars = 75µm

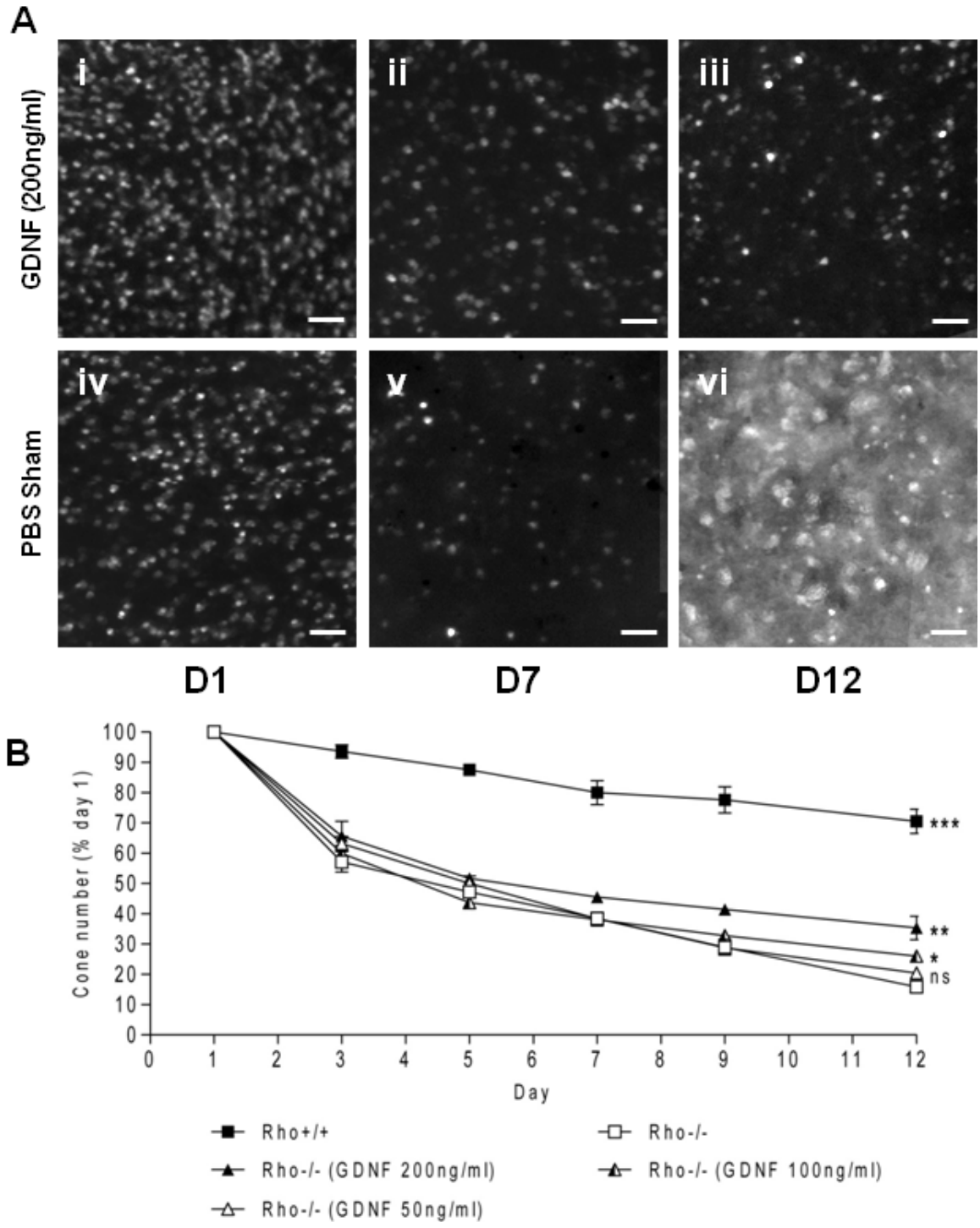

Figure 3.4 - GDNF confers limited protection against secondary cone loss in Rho-/- TgOPN1LW-EGFP+/- explants
GDNF administered to retinal explants (n=6 explants per group) in complete media protects cone photoreceptors from degeneration following advanced rod loss, but to a lesser extent than observed with CNTF **(A I-III)**. Individual cone photoreceptors clearly visible 12 days (D) post harvesting **(A III)**. In explants treated with an equal volume of PBS cone photoreceptors were largely absent by D12 and tissue had become autofluorescent, an indicator of tissue death in vitro **(A IV-VI)**. Neuroprotection was dose dependent with higher GDNF concentrations resulting in greater neuroprotection **(B)**. Anderson-Darling test for normality, $A^2 = 0.440$; p=0.291. * = p<0.05; ** = p<0.01; *** = p<0.001, n = 6 explants per group, two-way repeated measure ANOVA with CNTF dose and age as factors. ns = not significant. All scale bars = 75µm

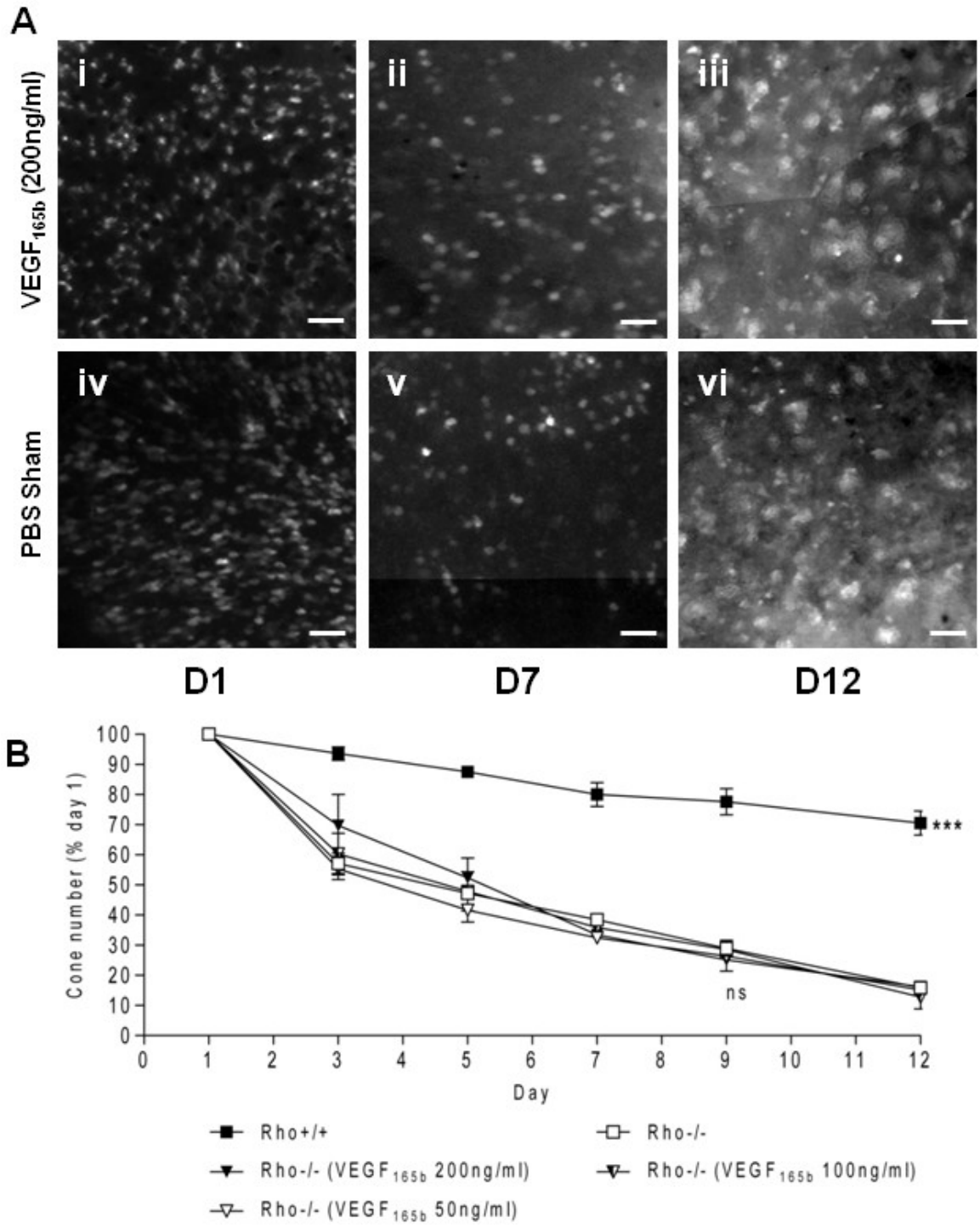

Figure 3.5 – $VEGF_{165b}$ does not confer any protection against secondary cone loss in Rho-/- TgOPN1LW-EGFP+/- explants
$VEGF_{165b}$ administered to retinal explants (n=6 explants per group) in complete media does not protective cone photoreceptors from degeneration following advanced rod loss **(A I-III)**. Individual cone photoreceptors were largely absent from $VEGF_{165b}$ and PBS sham treated explants by post harvest day (D) 12 **(A III, VI)**. No evidence was observed that neuroprotection was dose dependent with significant cell death observed at all doses. **(B)**. Anderson-Darling test for normality, $A^2 = 0.463$; $p=0.255$. *** = $p<0.001$, n = 6 explants per group, two-way repeated measure ANOVA with CNTF dose and age as factors. ns = not significant. All scale bars = 75µm

Chapter 4

Long-term dose-dependent neuroprotection of photoreceptors in a fluorescent reporter model of secondary cone degeneration in retinitis pigmentosa

INTRODUCTION

Retinitis pigmentosa (RP) is a genetically and phenotypically heterogeneous disorder affecting approximately 1 in 3000 individuals worldwide (Haim, 2002; Pagon and Daiger, 2005). Over 45 loci have been associated with RP, the majority of which contribute to only a small fraction of the overall disease, which makes the development of gene specific therapies problematic for all but the most prevalent alleles. Furthermore, in approximately ~30% of autosomal recessive (AR) RP and ~50% of autosomal dominant (AD) RP, the underlying genetic etiology remains elusive (Hartong et al., 2006). One of the most commonly affected genes in RP is rhodopsin (*RHO*), implicated in 8-10% of RP overall. However, whilst this might seem an attractive candidate for development of a gene-specific therapy, the majority of RP caused by *RHO* mutations is dominantly inherited - 25% of AD-RP compared to 1% of AR-RP – and the molecular mechanisms underlying disease pathology are highly variable, with seven mutation classes, many resulting in dominant negative effects (Mendes et al., 2005).

One of the most common presentations of RP is a rod-cone dystrophy, wherein rod photoreceptors degenerate due to an underlying genetic defect (e.g. *RHO*, *PDE6β*), followed by the secondary degeneration of cone photoreceptors. The mechanisms underlying the secondary loss of cone photoreceptors are incompletely understood, yet degeneration inevitably occurs despite the cones being genetically normal. Cone loss typically occurs once the primary rod degeneration has reached an advanced stage, with few rods remaining, which has led many to hypothesise that cone survival is dependent on rod derived trophic support, such as secretion of rod-derived cone viability factor, which has been shown to functionally preserve cones in late-stage RP (Leveillard et al., 2004; Yang et al., 2009).

Cumulatively, the absence of genetic and mechanistic understanding governing secondary cone loss in RP necessitates that approaches for preserving remaining cone photoreceptors in RP revolve around the administration of a neuroprotective proteins, typically low molecular weight ‘growth factors’. Numerous compounds have been demonstrated to have some efficacy in the preservation of cone photoreceptors in animal models of RP, including brain-derived neurotrophic factor (BDNF) (Okoye et

al., 2003), glial cell line-derived neurotrophic factor (GDNF) (McGee Sanftner et al., 2001) and ciliary neurotrophic factor (CNTF) (Liang et al., 2001).

In the previous chapter we identified CNTF as a particularly promising candidate molecule, which has been previously demonstrated in other studies to be highly protective of ganglion cells in models of oxidative stress and experimental glaucoma (Ji et al., 2004; Leaver et al., 2006; MacLaren et al., 2006a; Maier et al., 2004; Pease et al., 2009), and of photoreceptors in models of RP (Kassen et al., 2009; Liang et al., 2001; Lipinski et al., 2011a). However, as with all studies examining neuroprotection of cone photoreceptors, the time point of intervention is critically important. The clinical reality is that rod degeneration has typically reached an advanced stage by the time patients present to the clinic. Any neuroprotection strategy must be necessarily focus not just on preserving rod photoreceptors, but on the preservation of cone photoreceptors when rods are largely absent. Laing et al (2001) demonstrated robust protection of photoreceptors in rhodopsin knockout model of RP, but as the intervention was made at an early stage (3-5 days old) prior to onset of rod loss, both rod and cone photoreceptors were preserved, making it difficult to assess the clinical relevance. Herein, we examine the effectiveness of CNTF neuroprotection to preserve cone photoreceptors when the expression of the therapeutic transgene occurs when rod degeneration is already advanced.

As the most common causative gene implicated in RP, we utilized a rhodopsin knockout mouse ($Rho^{-/-}$) crossed to a transgenic fluorescent reporter mouse (B6.Cg-Tg(OPN1LW-EGFP) which expresses enhanced green fluorescent protein (EGFP) in the majority of cone photoreceptors. The fluorescent reporter acts a surrogate marker of cell viability, where continued fluorescence requires constant levels of EGFP production (Chalfie et al., 1994; Corish and Tyler-Smith, 1999), allowing the survival of cone photoreceptors to be assessed in vivo as they degenerate secondary to advanced rod loss. Significantly, this can be achieve in vivo using a confocal scanning laser ophthalmoscope (cSLO) which allows cone survival to be assessed non-invasively through repetitive imaging (Beck et al., 2010). We have previously demonstrated (Chapter 3) that individual cone photoreceptors can be resolved *in vitro* allowing

longitudinal quantification of cone numbers in response to treatment (Lipinski et al., 2011a). Herein, we have modified this technique to allow cone photoreceptors to be quantified *in vivo* from autofluorescence (AF) fundus images.

Whilst it is possible to administer neuroprotective compounds via repetitive intraocular injection of purified protein, the short half life of CNTF (~7 days) would necessitate that such injections were administered regularly (Chong et al., 1999). RP is a progressive disease and so neuroprotection would be required throughout the lifetime of a patient. Therefore, delivery of CNTF using gene therapy would be preferable, where long-term expression could be achieved following a single surgical intervention. Recombinant adeno-associated virus (rAAV) vectors have been used successfully to transfer therapeutic transgenes to the retina in numerous preclinical and clinical studies. Due to the high probability that cone photoreceptors will be subject to significant cellular stress in the model of RP, and CNTF acting through binding to cell surface expressed receptors, cone photoreceptors were not targeted directly for gene delivery. Instead, a recombinant AAV serotype 2 (rAAV2/2) vector was selected to package a modified secreted form of human CNTF by using a secreted form of CNTF, and a vector with tropism for ganglion cells and Müller glia when administered intravitreally, we aimed to preserve cone photoreceptors by indirectly via a paracrine mechanism.

Herein, we set out to demonstrate if neuroprotection of cone photoreceptors could be achieved by expression of a secreted CNTF protein from inner retinal neurons when delivered to adult retina where advanced rod loss was already evident. Gene transfer was carried out in adult $Rho^{+/-TgOPN1LW-EGFP+/-}$ mice at week 4-5, and cone survival quantified non-invasively using in vivo autofluorescence imaging initially week 8, when secondary loss of cones commences. Imaging was employed to longitudinally assess cone survival over a 22 week time course. Retinal functional and visual perception was also assessed throughout by electroretinography (ERG), and at week 30 by optomotor response (OMR) testing, to establish the extent of functional preservation.

CHAPTER SPECIFIC MATERIALS AND METHODS

Mice

Mice which express EGFP in cone photoreceptors and have a primary rod specific degeneration ($Rho^{-/-TgOPN1LW\text{-}EGFP+/-}$) were created through crossing of $B6^{TgOPN1LW\text{-}EGFP+/+}$ mice (homozygous for the OPN1LW-EGFP transgene insertion) with $Rho^{-/-}$ (homozygous for targeted rhodopsin knockout), followed by backcrossing of F1 progeny ($Rho^{+/-TgOPN1LW\text{-}EGFP+/-}$) to the parental $Rho^{-/-}$ line. Mice were genotyped at weaning by PCR as described in the general materials and methods section.

Vector construction

A recombinant AAV vector plasmid (herein termed pUF6.1_AAV2) was described previously, and was kindly provided by William W. Hauswirth, University of Florida, USA. cDNA clones of human neuronal growth factor (NGF; NM_002506) and human ciliary neurotrophic factor (CNTF, NM_000614) were purchased from Origene (Rockville, MD, USA). PCR was used to amplify the NGF secretion signal (Fwd, GTAC<u>GCGGCCGC</u>ATGTCCATGTTGTTC; Rev, GCTCTGTGAAAGCTGAGTGTGGTTCC) and the CNTF coding region minus the start codon and kozak consensus sequence (Fwd, GGAACCACACTCAGCTTTCACAGAGC, Rev, TCTA<u>GTCGAC</u>CTACATTTTCTTG) from the respective constructs. The two fragments were subsequently combined using SPLICE (Davies et al., 2007) and ligated into the UF6.1_AAV2 backbone using synthetic NotI and AccI restriction sites (underlined). An IRES.DsRed reporter was amplified from a previously created construct and ligated into the AccI site proximal to the CNTF stop codon. The correct orientation of the IRES.dsRED insert was confirmed by restriction digestion and gel electrophoresis, and fidelity of the final AAV2.CBA.CNTF.IRES.dsRED construct confirmed by sequencing along the full length.

Virus production and titration

Recombinant AAV serotype 2 (rAAV2/2) virus packaging the CNTF construct was produced by transient co-transfection of HEK293 in cell factories (HYPERflask; Corning, Tewksbury, MA, USA) followed by purification using iodixanol gradient centrifugation, as previously reported (Jacobson et al., 2006a; Zolotukhin, 2005). The purified rAAV2/2.CNTF virus was resuspended in sterile phosphate buffered saline (PBS) to a total volume of 100µl, and aliquoted into tubes which had been pre-blocked with 0.1% bovine serum albumen (BSA). The virus was titrated by qPCR using primers designed to amplify a 120bp fragment within the poly-A region, using vector plasmid and virus of known titre as standards. The virus titre was calculated to be $2x10^{13}$gp/ml.

Intraocular injection

The pupils of 4 week old $Rho^{-/-TgOPN1LW-EGFP+/-}$ or wild-type (C57Bl/6J) mice were dilated as above and a gel lubricant (Viscotears, Novartis, Frimley, UK) applied prior to positioning of a 6mm circular cover slip over the cornea to allow good visualization of the retina when viewed under a surgical microscope (M620 F20, Leica, Wetzlar, Germany). Injections were performed by advancing a Hamilton syringe with 10mm 34-guage needle (65N, Hamilton AG) trans-sclerally through the neural retina into the vitreous. 2µl of vector suspension or buffer (PBS) was delivered into the vitreous cavity close to the posterior pole; reflux was minimized by allowing the intraocular pressure to normalize for 30 seconds prior removing the needle rapidly. Orientation and stabilization of the eye was maintained throughout by holding the superior rectus muscle with notched forceps.

Autofluorescence (AF) imaging and cone quantification

The ocular fundi of each mouse were imaged using a confocal scanning laser ophthalmoscope (cSLO; Spectralis HRA, Heidelberg Engineering, Heidelberg, Germany) at weeks 8, 10, 12, 15, 18, 21, 24 and 30, as previously described (Charbel Issa et al., 2011). Briefly, following dilation a contact lens was placed on the cornea using a viscous coupling gel (0.3% w/v hypromellose to prevent cataract formation and to

improve and standardize image quality. The mouse was positioned on an imaging platform and the near-infrared (NIR) reflectance mode (820nm laser) used to achieve camera alignment at the confocal plane of the neural retina. Intrinsically EGFP expressing cone photoreceptors were imaged using the autofluorescence (AF) mode (480nm excitation) to capture high resolution images (1536 x 1536) recorded at a standardized detector sensitivity with automated real-time (ART) averaging. Cone numbers were quantified manually from each image, using vascular landmarks in the inferior retina to standardize the region of interest for each eye across the time course.

Electroretinography (ERG)

ERG recording was carried out using an Espion E2 system (Diagnosys LLC, Cambridge, UK) at 8, 10, 12 and 15 and week time points. Mice were anesthetized and their pupils dilated (see general materials and methods) prior to being placed on a heated platform, maintained at 37^{o}C by a circulating pump-water bath. A custom-made silver-coated nylon contact lens active electrode was manually positioned on each eye using hypromellose eye drops (0.5% methylcellulose) to maintain electrical conductivity and prevent corneal desiccation. Subdermal platinum needle electrodes were placed in the scruff (reference) and at the base of the tail (ground). Prepared animals were positioned inside the Ganzfeld dome of the Espion E2 system and light-adapted for 10 minutes using a 30Cd/m^2 polychromatic white light stimulus. For light-adapted responses, white flash stimuli of 3, 10 and 25cd.s/m^{2}were superimposed on a 30 cd/m^2 white background with 20 responses averaged using an ISI of 1 s. Dark adapted responses were not measured due to B6 Rho-/-OPN1LW-EGFP mice lacking rod function. Stimulus timing, duration and intensity were all controlled by the Espion software. b- wave amplitudes were quantified with the Espion software (Diagnosys LLC, Cambridge, UK).

Optomotor response (OMR)

A custom built optomotor system was produced consisting of a rotating cylinder which allowed speed and grating size to be precisely regulated. Mice were placed on a raised platform in the centre of the drum which was illuminated from above by a polychromatic white light stimulus (~1000 lux) and acclimatized to the drum for 1 minute, during which point the mouse was free to explore the raised platform. Each experimental run consisted of 1 minute clockwise rotation and 1 minute anti-clockwise rotation divided into alternating 30 second periods. The experimental run was repeated independently three times at each time point for each animal, and the number of responses averaged. The rotation of the square-wave grating elicited head tracking responses, with a single response consisting of a slow head-tracking motion in the direction of the drum's rotation followed by a rapid repositioning of the head to a central position.OMR is analogous to optokinetic nystagmus response (OKN), where eye tracking movements are measured in response to a square-wave grating of variable width and contrast moving across the visual field, in that the response is elicited unconsciously. To perform OKN in mice necessitates that the subject is completely restrained so that only the eyes are free to move in response to the drum's rotation, with eye tracking responses typically measured by movement of the pupil. OMR was chosen in this instance as it is substantially less invasive in that animals are not restrained other than being unable to move from the raised platform. The behaviour of each mouse in response to the rotating drum was recorded using a digital camera mounted directly above and head tracking responses scored manually with the scorer blinded as to which eye received CNTF treatment and which treatment group each mouse was in.

Statistics

Anderson-Darling test for normality on full data sets for each experiment revealed that the data was sampled from normally distributed population in the following cases: In vivo cone quantification, A^2=0.509, p=0.1983; low dose ERG, A^2=0.3402, p=0.4824; medium dose ERG, A^2=0.4483, p=0.2785; high dose ERG, A^2=0.7228, p=0.0594. Plotting of residuals versus fitted means for each experimental

group demonstrated that variance was equal within each group (plots not shown). Repetitive measures two-way ANOVA was used to analysis in vivo cone quantification with dose (independent variable) and time (repeated measure) as factors. Cone number was the dependent variable. Repetitive measures two-way ANOVA was used to analysis ERG responses with flash intensity (independent variable) and time (repetitive measure) as factors. Photopic b-wave amplitude was the dependent variable in each case, and each dose was analysed independently. Normality was not confirmed for optomotor response data: A^2=4.5536, p=<0.0005. Non-parametric Mann-Whitney U tests were used to compare mean head tracking responses elicited from treated and untreated eyes at each dose. Due to low sample size variance could not be plotted for groups when assessing CNTF levels following in vitro or in vivo vector transduction. Non-parametric Mann-Whitney U tests were applied in both instances to compare mean CNTF levels in transduced versus sham transduced cell supernatants (in vitro) or harvested eyes (in vivo). Bonferroni post tests were applied to all ANOVAs. The significance (p) level for all tests was set at 0.05.

RESULTS

Transduction of HEK293 cells demonstrates secretion of human CNTF

A monocistronic AAV vector genome was constructed containing the human CNTF therapeutic transgene and fluorescent reporter (DsRed) flanked by 5'- and 3'- inverted terminal repeats (ITR) derived from AAV serotype 2 (AAV2) (Fig. 4.1 A). Expression of the therapeutic transgene was driven by a ubiquitous chicken beta actin (CBA) promoter fused to the cytomegalovirus (CMV) early enhancer element (together termed CAG), whilst translation of the fluorescent reporter was driven independently from an upstream internal ribosome entry site (IRES). As human CNTF is not naturally secreted a 56bp sequence from nerve growth factor (NGF) 5'- terminus which encodes a C-terminal secretion signal was incorporated in frame immediately following the start codon. The vector genome was packaged into an unmodified AAV serotype-2 capsid to create recombinant virus (rAAV2/2.CNTF) with tropism for ganglion cells and Müller glia. The purified rAAV2/2.CNTF vector was titrated via qPCR using plasmid template and vector

stock of know concentration for comparison (data not shown) and the titre determined to be $1x10^{13}$gp/ml. rAAV2/2.CNTF function was assessed by transduction of HEK293 cells. Three days post transduction with $2x10^{10}$gp/well intracellular DsRed expression was clearly visible by fluorescence microscopy compared to sham (PBS) transduced cells (Fig.4.1B-C). The supernatant of rAAV2/2.CNTF and sham transduced cells was aspirated and assayed by ELISA to determine the concentration of human CNTF (Fig. 4.1 D). Human CNTF levels were significantly higher (~1250pg/ml)in media aspirated from wells transduced with rAAV2/2.CNTF than in PBS sham control wells (<8pg/ml; p=0.05, one-tailed Mann-Whitney U, n=3 well/group) indicating effective secretion of human CNTF from the vector construct.

To examine the in vivo levels of CNTF protein expression from therAAV2/2.CNTF vector, either low dose ($2x10^{8}$gp), medium dose ($2x10^{9}$gp) or high dose ($2x10^{10}$gp; n=3 eyes/group) vector was injected intravitreally in 4 week old $Rho^{-/-TgOPN1LW-EGFP+/-}$ mice and allowed to express, before eyes were harvested at week 8 (Fig. 4.1E). ELISA demonstrated high levels of human CNTF protein in eyes administered with high dose of vector(105.8±12.01pg/eye). Injection of medium dose vector resulted in lower levels of human CNTF (20.27±6.93pg/eye), whilst human CNTF levels were undetectable from eyes receiving the lowest vector dose. No CNTF was detected in contralateral PBS sham injected eyes (n=3) in any group(Fig. 4.1 E).

Autofluoescence imaging reveals robust preservation of cone photoreceptors for 30 weeks following human CNTF expression

Mice which express EGFP in cone photoreceptors and have a primary rod specific degeneration ($Rho^{-/-TgOPN1LW-EGFP+/-}$) were used to study the long term neuroprotective effects of human CNTF *in vivo*. $Rho^{-/-TgOPN1LW-EGFP+/-}$ mice were injected at 4 weeks old, receiving an intravitreal injection (2µl volume all injections) of PBS (sham) in one eye, and rAAV2/2.CNTF in the contralateral eye at either low dose ($2x10^{8}$gp; n=8 mice), medium dose ($2x10^{9}$gp; n=6 mice) or high dose ($2x10^{10}$gp; n=5 mice). The eye to be treated was randomised within cohorts to avoid systematic error.

A confocal scanning laser ophthalmoscope (cSLO), which is employed clinically to non-invasively assess retinal pathology by direct visualization of the retina through the pupil aperture, can be used in mice to assess the effects of a therapeutic intervention. The autofluorescence (AF) imaging mode can be used to visualize expression of fluorescent proteins within the retina, particularly EGFP, which has an excitation maximum proximate to that of the AF laser stimulus (Beck et al., 2010; Charbel Issa et al., 2011). AF imaging of the Rho$^{-/-TgOPN1LW-EGFP+/-}$mouse fundus reveals a pattern of punctuate white dots, where each dot corresponds to a single EGFP expressing cone photoreceptor (Figs. 4.2 and 4.3 A). Repetitive AF imaging allows the survival of individual cone photoreceptors to be tracked longitudinally, where fluorescence can be used as a surrogate marker of cell survival due to the short half life EGFP requiring a constant replenishment of protein to maintain visible levels of fluorescence (Chalfie et al., 1994; Corish and Tyler-Smith, 1999; Megason et al., 2006). More significantly, repetitive AF imaging allows cone photoreceptor numbers to be quantified longitudinally in each animal, giving a highly accurate real-time measurement of cell survival in response to a therapeutic intervention. Quantification is performed using vascular landmarks to define a region of interest (ROI) which remains constant throughout the life of the animal, and that can be identified regardless of eye rotation (Figs.4.2 and 4.3A). However, it should be noted that whilst the area imaged at each time point is constant for each animal, cSLO imaging only allows the central retina to be visualized, and so survival in the peripheral retina, where photoreceptors often survive until late stages of disease, cannot be quantified.

In Rho$^{-/-TgOPN1LW-EGFP+/-}$ mice there is a significant dorsal-ventral gradient of fluorescence, with a greater number of EGFP expressing cones located in the superior retina, and so the ROI was always defined between two vessels in the inferior retina where cone density is low enough to allow resolution of individual photoreceptors (Fig. 4.2). Cones were not quantified in the area immediately surrounding the optic disc or in the far periphery where confocal distortion makes resolution problematic. The ROI measured is not of uniform size between eyes due to differences in retinal vasculature, and so a comparison of absolute cone numbers within each ROI is not feasible; however, as the major vascular

landmarks remain consistent within each eye throughout an animal's life span, it is possible to express cone survival between two landmarks as a percentage relative to an initial time point (Fig. 4.2). Herein, cone numbers were evaluated at week 8 and cone numbers within each ROI compared relative to that baseline.

AF imaging showed robust EGFP expression across the retina at week 8 in all treatment and control groups, with distribution of fluorescent cones comparable between each group (Fig. 4.4 A-D). Cone numbers in the CNTF treatment groups and PBS-sham group showed a significant decline between week 8 and week 10 ($p<0.001$, all repeated measures two-way ANOVA with Bonferroni post-test. High dose n=5; medium dose n=6; low dose, n=8) indicating a loss of cone photoreceptors regardless of CNTF dose (Fig 4.3 B). In the PBS control groups degeneration of cone photoreceptors continued with significantly fewer cones remaining at each time point compared to the preceding measurement ($p<0.001$, all repeated measures two-way ANOVA with Bonferroni post-test. High dose n=5; medium dose n=6; low dose, n=8) until week 24, at which point cone numbers reached zero (Figs. 4.3B and 4.4). By contrast, whilst cone photoreceptor numbers in the high dose treatment group ($2x10^{10}$gp rAAV2/2.CNTF) declined significantly between weeks 10 and 12 ($p<0.05$,repeated measures two-way ANOVA with Bonferroni post-test, n=5), they did not decline significantly further between weeks 12 and 15 ($p>0.05$, repeated measures two-way ANOVA with Bonferroni post-test, n=5). Decline in cone numbers was slightly significant over the remainder of the time course ($p<0.05$ weeks 12 to 30, repeated measures two-way ANOVA with Bonferroni post-test, n=5) with cone numbers stabilizing at ~62% (Fig. 4.3). Cone number in the high dose treatment group were significantly higher than those in the paired PBS sham treated group from week 12 onwards ($p=<0.001$ all weeks, repeated measures two-way ANOVA with Bonferroni post-test, n=5).

Cone photoreceptor numbers declined in the medium dose group ($2x10^{9}$gp rAAV2/2.CNTF) between weeks 10 and 12 ($p<0.01$, repeated measures two-way ANOVA with Bonferroni post-test, n=6) but not between weeks 12 and 15 ($p>0.05$ repeated measures two-way ANOVA with Bonferroni post-test,

n=6). Decline in cone numbers was significant over the remainder of the time course ($p<0.001$ week 15 to week 30, repeated measures two-way ANOVA with Bonferroni post-test, n=6) with cone numbers stabilizing at ~44% (Fig. 4.3 B). Cone number in the medium dose treatment group were significantly higher than those in the paired PBS sham treated group from week 15 onwards ($p=<0.001$ all weeks, repeated measures two-way ANOVA with Bonferroni post-test, n=6). Both medium and high dose groups demonstrate robust long-term neuroprotection of cone photoreceptors, with significantly greater numbers of cones remaining in the high dose group compared the medium dose group by week 12($p<0.01$), becoming highly significant by week 15 ($p<0.001$, repeated measures two-way ANOVA with Bonferroni post-test. High dose n=5; medium dose n=6).

Cone degeneration in the low dose group ($2x10^8$gp rAAV2/2.CNTF) followed closely the course of the paired sham treated PBS control group, with significant week on week degeneration apparent until week 24($p=<0.001$ all weeks, repeated measures two-way ANOVA with Bonferroni post-test, n=8)at which point cone number was effectively reduced to zero (Fig. 4.3 B and 4.4). This indicates that the level of CNTF expression in the low dose treatment group is below the threshold for neuroprotection of cones photoreceptors in this model of RP.

Imaging of PBS sham and low dose treatment groups using the near-infrared reflectance mode (NIR) shows the emergence of patches of increased reflectance at late time points (Figs. 4.4 C-D and 4.5), which are likely areas of RPE atrophy, indicative of late stage RP.

ERG function is suppressed by CNTF and is not preserved beyond 12 weeks

Electroretinography (ERG) allows for field potential changes across the cornea in response to light stimuli to be measured as a means of assessing retinal function. The major ERG wave components are evoked by activation of distinct cell types, where the a-wave (a negative deflection) derives from activation of first order neurons, i.e. photoreceptors, and the b-wave (a positive deflection) derives from the subsequent activation of second order neurons, specifically ON-type bipolar cells. In $Rho^{-/-TgOPN1LW-EGFP+/-}$ the rods are

not receptive to light due to the absence of rhodopsin, and so primary light sensation is mediated only by cone photoreceptors. As the murine outer retina is comprised predominantly of rods - ~97% rods compared to 3% cones - the a-wave in Rho$^{-/-TgOPN1LW-EGFP+/-}$mice is large absent. The b-wave in Rho$^{-/-TgOPN1LW-EGFP+/-}$ is greatly reduced, where rod bipolar (all ON-type) no longer contribute; however, the b-wave is still measureable, and can be used to give an indication of residual cone function. Whilst in wild-type mice the light adaptation state of the retina is critical for isolating responses from either rod or cone photoreceptors, where the former require dark-adaptation and respond to extremely low level light stimuli, and the later respond to higher light intensities at which rods function is saturated, in Rho$^{-/-TgOPN1LW-EGFP+/-}$ mice this is not strictly necessary. However, b-wave responses were recorded in a light adapted state to make observations more comparable to published ERG protocols.

Compared to the paired PBS sham control group, the photopic b-wave amplitude at week 8 was significantly reduced at an of intensity 25 cd.s/m^2 in the high dose treatment group ($p<0.001$, repeated measures two-way ANOVA with Bonferroni post-test, n=5), indicating suppression of cone function in response to human CNTF (Fig. 4.6 A). The b-wave amplitude continued to be significantly reduced at week 10 compared to the PBS sham group ($p<0.001$, repeated measures two-way ANOVA with Bonferroni post-test, n=5), but was not significantly different at week 12 when ERG responses from both CNTF treated and PBS sham treated eyes were absent ($p>0.05$, repeated measures two-way ANOVA with Bonferroni post-test, n=5) (Fig. 4.6 C).

The b-wave amplitude of medium dose treated eyes were significantly reduced compared to paired PBS sham treated eyes at the highest intensity (25cd.s/m^2) light stimulus at week 8 ($p<0.01$) (Fig. 4.6 A) and week 10 ($p<0.05$, repeated measures two-way ANOVA with Bonferroni post-test, n=6) (Fig. 4.6 B).

No reduction in b-wave amplitude was observed with the low dose (Fig 4.6 A-C) treatment group compared to paired PBS sham at any time point or intensity. At weeks 12 and 15 b-wave ERG amplitude was not recordable above background noise in any treatment or sham control group. These results indicate

that CNTF results in dose dependent suppression of the murine cone ERG, and that CNTF does not lead to preservation of recordable cone function beyond that exhibited in sham treatment groups.

OMR responses can be elicited from CNTF treated eyes at 30 week

Optomotor response (OMR) utilizes a full field visual stimulus, classically a rotating drum with vertically orientated black/white stripes of a defined width and contrast in to which the animal is placed, to evoke an involuntary visual reflex (Fig. 4.7 A-B). The response is characterized by a slow head tracking motion in the direction of the drum's rotation, interspersed by a rapid head movement in the opposite direction to reorientate the head to a central position. Similar to optokinetic nystagmus (OKN) response, where each eye drives the slow phase eye movement in the opposite direction to the other (Harvey et al., 1997; Hobbelen and Collewijn, 1971), head tracking in OMR is driven from each eye independently and occurs in the temporal-to-nasal direction. Thus, when the drum rotates clockwise, the left eye drives a left-to-right head tracking response, and when the drum rotates anti-clockwise the right eye drives a right-to-left head tracking response (Fig. 4.7 B). Consequently, OMR can be used to distinguish the visual perception of each eye independently (Douglas et al., 2005).

OMR was initially performed on uninjected control $Rho^{-/-TgOPN1LW\text{-}EGFP+/-}$ mice (n=5) to determine the spatial frequency (grating width/rotation speed)that elicited the greatest response (data not shown); a 0.2 cyc/deg exposure was used for all subsequent OMR exposures. To explore whether CNTF treated eyes had a preserved OMR, despite the absence of a recordable ERG, experimental animals were examined at week 30. In all groups no head tracking was elicited by stimulation of PBS sham treated eyes. Head tracking events elicited from high dose treated eyes were significantly greater in frequency than paired PBS control eyes in all animals ($p=0.0143$, one-tailed Mann-Whitney U, n=4) (Fig. 4.7 C-D). Head tracking motion was well defined, though the period of tracking - how long the slow head movement follows the drum's rotation before the animal rapidly reorientate to a central position - was noticeably shorter than in 8 week $Rho^{-/-TgOPN1LW\text{-}EGFP+/-}$, potentially indicating a restriction in visual field.

Mice receiving medium dose rAAV.CNTF demonstrated greater levels of head tracking from treated eyes compared to PBS sham controls (p=0.025, one-tailed Mann-Whitney U, n=6) (Fig. 4.7 C).The number of head tracking events was lower in medium dose treatment group than in the high dose treated group, indicating the preservation of visual function is dose dependent. Low dose treated eyes did not exhibit significantly greater frequency of head tracking than paired sham treated eyes.

Linear regression analysis of OMR responses versus residual cone number at week 30 reveals a significant positive correlation (r2=0.80, F=33, p=0.0004), indicating that animals with greater numbers of cone photoreceptors remaining perform better on visually guided tasks such as OMR.

DISCUSSION

In this chapter we aimed to examine the efficacy of CNTF in preventing secondary cone photoreceptor degeneration when the intervention was made in adult mice with advanced stage rod degeneration. An rAAV2/2 vector was used to express a secretable form of human CNTF from inner retinal neurons following intravitreal delivery. Autofluorescence fundus imaging was employed quantitatively to longitudinally assess the survival of intrinsically fluorescent cone photoreceptors in response to secreted human CNTF. The use of vascular landmarks to define regions of interest which remained constant throughout the animal's lifetime led to highly reproducible quantification. The demonstration of robust dose-dependent preservation of cone photoreceptors - stable for at least 22 weeks – strongly indicates that CNTF is able to sustain cone photoreceptors long-term. Functional assessment demonstrated that the light adapted photopic ERG was suppressed by CNTF, and that a detectable ERG was not observed beyond week 15. However, OMR testing revealed that mice still retain the ability to identify high contrast visual stimuli at week 30, indicating the preservation of functionally useful vision in response to CNTF treatment, despite the absence of a recordable ERG.

Protection of photoreceptors in models of RP has previously been demonstrated using a number of compounds, including GDNF, BDNF and CNTF (Liang et al., 2001; McGee Sanftner et al., 2001;

Ohnaka et al., 2012; Okoye et al., 2003). While these studies indicate that photoreceptor neuroprotection can be achieved in models of RP, it is often the case that intervention was carried out in juvenile animals (e.g. 3-5 days) before significant rod degeneration had occurred. There is a significant body of evidence to suggest that CNTF has a neuroprotective effect on rod photoreceptors (Cayouette and Gravel, 1997; LaVail et al., 1992; LaVail et al., 1998) and consequently, one would expect cone photoreceptors to be additionally preserved (e.g. Liang et al., 2001). However, the clinical reality is that, whilst rod degeneration often occurs over many years and so theoretically a wide window exists in which to intervene, patients typically do not present to the clinic until the degeneration has reached an advanced stage, with majority of rod photoreceptors already absent.

In the present study, CNTF was expressed following delivery of the therapeutic transgene to inner retinal neurons at week 4-5, when retinogenesis is complete and rod photoreceptor degeneration has already begun. Expression of a transgene from rAVV vectors typically takes 2-3 weeks to reach its peak, and so in eyes receiving rAAV2/2.CNTF, one would expect maximum levels of CNTF expression to be reached at week 7-8, at which stage the retinal degeneration in $Rho^{-/-}$ animals is well advanced, with >50% of photoreceptors expected to have degenerated (Humphries et al., 1997).Secondary cone loss is observed from week 8 onwards, with the major phase of cone degeneration occurring between weeks 10 and 15, as observed in the PBS sham treated groups (Fig. 4D). Consequently, by intervening in early adulthood, our experimental model closely reproduces the clinical situation which is likely to be encountered, where intervention occurs only after significant rod loss.

The use of in vivo autofluorescence imaging to quantify cone photoreceptor survival longitudinally, rather than relying on post mortem histology at each time point, allowed for highly reproducible real-time comparisons of secondary cone degeneration between several treatment groups and their paired PBS sham controls. Whilst the use of viral vectors to deliver the therapeutic transgene limited control of dosing to regulating the number of genome particle administered, the level of human CNTF protein detected in by ELISA in week 8 eyes was different between vector doses, being highest in eyes

receiving $2x10^{10}$gp (105.8±12.01pg/eye). Human CNTF was not detected in eyes of the lowest dose treatment group, indicating that CNTF expression is either below the level of detection by ELISA (8pg/ml) or expression is absent. Cone survival over the time course appeared to correlate well to the vector dose administered and the levels of CNTF protein detected, with significantly higher levels of cone survival in high dose treatment group compared to the medium dose. Cone survival was not observed to be significantly improved in the lowest dose treatment group compared to PBS sham, indicating that there is a threshold level of CNTF protein required for neuroprotection of cone photoreceptors in RP. That cone numbers stabilized during the time course, and that the plateau in cone numbers occurred at different levels in each treatment group, further indicates that there is a strong correlation between the amount of available CNTF protein and the survival of cones photoreceptors. The stabilisation of cone numbers in the high dose treatment group is highly encouraging that neuroprotection might be maintained in the long-term, without significant further decline throughout the animal's lifetime, and suggests that CNTF might be clinically applicable for the preservation of cone photoreceptors in RP.

Functional assessment demonstrated suppression of ERG amplitude, a property which has been observed in several previous studies (Bok et al., 2002; Buch et al., 2006; McGill et al., 2007; Schlichtenbrede et al., 2003b). CNTF suppression of phototransduction is thought to affect rod photoreceptors more severely than cones through regulation of molecules in the rod phototranscution pathway, such as rhodopsin and transducin, leading to a reduction in rod outer segment (OS) length and consequently a reduction in light sensitivity. However, in the context of RP where the majority of rod photoreceptors are likely to be absent, a CNTF induced reduction in rod function is likely to be of little concern.

The effects of CNTF on cone phototransduction are not well understood, but similar reduction in the length of the cone OS has been reported. In this study, a reduction of up to 50% was observed in the amplitude of the photopic b-wave in the high dose treatment group. Light adapted b-wave amplitude was also reduced in the medium dose group, but to a lesser extent, and was not significantly reduced in the

low dose group compared to PBS sham, indicating that ERG suppression is dose-dependent. It has been suggested that a therapeutic dose range exists in which CNTF exhibits a neuroprotective effect but does not adversely affect photoreceptor function (McGill et al., 2007). Our observations would indicate that the neuroprotective dose range of CNTF overlaps significantly with the dose required to adversely impact cone phototransduction. However, it is conceivable that the effects of CNTF on cone phototransduction are more pronounced in a model of RP, where CNTF will be available at higher relative concentration per cell than if rods were present. The b-wave amplitude in all groups reached unrecordable amplitude in all groups by week 15, regardless of the extent of suppression at previous weeks. Firstly, this indicates that whilst CNTF does suppress b-wave amplitude, it does not appear to expedite the loss of ERG response; secondly, that CNTF is not able to preserve a detectable ERG, regardless of dose.

In light of the ERG suppression we determined to examine the extent to which functional vision remained in the late stages of retinal degeneration using optomotor response (OMR). OMR can be used to elicit an unconscious head tracking response independently from each eye based on the direction in which the stimulus moves relative to the eye (Douglas et al., 2005). This enabled us to compare the vision of treated and untreated eyes in each animal individually simply by alternating the rotation of the stimulus. OMR was performed at week 30, when cone photoreceptors were largely absent in control eyes. When eyes treated with high dose rAAV2/2.CNTF were stimulated, by movement of the high contrast drum in a temporal-to-nasal direction relative to the eye, slow head tracking movements were clearly distinguishable. Head tracking occurred with significantly higher frequency in treated eyes than in contralateral eyes which received a PBS sham, where tracking was almost uniformly absent. Eyes treated with medium dose vector elicited occasional head tracking responses, through at a lower frequency than the high dose group.

Whilst intra-animal variation was low, i.e. each animal responded with a similar frequency on the three occasions it was tested, inter-animal variation was observed within groups, where some animals responded with greater frequency than others despite receiving identical treatment. Post-hoc analysis

revealed that the number of residual cone photoreceptors present at week 30 correlated to the animal's OMR performance, strongly indicating that visual perception in late stage degeneration is directly linked to the number of cone photoreceptors remaining. This is important as is strongly supports that those photoreceptors remaining are functional and can mediate a visually guided response even in a retina with significant rod degeneration and an absent photopic ERG.As mentioned previously, cone survival was quantified from cSLO images, and so is a measure of those cones surviving in the central retina only, where the peripheral retina is difficult to image clearly due to confocal distortion and the relatively small pupil aperture of the mouse. However, as a visual response is more likely to be driven from activation of central cones than those in the periphery, correlating cone survival as measured by cSLO with OMR is valid.

The ability to respond to a visual stimulus such as a rotating square-wave grating of fixed width and contrast is mediated by how cones are distributed across the retina, where contrast sensitivity and spatial resolution are, as with colour perception, functions of how signals arising from the activation of multiple cones over a finite area by individual photons are integrated (Williams et al., 1993). Consequently, a reduction in the density of cones, particularly in the central retina, is likely to correlate to a reduction in visual acuity. That the relationship between photoreceptor number and OMR appears linear is indicative that the visual response elicited is proportional to the number of photoreceptors surviving, rather than a difference in sensitivity of the remaining cones in each group.

The presence of an optomotor response in the absence of an ERG initially appears counterintuitive, where one would usually expect to observe detectable levels of electrophysiological activity when eliciting a visual response. ERGs are recorded by measuring deviations in corneal field potential which are propagated following activation of photoreceptors by light. The propagation of a field potential requires a summed response from many photoreceptors activated in unison. It also requires the correct orientation of cells relative to one another and to the incident light, so that the field potential is propagated in the same direction. In our experimental model the degeneration of rod photoreceptors,

resulting in the compression of remaining cone photoreceptors between the inner retina and the RPE. This leads to significant alterations in cone photoreceptor morphology and orientation, likely reducing cone sensitivity, where the outer segment is no longer aligned relative to the incident light, and having significant impact on the generation of a uniform field potential. In contrast, OMR measures a physical response to a light stimulus. Due to amplification and processing of the visually evoked signal between the eye and brain, and within the visual cortex, a response can be generated with input from only a small number of cells. Consequently, it is possible to have a number of cells below the threshold needed to evoke a change in corneal field potential measureable by ERG, but which can still elicit a visual response.

In conclusion we have demonstrated that a secreatable neuroprotective compound can confer significant protections against secondary cone loss in a mouse model of RP. The treatment was administered by a single intravitreal injection of rAAV designed to target cells of the inner retina, and was demonstrated to result in long-term neuroprotection of cone photoreceptors up to 30 weeks. Despite observing that electrophysiological activity was not recordable beyond 15 weeks, it was shown that mice retain the ability to respond to visual stimulation (OMR) up to week 30, and that visual acuity is proportional to the number of cone photoreceptors remaining. The non-invasive nature of the treatment, coupled with the apparent long-term maintenance of cone photoreceptor neuroprotection with associated visual function, strongly indicates that neuroprotective strategies might be a viable therapeutic avenue for the treatment of end-stage RP in humans.

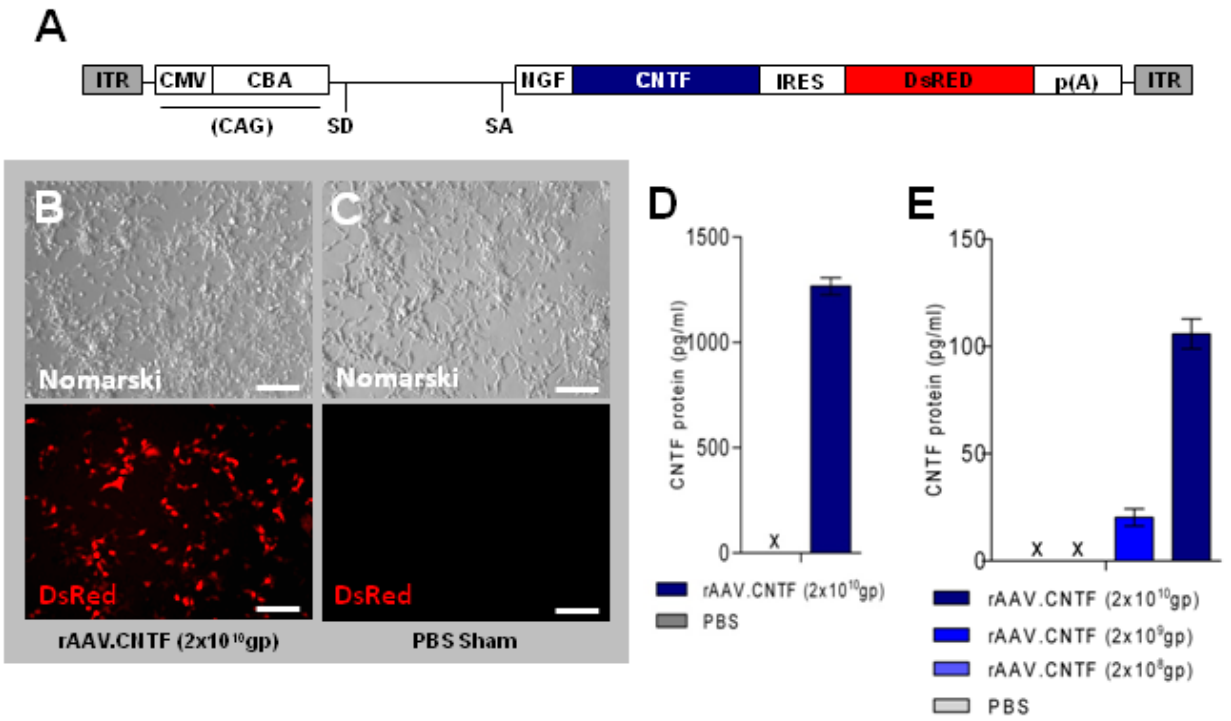

Figure 4.1–Modification of CNTF results in secretion when expressed in vitro and in vivo by recombinant AAV vector
Schematic representation of the CNTF expression construct **(A)**. ITR = inverted terminal repeat; CMV = cytomegalovirus enhancer; CBA = chicken beta actin promoter; SD = splice donor site; SA = splice acceptor site; NGF = neuron growth factor secretion signal; CNTF = ciliary neurotrophic factor cDNA; IRES = internal ribosome entry site; DsRed = fluorescent reporter; p(A) = poly-adenylation signal. The human ciliary neurotrophic factor (CNTF) cDNA is expressed ubiquitously from the CBA promoter and has been modified to be secreted by the addition of the leading peptide from neuron growth factor (NGF). The AAV2 based expression construct was packaged in an AAV serotype 2 capsid to produce recombinant AAV2/2 vector (rAAV2/2)which targets Müller glia and ganglion cells following intravitreal administration. Secretion of CNTF was examined in vitro by transduction of HEK293 cells with rAAV2/2.CNTF vector at $2x10^{10}$ genome particles (gp) per well. The independently translated fluorescent reporter gene (DsRed) was clearly observable in transduced wells **(B)** but not in PBS treated wells **(C)**. Human CNTF protein was detectable in supernatant aspirated from rAAV.CNTF transduced wells but not PBS treated wells (n=3 wells per group) **(D)**. Human CNTF protein could be recovered from eyes administered rAAV.CNTF vector (Rho-/- TgOPN1LW-EGFP+/- mice, n=3 eyes/group, injection at postnatal week 4, harvesting at postnatal week 8) **(E)**.Scale bars = 50µm. X = bars with zero value.

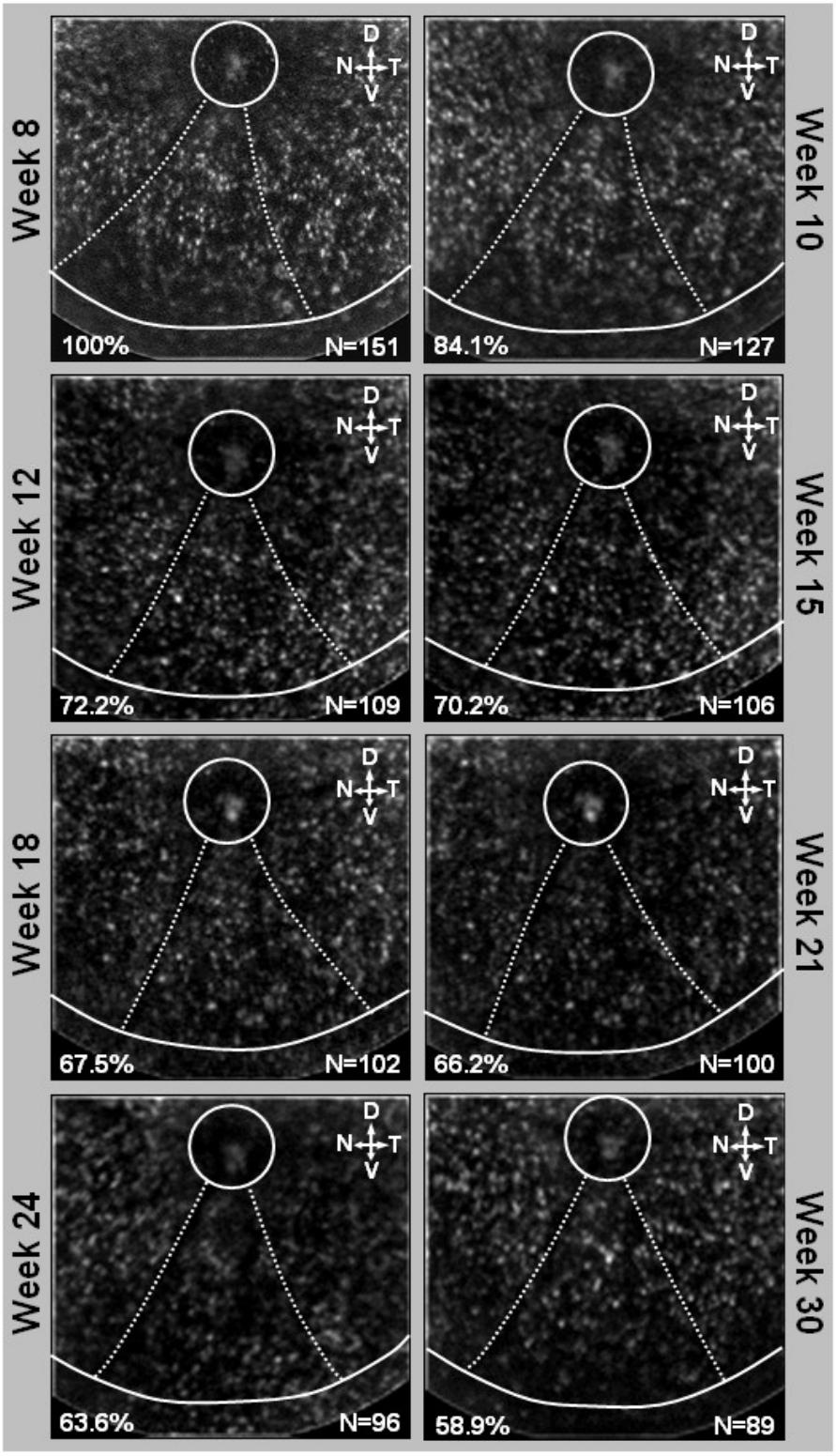

Figure 4.2 – Individual cone photoreceptors can be resolved on cSLO autofluorescence imaging allowing cone survival to be quantified repetitively in each animal using vascular landmarks to define a region of interest (ROI).
Representative images of a Rho-/- TgOPN1LW+/- eye (OS/left) treated with high dose ($2x10^{10}$gp) CNTF over the30 week time course. The absolute number of cone photoreceptors (N) in the ROI is defined between two blood vessels (dotted lines). Confocal distortion renders cone resolution difficult in the peripheral retina and area surrounding the optic disc (solid white lines) - these areas are excluded from quantification. Percentage survival is expressed as a function of cone number within the ROI at week 8. D = dorsal, V = ventral, N= nasal, T= temporal.

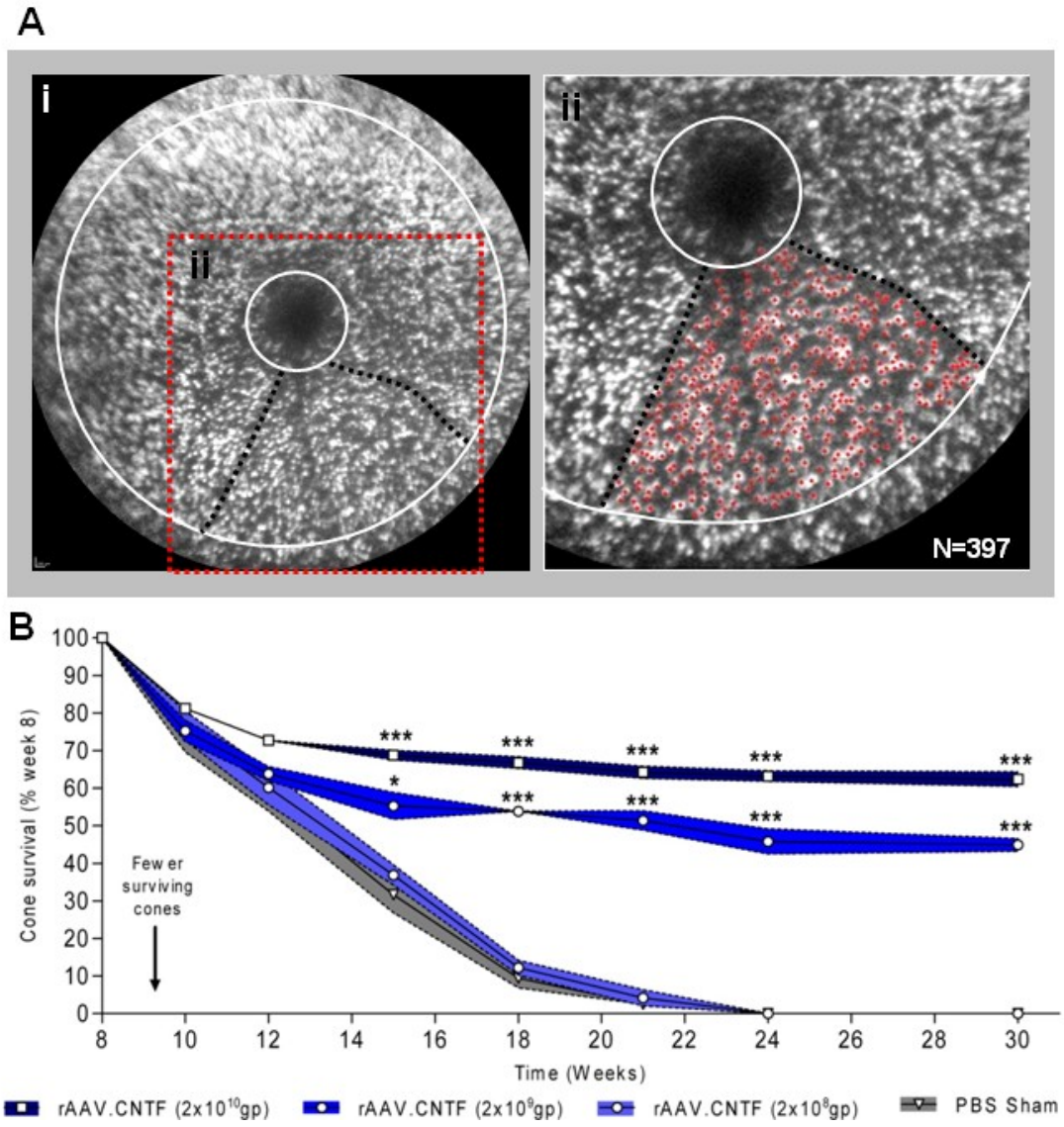

Figure 4.3–CNTF secretion leads to significant dose dependent protection of cone photoreceptors in vivo
Cone photoreceptors (white dots) are quantified (red crosses) at each time point using vascular landmarks (black dotted lines) to define a region of interest which remains constant in each animal throughout the experimental time course **(A)**. Quantification of cone survival in Rho-/- TgOPN1LW-EGFP+/- injected at postnatal week 4 with high dose rAAV.CNTF (dark blue), medium dose rAAV.CNTF (bright blue), low dose rAAV.CNTF (light blue), or PBS sham (grey)**(B)**. Cone survival is expressed as a function of the cone number at postnatal week 8. Significantly greater numbers of cones are preserved in the high and medium dose treatment groups compared to the PBS sham treatment group. Low dose CNTF did not result in significantly increased cone survival compared to PBS sham treatment. Anderson-Darling test for normality, $A^2 = 0.509$; $p=0.198$. * = $p<0.05$; ** = $p<0.01$; *** = $p<0.001$, two-way repeated measures ANOVA with dose and time as factors. High dose group n=5, medium dose group n=6, low dose group n=8, at week 30 time point.

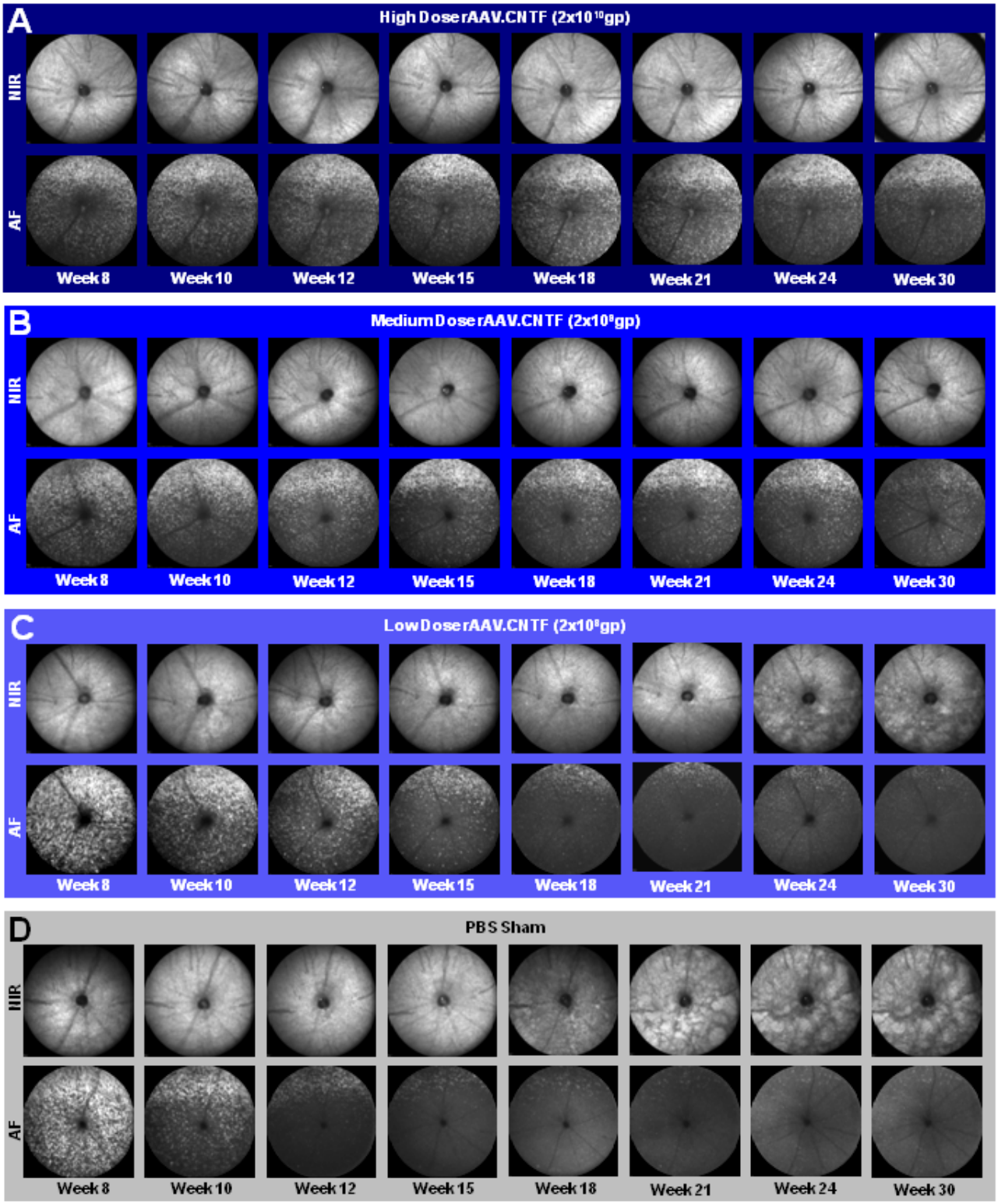

Figure 4.4 – CNTF prevents secondary cone loss in a dose dependent manner in an in vivo model of retinitis pigmentosa
Representative near infrared (NIR) and autofluorescence (AF) fundus images of Rho-/- TgOPN1LW-EGFP+/- mice assigned to each of the treatment groups: High dose rAAV.CNTF **(A)**, medium dose rAAV.CNTF **(B)**, low dose rAAV.CNTF **(C)**, or PBS sham **(D)**. CNTF doses are given as genome particles (gp) administered per eye in 2µl volume. Cone photoreceptors are observed on the autofluorescence (AF) mode as punctuate white dots which can be quantified longitudinally over 30 weeks. RPE atrophy can be observed as areas of increased brightness on the near-infrared reflectivity (NIR) mode, particularly at later time points in low dose and PBS sham treatment groups.

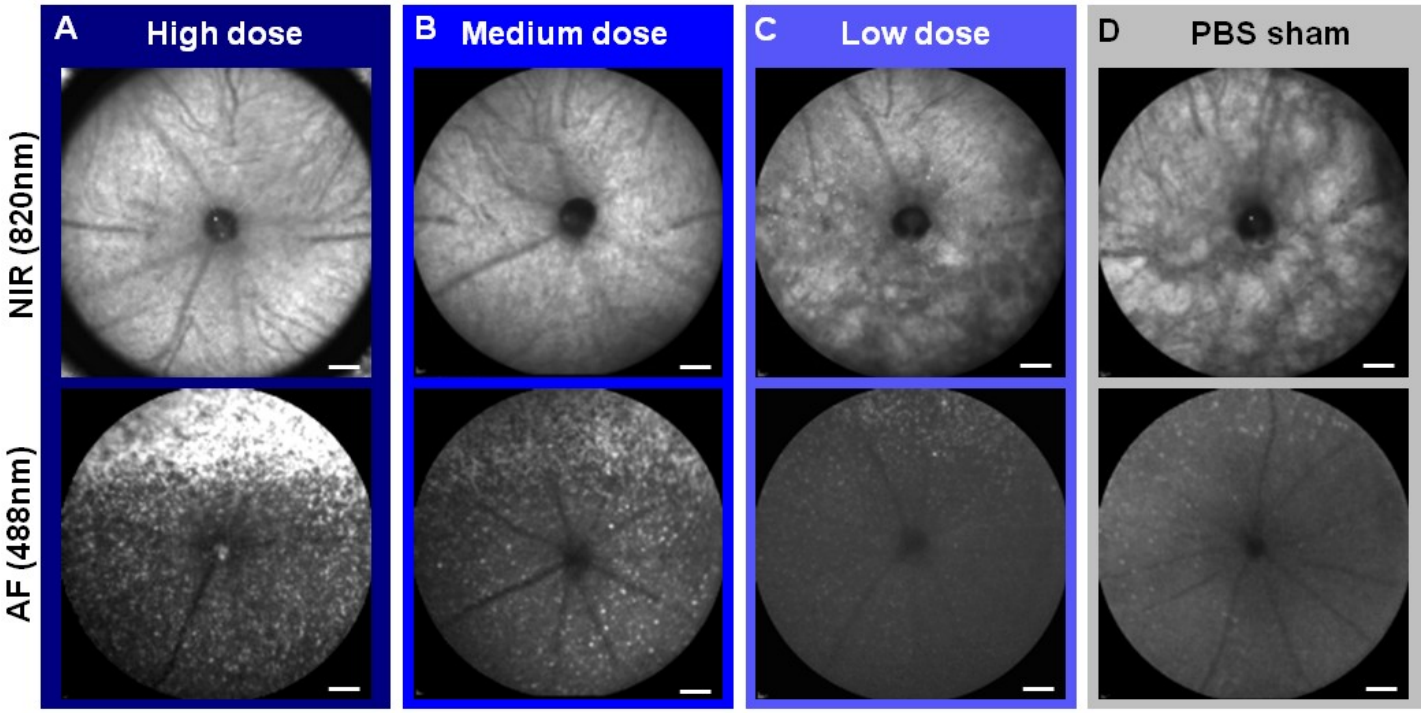

Figure 4.5 – Representative autofluorescence and near infrared images demonstrate cone preservation is dose dependent
Enlargered fundus images of Rho-/- TgOPN1LW-EGPF+/- mice at post natal week 30 demonstrate clearly that greater numbers of cone photoreceptors are present in high dose ($2x10^{10}$gp) treated eyes **(A)** than PBS sham treated eyes **(D)**, where fluorescent cones (white dots) are largely absent. Hyperfluorescent areas are apparent on NIR images in low dose ($2x10^{8}$gp) **(C)** and PBS sham treatment groups **(D)** indicating pigment changes most likely associated with RPE atrophy. Cone survival is dose dependent, with fewer cones surviving at week 30 in medium dose (2x109gp) treatment group **(C)** compared to the high dose group. Scale bars = ~100µm.

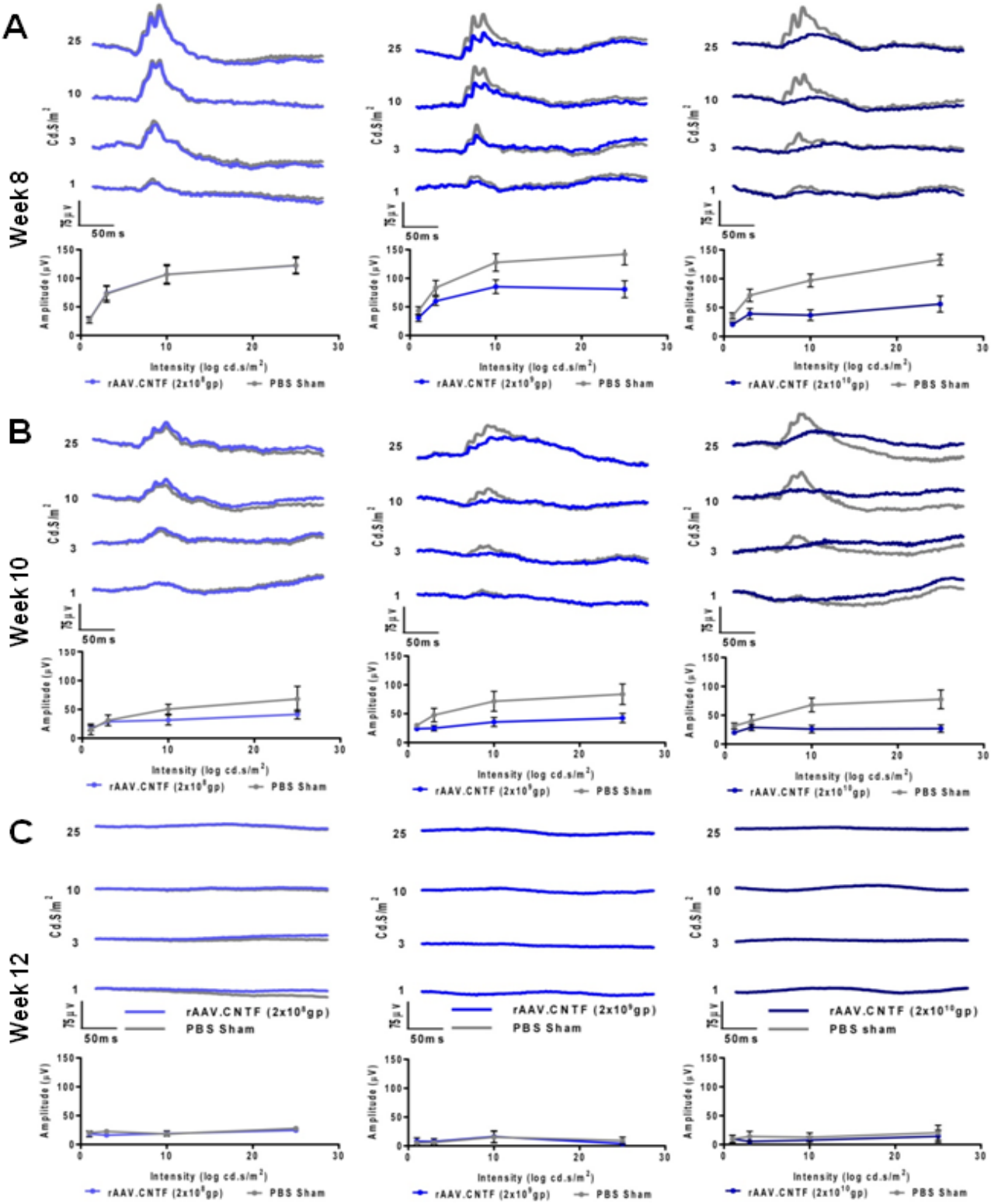

Figure 4.6 – ERG function is suppressed by CNTF in a dose-dependent manner and it not preserved beyond week 12
Representative ERG recordings from Rho-/- TgOPN1LW-EGFP+/- mice treated in one eye with high dose rAAV.CNTF (dark blue), medium dose rAAV.CNTF (bright blue) or low dose rAAV.CNTF (light blue) compared to the paired PBS sham eye (grey)**(A-C)**. Photopic (light adapted) b-wave amplitude was measured in response to 1Hz flash series at 1, 3, 10 and 25 Cd.S/m^2 over a 30Cd/m^2 polychromatic white light background. B-wave amplitude was not reduced in low dose treated eyes compared to paired PBS sham treated eyes. Photopic b-wave amplitude was reduced in medium and high dose groups compared to paired PBS sham treated eyes. The photopic b-wave amplitude was absent or below recordable levels in all groups by week 12.

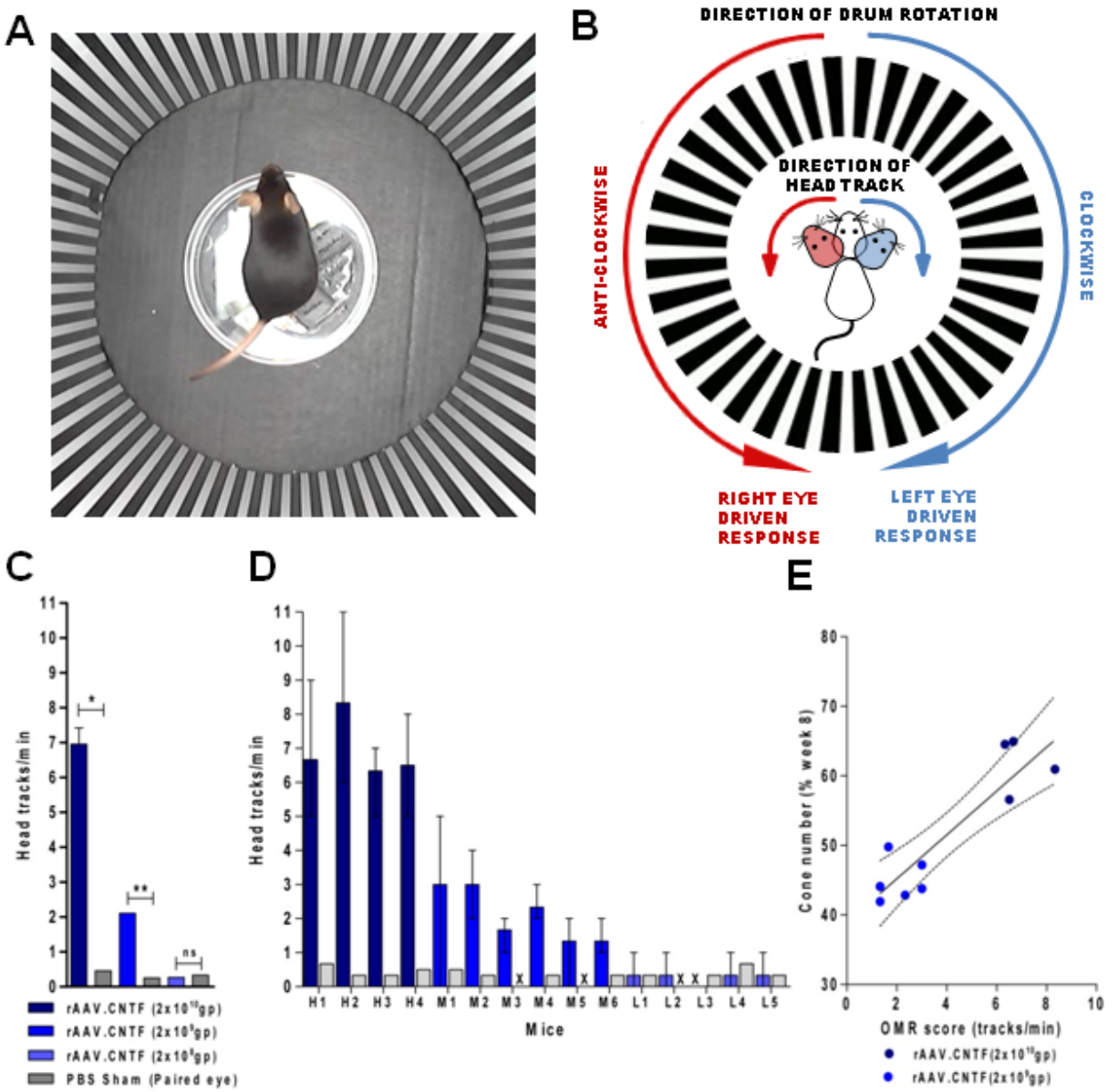

Figure 4.7 –Reponses to visual stimuli can be elicited at week 30 from high and medium dose rAAV.CNTF treated eyes
Mice were examined at week 30for the presence of an optomotor response (OMR), an unconscious turning of the head in reaction to a high contrast stimulus moving horizontally across the visual field. Mice were placed on a raised platform in the centre of a rotating drum with a black/white square-wave grating pattern **(A)**. In OMR testing the direction of the drum's rotation dictates which eye drives the head tracking response, enabling the vision of rAAV.CNTF treated and PBS sham treated eyes to be tested independently within each animal by alternating the direction of rotation **(B)**. Each animal was tested three times, with each test consisting of 1 minute acclimatization to the drum (no rotation), followed by 1 minute clockwise rotation and 1 minute anti-clockwise rotation divided into alternating 30 second periods. Responses were filmed using a digital camera mounted directly above the drum and the number of head tracking movements scored manually. OMR responses were elicited with significantly greater frequency from high dose rAAV.CNTF treated eyes than paired PBS sham treated eyes (* = 0.0445, one-tailed Wilcoxon matched pairs, n=4 eyes per group)**(C)**. OMR responses were also observed in medium dose rAAV.CNTF treated eyes compared to paired PBS sham treated eyes (* = 0.0156, one-tailed Wilcoxon matched pairs, n=6 eyes per group) though frequency of head tracking was less than elicited from high dose treated eyes. There was no evidence of significant head tracking being driven from low dose rAAV.CNTF treated eyes compared to paired PBS sham treated eyes (p=0.3864, one-tailed Wilcoxon matched pairs, n=5 eyes per group). Mean head tracking responses (average of three tests) are shown for individual mice (D). The OMR scores of individual mice correlate significantly to the number of cones remaining in treated eyes at week 30 (linear regression, r^2= 0.80, p=0.0004, error (dotted lines) = 95% confidence interval). Error bars all = s.d. X = bars with zero value.

General Discussion

This body of work set out to address whether neuroprotection might be a feasible treatment strategy for the preservation of cone photoreceptors in RP, where those cells frequently degenerate secondarily to rod photoreceptors, despite being genetically healthy (Lipinski et al., 2013). Due to the unknown cause of secondary cone loss, and the often unelucidated genetic etiology underlying primary rod degeneration, the development of a broadly applicable therapeutic approach is critical for the future treatment of this disease, at least in the immediate future. This topic was addressed on several fronts: the study of a model with reported cone degeneration (chapter 1), the assessment of an alternative gene delivery vector for targeting photoreceptors directly (chapter 2), the screening of neuroprotective compounds effective against secondary cone loss (chapter 3), and the assessment of the compound observed to be most neuroprotective – CNTF – using in vivo imaging of fluorescent cone photoreceptors in a rhodopsin knockout model of RP (chapter 4).

Chapter 1

In chapter 1,a combination of histology and electrophysiology was used to characterize a novel dominantly inherited cone degeneration in the B6.Cg-Tg(OPN1LW-EGFP)mouse model. Anatomical studies revealed significant loss of S-cones, indicating that the observed degeneration was independent of EGFP expression, which occurs only in MWS-opsin expressing cone photoreceptors (Beck et al., 2010; Fei and Hughes, 2001; Lipinski et al., 2011b).The distribution of MWS- and SWS-opsins in the B6.Cg-Tg(OPN1LW-EGFP) mouse was in line with previous studies and with congenic controls, with SWS-opsin largely restricted to cones of the inferior retina and MWS-opsin expressed throughout the retina except in the peripheral ventral retina (Ahnelt and Kolb, 2000).The presence of a small population of S-cones in the ventral retina allowed the electrophysiological function of non-EGFP expressing cone photoreceptors to be examined. The use of flicker ERG in conjunction with a short-wavelength stimulus (365nm) to isolate an S-cone driven response is not widespread, but has been demonstrated to be possible in several studies (Ekesten et al., 2001; Jacobs and Williams, 2007; Lyubarsky et al., 1999; Naarendorp et

al., 2010). Despite the separation between the peak absorbances (λ_{max}) of the two opsins (~149nm), it remains unclear the extent to which co-expressed MWS-opsin contributes to or modifies the ERG response observed when a short-wave-length stimulus is used. Whilst the number of non EGFP-expressing cone photoreceptors was observed to decline at an equal rate to the EGFP-expressing population, and this corresponded to a reduction in ERG amplitude in response to the 365nm flicker stimulus, indicating a global cone degeneration, it's likely that the exclusion of EGFP toxicity as the cause of cone degeneration would only be achieved through detailed end-point analysis of mice older than those examined here. In such mice, where cone degeneration has progressed further, the absence of a residual S-cone population would strongly support the hypothesis of an underlying genetic cause.

FISH analysis revealed that the OPN1LW-EGFP transgene was inserted in a region homologous to two human diseases affecting the macular, NCMD and PBCRA. Although mice do not possess a macular, and murine disease phenotypes consequently do not often correspond precisely to clinical observations in humans, the etiology of numerous retinal diseases have been identified in humans as a result of examining mouse models, due in part to the close genetic homology of the two species. One such example is the observation in mice of abnormal photoreceptor development followed by slow degeneration of both rod and cone photoreceptors which lead to the identification of mutations within the peripherin 2 (*Prph2*) gene. Shortly thereafter chromosome mapping lead to a *Prph2* homolog (*PRPH2*) being identified on human chromosome 6p21, mutation of which was linked to generalized autosomal dominant retinitis pigmentosa and macular dystrophies (Kajiwara et al., 1991; Kalyanasundaram et al., 2009; Travis et al., 1991). Consequently, whilst murids do not possess a macular, the study of retinal degenerations in small animal models has the potential to reveal genetic etiologies underlying human retinal diseases, even when the phenotypic correlation is not precise.

Mapping of the OPN1LW-EGFP transgene by FISH demonstrated that the insertion was located on chromosome 10B2-10B3. The homologous region in humans, chromosome 6q16-6q21, is associated with a number of dominantly inherited retinal disorders, including North Carolina macular dystrophy

(NCMD) and progressive bifocal chorioretinal atrophy (PBCRA) (Godley et al., 1996; Small, 1998).It was proposed in chapter 1 that the retinal degeneration observed in the B6.Cg-Tg(OPN1LW-EGFP) mouse model is linked to insertion of the transgene between the *Ascc3* and *Sim1* genes. Based on publically available databases (e.g. NCBI) this region does not contain any annotated genes, raising the question of how the transgene's insertion into this region might give rise to a cone-specific retinal degeneration? It has become increasingly apparent in recent years that the functional genome is not comprised solely of protein-encoding genes, and that other elements, particularly non-coding RNAs, are important for correct cellular homeostasis. Whilst non-coding RNAs have not previously been associated to any retinal degeneration in humans, they have been implicated in human disease, predominantly in the context of micro RNA (miRNA) disruption in the development of cancer. Furthermore, non-coding RNAs appear to be particularly important for neuronal development, with approximately 70% of discovered miRNAs expressed in the brain, many of which are neuron specific (Cao et al., 2006; Esteller, 2011). Consequently, it is conceivable that the function of neurons, such as cone photoreceptors, could be adversely affected by the disruption of non-coding elements within the intergenic region into which the OPN1LW-EGFP transgene has inserted, though without any direct evidence this remains speculative.

The proposed site of disruption, intergenic to *Ascc3* and *Sim1*, falls outside the locus currently described as being associated with NCMD (Small, 1998), and so it is unclear how the cone degeneration observed in the B6.Cg-Tg(OPN1LW-EGFP) mouse might directly correlates to the human disease. The NCMD locus is currently defined by linkage analysis, and although fine resolution mapping has narrowed the likely location, a precise genetic target has not been identified (Small et al., 1999). It is worth noting that as with all rare conditions the linkage analysis in the studies by Small et al (1998; 1999) were necessarily performed on a limited number of families, and that several families showed linkage of markers outside of the proposed region (D6S249-D6S1671), indicating the locus might potentially be larger than reported.

Further work is required to analysis the precise impact of the transgenic insertion in the B6.Cg-Tg(OPN1LW-EGFP) mouse model. Of particular importance would be to establish the precise location of the insertion within the 40kb intregenic region between *Ascc3* and *Sim1*, and subsequently to assess if any non-coding RNAs are expressed within that region. Unfortunately, as this model appears to have a primary degeneration of cone photoreceptors, it is unlikely to inform us further as to the mechanisms underlying secondary cone loss in RP. In the long term, elucidating the mechanism by which cone photoreceptors degenerate – is it loss of trophic support, or an increase in physical stress, or a combination of both – is key to the development of future therapies, where understanding the root cause makes it more likely to be able to effectively halt the degenerative process.

Chapter 2

In chapter 2, it was demonstrated that VEEV-G pseudotyped lentivirus vector is well tolerated in the anterior chamber, resulting in transduction of the corneal endothelium and trabecular meshwork, but is unlikely to be suitable for photoreceptor gene delivery. Robust RPE expression was achieved with both vector pseudotypes in accordance with results observed in previous studies (Balaggan et al., 2006; Cheng et al., 2005; Pang et al., 2006), perhaps indicating a receptor non-specific mechanism of vector internalization, such as phagocytosis along with shed outer segment discs. Pseudotyped lentivirus vectors could consequently be of use for the delivery of neuroprotective transgenes to the RPE, or for the expression of a therapeutic transgene to correct a specific deficit within the RPE, such as mer tyrosin kinase (MERTK) or RPE65 for the treatment of leber's congenital amaurosis. However, the RPE can be specifically targeted using rAAV vectors, particularly serotypes 1 and 4 which do not transduce photoreceptors efficiently (Ali et al., 1996; Le Meur et al., 2007; Lebherz et al., 2008). Additionally, the coding sequences for neuroprotective proteins and all currently identified RPE expressed genes associated with retinal diseases are typically small, allowing them to be packaged into single rAAV virions (Lipinski et al., 2013). There is, therefore, likely to be little utility for lentivirus in terms of developing either a

broadly applicable therapy for the neuroprotection of cone photoreceptors in RP, or for improving current gene delivery strategies for the treatment of monogenic diseases affecting the RPE.

Limited evidence was observed that lentivirus vectors may be used successfully to target human photoreceptors directly, potentially indicating a use in the treatment of specific retinal diseases affecting photoreceptors, such as Stargardt's or Usher's 1B, for which the coding sequences are slightly too large to be packaged effectively in rAAV vectors. The VEEV-G pseudotype – derived from a highly neurotrophic virus – was less effective at targeting photoreceptors than VSV-G, suggesting that the appropriate receptors for VEEV-G may not be present on photoreceptors. Furthermore, that photoreceptors could be targeted with VSV-G – which has broad cellular tropism – indicates that binding to surface receptors and subsequent internalization of the lentivirus virion are not significantly limiting steps to transduction. How then to explain the absence of photoreceptor transduction in vivo? One hypothesis is that lentivirus access to the photoreceptor cell bodies is physically restricted in vivo by a number of factors, including virion size, the presence of a viral envelope, the shedding of outer segment discs towards the RPE, and the phagocytotic nature of the RPE itself (Gruter et al., 2005). Evidence that physical barriers prevent the transduction of photorecptors in vivo can be noted in numerous studies which demonstrate effective photoreceptor gene expression following subretinal vector administration before retinogensis is complete (Davis et al., 2008; Kong et al., 2008; Pang et al., 2006). In the ex vivo culture system the retinal morphology is likely to be significantly disrupted, and barriers, such as the outer limiting membrane and outer segments, are likely to be either compromised or absent. This is particularly the case herein where the tissue was removed from a patient suffering a chronic rhegmatogenous retinal detachment with associated proliferative vitroretinopathy. Due to the chronic nature of this detachment the tissue is likely to have been degenerative, with breakdown of the outer segments (Kroll and Machemer, 1969a, b; Lewis et al., 2002) in addition to some degree of photoreceptor apoptosis (Anderson et al., 1983; Cook et al., 1995; Erickson et al., 1983).The absence of these barriers may allow photoreceptor transduction to occur,

implying that if such barriers can be circumvented in vivo, lentivirus may an effective therapeutic vector. Without causing damage to the retina, however, it is unclear how this might be achieved.

Chapter 3

In chapter 3 a novel *ex vivo* model of RP was established whereby the neuroprotective effects of various compounds could be assessed longitudinally through the quantification of intrinsically fluorescent cone photoreceptors. Using this model it was demonstrated that CNTF, and to a lesser extent GDNF, were effective at attenuating the secondary loss of cones. The use of retinal explants with intrinsic fluorescence to analyse cone survival is a powerful technique for the screening of potentially neuroprotective compounds, yet the numerous benefits which make accurate cone quantification possible have corollary drawbacks, particularly with how well the observations might be replicated in vivo.

One of the greatest benefits is that multiple retinal explants can be harvest from each animal, where each explant can be exposed independently to a given treatment condition, and thus represents an individual experimental unit. Whilst it is important to ensure that explants taken from multiple animals are randomly assigned across treatment groups, the ability to harvest a large number of explants from each mouse greatly reduces the number of animals required, with associated welfare and cost benefits.

It is also possible to precisely control the dosing of a given treatment ex vivo, where a certain concentration of a compound can be administered during media changes on a daily basis. In contrast to in vivo administration, where repetitive dosing is often separated by a number of days, ex vivo administration in media ensures a near constant concentration throughout the experimental time course. Unfortunately, whilst being tightly controlled, ex vivo dosing levels give little indication as to what the therapeutic dose is likely to be in vivo, where the compound may be absorbed by tissues other than the retina or be actively broken down.

The presence of the retina only in culture makes it possible to examine the effect of a compound on cone survival in isolation of confounding variables, such immunogenic reactions, or clearance of the

compound through metabolism or breakdown. The corollary of this, however, is that it is not possible to analysis compounds which mediate through tissues not present in the ex vivo culture environment, such as those (discussed below) which might mediate an effect through the RPE, which may lead to the ex vivo culture model returning falsely negative results.

The use of intrinsic fluorescence as a surrogate marker of cell survival, where constant production of protein is required for cells to remain fluorescent due to the short-half life of EGFP (Chalfie et al., 1994; Corish and Tyler-Smith, 1999; Megason et al., 2006), allows cone photoreceptor survival to be quantified with great accuracy, and despite various shortcomings, the ex vivo model presented herein represents one of the best ways currently described to evaluate the likely effectiveness of neuroprotective compounds.

The neuroprotective effects of CNTF are thought to be mediated through Müller cell activation resulting in STAT3 and ras-MAPK signalling following interaction with CNTFRα (Peterson et al., 2000). However, in the vertebrate retina CNTFRα expression is restricted to inner retinal neurons, particularly ganglion cells, and to rod outer segments (Fuhrmann et al., 1998), with no evidence of CNTFRα expression in photoreceptor cell bodies (Peterson et al., 2000). Müller cells are also thought not to express CNTFRα and not to be directly affected by CNTF administration. However, in neurons CNTFRα is anchored to the membrane by a unique glycosylphosphatidylinositol (GPI) linkage which under certain physiological conditions is degraded, allowing CNTFRα to be released from the membrane and solubilised. In the retina this release occurs primarily from amacrine and horizontal cells. Soluble CNTFRα is able to bind free CNTF (Davis et al., 1993) and signal via the LIFRβ/gp130 heterodimer (Peterson et al., 2000), resulting in Müller cell activation mediated by Jak/STAT3 induction (Kassen et al., 2009). Soluble CNTFRα does not appear to interact with photoreceptors directly, with no STAT3 or ras-MAPK activation reported (Peterson et al., 2000). In contrast, Müller cells do express receptors for GDNF, namely tyrosine kinase Ret and Growth factor receptor alpha-1, (GFRα-1) (Hauck et al., 2006),

and downstream signalling following receptor binding is likely to be through a similar Jak/STAT or MAPK/ERK pathway to that of CNTF.

Activated or reactive astrocytes have been shown to play an essential role in neuronal survival in response to injury, with their ablation resulting in rapid neuronal death following injury in the adult CNS (Bush et al., 1999). One primary mechanism of activated glial cell-mediated neuroprotection is thought to involve reduction of glutamate-induced cytotoxicity (Bush et al., 1999; Delyfer et al., 2005a). CNTF has previously been shown to promote glial uptake of extracellular glutamate through up regulation of glutamate transporters (Beurrier et al., 2010). However, GDNF is thought not to reduce levels of extracellular glutamate, as shown in the rd1 mouse model of RP (Delyfer et al., 2005b), perhaps contributing to the greater neuroprotective effects of CNTF in our *ex vivo* culture model. Müller cell activation is also noted to alter expression of various neurotrophic factors, including CNTF, GDNF, basic fibroblast growth factor (bFGF) and nerve growth factor (NGF) (Harada et al., 2002), which will additionally contribute towards neuroregulation (Bringmann and Reichenbach, 2001).

Due to the presence of Müller cells in our retinal explants, as well as the presence of glutamine in the culture media, the neuroprotective mechanisms occurring in this *ex vivo* culture system are likely to be similar to those *in vivo* described above. However, cone survival in this organ culture system will invariably be affected by additional stresses not normally associated with RP, particularly the trauma of the tissue dissection. Such stresses likely contribute to the slow degeneration of cones found in positive control explants, despite this tissue having genetically normal rod photoreceptors.

VEGF antagonists have become the gold standard treatment for wet AMD, where they limit angiogenesis. However, endogenous VEGF is required for proper visual function, Müller cell survival, and is a critical neurotrophic agent in response to ischemic injury (Nishijima et al., 2007; Saint-Geniez et al., 2008). Consequently, long-term inhibition of VEGF may negatively affect neuronal survival. Recently, C-terminal splice variants (b-isoforms) have been described to be anti-angiogenic (Konopatskaya et al., 2006) and potentially neuroprotective (Magnussen et al., 2010). However, we

observed no neuroprotective effects in our *ex vivo* model. Reassuringly, however, no acceleration of cone loss was seen at the doses tested, which is encouraging in the context of potential clinical applications for $VEGF_{165b}$ for inhibiting angiogenesis in AMD, where foveal cones may be stressed.

The data here confirm that CNTF has potent neuroprotective properties, and is effective at slowing the loss of cone photoreceptors secondary to advanced rod degeneration, making it an appropriate compound for the preservation of cones in RP.

Chapter 4

In chapter 4, it was demonstrated that expression of human CNTF in a mouse model with advanced stage rod degeneration can significantly reduce the extent of secondary cone loss, and preserve limited vision despite suppression of electrophysiological responses.

Protection of photoreceptors in models of RP has previously been demonstrated using a number of compounds, including GDNF, BDNF and CNTF (Liang et al., 2001; McGee Sanftner et al., 2001; Ohnaka et al., 2012; Okoye et al., 2003). While these studies indicate that photoreceptor neuroprotection can be achieved in models of RP, it is often the case that intervention was carried out in juvenile animals (e.g. 3-5 days) before significant rod degeneration had occurred. There is a significant body of evidence to suggest that CNTF has a neuroprotective effect on rod photoreceptors (Cayouette and Gravel, 1997; LaVail et al., 1992; LaVail et al., 1998) and consequently, one would expect cone photoreceptors to be additionally preserved (e.g. Liang et al., 2001). However, the clinical reality is that, whilst rod degeneration often occurs over many years and so theoretically a wide window exists in which to intervene, patients with sporadic RP (no family history) typically do not present to the clinic until the degeneration has reached an advanced stage, with the majority of rod photoreceptors already absent.

In this chapter, CNTF was expressed following delivery of the therapeutic transgene to inner retinal neurons at week 4-5, when retinogenesis is complete and rod photoreceptor degeneration has already begun. Expression of a transgene from rAVV vectors typically takes 2-3 weeks to reach its peak,

and so in eyes receiving rAAV2/2.CNTF, one would expect maximum levels of CNTF expression to be reached at week 7-8, at which stage the retinal degeneration in $Rho^{-/-}$ animals is well advanced, with >50% of photoreceptors expected to have degenerated (Humphries et al., 1997). Secondary cone loss is observed from week 8 onwards, with the major phase of cone degeneration occurring between weeks 10 and 15, as observed in the PBS sham treated groups (Fig. 4D). Consequently, by intervening in early adulthood, our experimental model closely reproduces the clinical situation which is likely to be encountered, where intervention occurs only after significant rod loss.

The use of in vivo autofluorescence imaging to quantify cone photoreceptor survival longitudinally, rather than relying on post mortem histology at each time point, allowed for highly reproducible real-time comparisons of secondary cone degeneration between several treatment groups and their paired PBS sham controls. Whilst the use of viral vectors to deliver the therapeutic transgene limited control of dosing to regulating the number of genome particle administered, the level of human CNTF protein detected in by ELISA in week 8 eyes was different between vector doses, being highest in eyes receiving $2x10^{10}$gp (105.8±12.01pg/eye). Human CNTF was not detected in eyes of the lowest dose treatment group, indicating that CNTF expression is either below the level of detection by ELISA (8pg/ml) or expression is absent. Cone survival over the time course appeared to correlate well to the vector dose administered and the levels of CNTF protein detected, with significantly higher levels of cone survival in high dose treatment group compared to the medium dose. Cone survival was not observed to be significantly improved in the lowest dose treatment group compared to PBS sham, indicating that there is a threshold level of CNTF protein required for neuroprotection of cone photoreceptors in RP. That cone numbers stabilized during the time course, and that the plateau in cone numbers occurred at different levels in each treatment group, further indicates that there is a strong correlation between the amount of available CNTF protein and the survival of cones photoreceptors. The stabilisation of cone numbers in the high dose treatment group is highly encouraging that neuroprotection might be maintained in the long-term, without significant further decline throughout the animal's lifetime, and suggests that CNTF might

be clinically applicable for the preservation of cone photoreceptors in RP. This data is in accordance with observations of neuroprotection in human trials using subretinal implantation of encapsulated cells which demonstrate using adaptive-optics SLO imaging that photoreceptors are anatomically preserved for several years by CNTF secretion (Talcott et al., 2011).

Functional assessment demonstrated suppression of ERG amplitude, a property which has been observed in several previous studies (Bok et al., 2002; Buch et al., 2006; McGill et al., 2007; Schlichtenbrede et al., 2003b). CNTF suppression of phototransduction is thought to affect rod photoreceptors more severely than cones through regulation of molecules in the rod phototranscution pathway, such as rhodopsin and transducin, leading to a reduction in rod outer segment (OS) length and consequently a reduction in light sensitivity. However, in the context of RP where the majority of rod photoreceptors are likely to be absent, a CNTF induced reduction in rod function is likely to be of little concern.

The effects of CNTF on cone phototransduction are not well understood, but similar reduction in the length of the cone OS has been reported. In this study, a reduction of up to 50% was observed in the amplitude of the photopic b-wave in the high dose treatment group. Previous studies have reported a reduction in ERG amplitude of 45-70% immediately following intravitreal injection of CNTF, with suppression of 30-50% for at least 6 months (Bok et al., 2002; Liang et al., 2001; McGill et al., 2007). Whilst this data appears to correspond to the reductions in ERG amplitude observed here, it is difficult to correlate the levels of ERG suppression when CNTF is expressed continuously, as here, with those studies which examined ERG amplitude following a single bolus of up to 10μg CNTF protein.

Light adapted b-wave amplitude was also reduced in the medium dose group, but to a lesser extent, and was not significantly reduced in the low dose group compared to PBS sham, indicating that ERG suppression is dose-dependent. Functional suppression has been noted in human patients receiving secreted CNTF treatment from encapsulated cell implants, with visual field sensitivity recordings being reduced to a greater extent in CNTF treated eyes than in untreated eyes (Birch et al., 2013).

It has been previously suggested that a therapeutic dose range exists in which CNTF exhibits a neuroprotective effect but does not adversely affect photoreceptor function (McGill et al., 2007). Our observations would indicate that the neuroprotective dose range of CNTF overlaps significantly with the dose required to adversely impact cone phototransduction. However, it is conceivable that the effects of CNTF on cone phototransduction are more pronounced in a model of RP, where CNTF will be available at higher relative concentration per cell than if rods were present, than in wild-type mice. As previously reported for transgenic rhodopsin knockout mice, the b-wave amplitude in all groups reached non-recordable amplitude in all groups by week 15 (Humphries et al., 1997). That the ERG amplitude reached un-recordable levels at the same time point in all treated and un treated group indicates that, firstly, that whilst CNTF does suppress b-wave amplitude, it does not appear to expedite the loss of ERG response, and secondly, that CNTF is not able to preserve a detectable ERG, regardless of dose.

In light of the ERG suppression it was determined to examine the extent to which functional vision remained in the late stages of retinal degeneration using optomotor response (OMR). OMR can be used to elicit an unconscious head tracking response independently from each eye based on the direction in which the stimulus moves relative to the eye (Douglas et al., 2005). This enabled a comparison of the vision of treated and untreated eyes in each animal individually simply by alternating the rotation of the stimulus. OMR was performed at week 30, when cone photoreceptors were largely absent in control eyes. When eyes treated with high dose rAAV2/2.CNTF were stimulated, by movement of the high contrast drum in a temporal-to-nasal direction relative to the eye, slow head tracking movements were clearly distinguishable. Head tracking occurred with significantly higher frequency in treated eyes than in contralateral eyes which received a PBS sham, where tracking was almost uniformly absent. Eyes treated with medium dose vector elicited occasional head tracking responses, through at a lower frequency than the high dose group. The number of residual cone photoreceptors present at week 30 correlated to the animal's OMR performance, strongly indicating that visual perception in late stage degeneration is linked to the number of cone photoreceptors remaining. However, it was notable that the period of head tracking,

i.e. the time that the slow movement of the mouse's head tracked the rotation of the drum before the head righted to central location, appeared to be decreased in 30 week CNTF treated eyes compared to wildtype OMR responses (data not shown). This indicates that whilst remaining cone photoreceptors in CNTF treated eyes are functional, that there may be a reduction in visual field or contrast sensitivity, most likely due to the reduction in cone photoreceptor numbers and the consequent disruption of the photoreceptor mosaic.

The presence of an optomotor response in the absence of an ERG initially appears counterintuitive, where one would usually expect to observe detectable levels of electrophysiological activity when eliciting a visual response. ERGs are recorded by measuring deviations in corneal field potential which are propagated following activation of photoreceptors by light. The propagation of a field potential requires a summed response from many photoreceptors activated in unison. It also requires the correct orientation of cells relative to one another and to the incident light, so that the field potential is propagated in the same direction. In this experimental model the degeneration of rod photoreceptors, resulting in the compression of remaining cone photoreceptors between the inner retina and the RPE, leads to significant alterations in cone photoreceptor morphology and orientation, likely reducing cone sensitivity - where the outer segment is no longer aligned relative to the incident light - having a significant impact on the generation of a uniform field potential. In contrast, OMR measures a physical response to a light stimulus. Due to amplification and processing of the visually evoked signal between the eye and brain, and within the visual cortex, a response can be generated with input from only a small number of cells. Consequently, it is possible to have a number of cells below the threshold needed to evoke a change in corneal field potential measureable by ERG, but which can still elicit a visual response.

These last two chapters, where CNTF was identified using an accurate screening model to be highly neuroprotective of cone photoreceptors, and was then expressed via rAAV vector in a modified secretable form from inner retinal neurons in vivo, resulting in a significant increase in cone survival and the preservation of functional vision, strongly indicates that neuroprotection is an possible strategy for the

treatment of end-stage rod-cone dystrophies in RP. Furthermore, the work demonstrates that cones can be preserved without direct transduction, and that neuroprotection can be sustained long-term following a single intervention – important facets of an optimized gene therapy approach. However, certain issues surrounding CNTF neuroprotection remain.

First, the extent of neuroprotection, i.e. the level at which cone numbers stabilize following treatment, and the suppression of electrophysiological response, seem to be dose dependent, and to overlap. Consequently, successful CNTF neuroprotection is likely to involve a 'trade-off' between the numbers of cone photoreceptors preserved, and the functionality of those cells remaining. Currently, with dosing controlled crudely by an alteration of the vector titre administered, striking an appropriate balance might prove problematic. It might therefore be necessary to include certain regulatory elements in any vector destined for clinical evaluation, such as an inducible promoter, enabling CNTF expression from the transgene to be switched off should electrophysiological suppression become intolerably great.

Second, whilst it was demonstrated that the preserved cone photoreceptors are able to illicit an unconscious head-turning response in treated mice, it is unclear as to what degree of functional vision this might relate to. The pair-wise experimental layout used herein was designed to make detection of small differences in cone survival possible by greatly reducing inter-animal variation, and so further tests of functional vision, such as the Morris water maze or visual cliff, were not carried out. For such tests it was deemed impractical to test each eye individually, or that doing so, e.g. by suturing each eye closed in turn, would adversely affect the animal's behaviour on the test. Furthermore, such tests often require a certain amount of prior learning before useful results can be generated, and the mice in this investigation were not given such training at an age before onset of the retinal degeneration. It would, however, be possible in CNTF treated animals to perform other examinations, such as measurements of cortical blood flow following stimulation of the treated eye versus the untreated eye. Cortical blood flow has been demonstrated to increase in response to a visual stimulus (Pearson et al., 2012; Singh et al., 2013), and such an increase following stimulation of the treated eye would provide strong evidence that visual

information from remaining cone photoreceptors is being relayed to the brain, and would be support of the OMR data, where head tracking requires cognitive processing, albeit subconscious.

It is worth noting that measurements of visual acuity or function in mice following CNTF treatment may not correlate to those observed in human patients, where as mentioned previously, the presence of the macular complicates phenotypic correlation. It is possible that CNTF may lead to preservation of central cones, and thus central vision, and consequently lead to preservation of functional vision at a high level.

In conclusion, herein it has been demonstrated that cone photoreceptors can be preserved in a model of retinitis pigmentosa by neuroprotective compounds. That long-term neuroprotection can be achieved following a single gene therapy intervention gives rise to the possibility that a widely applicable and safe therapy for retinitis pigmentosa might be possible.

Bibliography

Abramoff, M.D., Magelhaes, P.J., Ram, S.J., 2004. Image Processing with ImageJ. Biophotonics International 11, 36-42.

Acland, G.M., Aguirre, G.D., Bennett, J., Aleman, T.S., Cideciyan, A.V., Bennicelli, J., Dejneka, N.S., Pearce-Kelling, S.E., Maguire, A.M., Palczewski, K., Hauswirth, W.W., Jacobson, S.G., 2005. Long-term restoration of rod and cone vision by single dose rAAV-mediated gene transfer to the retina in a canine model of childhood blindness. Mol Ther 12, 1072-1082.

Acland, G.M., Aguirre, G.D., Ray, J., Zhang, Q., Aleman, T.S., Cideciyan, A.V., Pearce-Kelling, S.E., Anand, V., Zeng, Y., Maguire, A.M., Jacobson, S.G., Hauswirth, W.W., Bennett, J., 2001. Gene therapy restores vision in a canine model of childhood blindness. Nat Genet 28, 92-95.

Aguirre, G.D., Baldwin, V., Pearce-Kelling, S., Narfstrom, K., Ray, K., Acland, G.M., 1998. Congenital stationary night blindness in the dog: common mutation in the RPE65 gene indicates founder effect. Mol Vis 4, 23.

Ahnelt, P.K., Kolb, H., 2000. The mammalian photoreceptor mosaic-adaptive design. Prog Retin Eye Res 19, 711-777.

Akache, B., Grimm, D., Pandey, K., Yant, S.R., Xu, H., Kay, M.A., 2006. The 37/67-kilodalton laminin receptor is a receptor for adeno-associated virus serotypes 8, 2, 3, and 9. J Virol 80, 9831-9836.

Akimoto, M., Cheng, H., Zhu, D., Brzezinski, J.A., Khanna, R., Filippova, E., Oh, E.C., Jing, Y., Linares, J.L., Brooks, M., Zareparsi, S., Mears, A.J., Hero, A., Glaser, T., Swaroop, A., 2006. Targeting of GFP to newborn rods by Nrl promoter and temporal expression profiling of flow-sorted photoreceptors. Proc Natl Acad Sci U S A 103, 3890-3895.

Alge, C.S., Suppmann, S., Priglinger, S.G., Neubauer, A.S., May, C.A., Hauck, S., Welge-Lussen, U., Ueffing, M., Kampik, A., 2003. Comparative proteome analysis of native differentiated and cultured dedifferentiated human RPE cells. Invest Ophthalmol Vis Sci 44, 3629-3641.

Ali, R.R., Reichel, M.B., De Alwis, M., Kanuga, N., Kinnon, C., Levinsky, R.J., Hunt, D.M., Bhattacharya, S.S., Thrasher, A.J., 1998. Adeno-associated virus gene transfer to mouse retina. Hum Gene Ther 9, 81-86.

Ali, R.R., Reichel, M.B., Thrasher, A.J., Levinsky, R.J., Kinnon, C., Kanuga, N., Hunt, D.M., Bhattacharya, S.S., 1996. Gene transfer into the mouse retina mediated by an adeno-associated viral vector. Hum Mol Genet 5, 591-594.

Alizadeh, M., Wada, M., Gelfman, C.M., Handa, J.T., Hjelmeland, L.M., 2001. Downregulation of differentiation specific gene expression by oxidative stress in ARPE-19 cells. Invest Ophthalmol Vis Sci 42, 2706-2713.

Anderson, D.H., Stern, W.H., Fisher, S.K., Erickson, P.A., Borgula, G.A., 1983. Retinal detachment in the cat: the pigment epithelial-photoreceptor interface. Invest Ophthalmol Vis Sci 24, 906-926.

Applebury, M.L., Antoch, M.P., Baxter, L.C., Chun, L.L., Falk, J.D., Farhangfar, F., Kage, K., Krzystolik, M.G., Lyass, L.A., Robbins, J.T., 2000. The murine cone photoreceptor: a single cone type expresses both S and M opsins with retinal spatial patterning. Neuron 27, 513-523.

Arsuaga, J., Tan, R.K., Vazquez, M., Sumners, D.W., Harvey, S.C., 2002. Investigation of viral DNA packaging using molecular mechanics models. Biophys Chem 101-102, 475-484.

Auricchio, A., Kobinger, G., Anand, V., Hildinger, M., O'Connor, E., Maguire, A.M., Wilson, J.M., Bennett, J., 2001. Exchange of surface proteins impacts on viral vector cellular specificity and transduction characteristics: the retina as a model. Hum Mol Genet 10, 3075-3081.

Azzouz, M., Le, T., Ralph, G.S., Walmsley, L., Monani, U.R., Lee, D.C., Wilkes, F., Mitrophanous, K.A., Kingsman, S.M., Burghes, A.H., Mazarakis, N.D., 2004. Lentivector-mediated SMN replacement in a mouse model of spinal muscular atrophy. J Clin Invest 114, 1726-1731.

Bainbridge, J.W., Tan, M.H., Ali, R.R., 2006. Gene therapy progress and prospects: the eye. Gene Ther 13, 1191-1197.

Balaggan, K.S., Binley, K., Esapa, M., Iqball, S., Askham, Z., Kan, O., Tschernutter, M., Bainbridge, J.W., Naylor, S., Ali, R.R., 2006. Stable and efficient intraocular gene transfer using pseudotyped EIAV lentiviral vectors. J Gene Med 8, 275-285.

Baltmr, A., Duggan, J., Nizari, S., Salt, T.E., Cordeiro, M.F., 2010. Neuroprotection in glaucoma - Is there a future role? Exp Eye Res 91, 554-566.

Beck, S.C., Schaeferhoff, K., Michalakis, S., Fischer, M.D., Huber, G., Rieger, N., Riess, O., Wissinger, B., Biel, M., Bonin, M., Seeliger, M.W., Tanimoto, N., 2010. In vivo analysis of cone survival in mice. Invest Ophthalmol Vis Sci 51, 493-497.

Bemelmans, A.P., Bonnel, S., Houhou, L., Dufour, N., Nandrot, E., Helmlinger, D., Sarkis, C., Abitbol, M., Mallet, J., 2005. Retinal cell type expression specificity of HIV-1-derived gene transfer vectors upon subretinal injection in the adult rat: influence of pseudotyping and promoter. J Gene Med 7, 1367-1374.

Bennett, J., Maguire, A.M., Cideciyan, A.V., Schnell, M., Glover, E., Anand, V., Aleman, T.S., Chirmule, N., Gupta, A.R., Huang, Y., Gao, G.P., Nyberg, W.C., Tazelaar, J., Hughes, J., Wilson, J.M., Jacobson, S.G., 1999. Stable transgene expression in rod photoreceptors after recombinant adeno-associated virus-mediated gene transfer to monkey retina. Proc Natl Acad Sci U S A 96, 9920-9925.

Bennicelli, J., Wright, J.F., Komaromy, A., Jacobs, J.B., Hauck, B., Zelenaia, O., Mingozzi, F., Hui, D., Chung, D., Rex, T.S., Wei, Z., Qu, G., Zhou, S., Zeiss, C., Arruda, V.R., Acland, G.M., Dell'Osso, L.F., High, K.A., Maguire, A.M., Bennett, J., 2008. Reversal of blindness in animal models of leber congenital amaurosis using optimized AAV2-mediated gene transfer. Mol Ther 16, 458-465.

Berns, K.I., 1996. Paroviridae: the viruses and their replication, Fields, B.N. (Ed.), Fundamental Virology. Lippincot-Raven, Philadelphia, New York, pp. 1017–1042.

Beurrier, C., Faideau, M., Bennouar, K.E., Escartin, C., Kerkerian-Le Goff, L., Bonvento, G., Gubellini, P., 2010. Ciliary neurotrophic factor protects striatal neurons against excitotoxicity by enhancing glial glutamate uptake. PLoS One 5, e8550.

Biel, M., Seeliger, M., Pfeifer, A., Kohler, K., Gerstner, A., Ludwig, A., Jaissle, G., Fauser, S., Zrenner, E., Hofmann, F., 1999. Selective loss of cone function in mice lacking the cyclic nucleotide-gated channel CNG3. Proc Natl Acad Sci U S A 96, 7553-7557.

Birch, D.G., Lockr, K.G., Travis, P., Martin, K., Austin, R., Weng, T., Duncan, J.L., 2013. Long-term follow-up of patients with retinitis pigmentosa (RP) receiving sustained-release CNTF through intraocular encapsulated cell technology implants, ARVO annual meeting, Seattle, WA.

Bok, D., Yasumura, D., Matthes, M.T., Ruiz, A., Duncan, J.L., Chappelow, A.V., Zolutukhin, S., Hauswirth, W., LaVail, M.M., 2002. Effects of adeno-associated virus-vectored ciliary neurotrophic factor on retinal structure and function in mice with a P216L rds/peripherin mutation. Exp Eye Res 74, 719-735.

Boye, S.E., Alexander, J.J., Boye, S.L., Witherspoon, C.D., Sandefer, K., Conlon, T., Erger, K., Sun, J., Ryals, R.C., Chiodo, V., Clark, M., Girkin, C.A., Hauswirth, W.W., Gamlin, P.D., 2012. The human rhodopsin kinase promoter in an AAV5 vector confers rod and cone specific expression in the primate retina. Hum Gene Ther.

Bringmann, A., Reichenbach, A., 2001. Role of Muller cells in retinal degenerations. Front Biosci 6, E72-92.

Brown, B.D., Cantore, A., Annoni, A., Sergi, L.S., Lombardo, A., Della Valle, P., D'Angelo, A., Naldini, L., 2007. A microRNA-regulated lentiviral vector mediates stable correction of hemophilia B mice. Blood 110, 4144-4152.

Brown, K.T., 1968. The eclectroretinogram: its components and their origins. Vision Res 8, 633-677.

Buch, P.K., MacLaren, R.E., Duran, Y., Balaggan, K.S., MacNeil, A., Schlichtenbrede, F.C., Smith, A.J., Ali, R.R., 2006. In contrast to AAV-mediated Cntf expression, AAV-mediated Gdnf expression enhances gene replacement therapy in rodent models of retinal degeneration. Mol Ther 14, 700-709.

Buch, P.K., Mihelec, M., Cottrill, P., Wilkie, S.E., Pearson, R.A., Duran, Y., West, E.L., Michaelides, M., Ali, R.R., Hunt, D.M., 2011. Dominant cone-rod dystrophy: a mouse model generated by gene targeting of the GCAP1/Guca1a gene. PLoS One 6, e18089.

Bulina, M.E., Lukyanov, K.A., Britanova, O.V., Onichtchouk, D., Lukyanov, S., Chudakov, D.M., 2006. Chromophore-assisted light inactivation (CALI) using the phototoxic fluorescent protein KillerRed. Nat Protoc 1, 947-953.

Bush, T.G., Puvanachandra, N., Horner, C.H., Polito, A., Ostenfeld, T., Svendsen, C.N., Mucke, L., Johnson, M.H., Sofroniew, M.V., 1999. Leukocyte infiltration, neuronal degeneration, and neurite outgrowth after ablation of scar-forming, reactive astrocytes in adult transgenic mice. Neuron 23, 297-308.

Calame, M., Cachafeiro, M., Philippe, S., Schouwey, K., Tekaya, M., Wanner, D., Sarkis, C., Kostic, C., Arsenijevic, Y., 2011. Retinal degeneration progression changes lentiviral vector cell targeting in the retina. PLoS One 6, e23782.

Cao, X., Yeo, G., Muotri, A.R., Kuwabara, T., Gage, F.H., 2006. Noncoding RNAs in the mammalian central nervous system. Annu Rev Neurosci 29, 77-103.

Carter-Dawson, L.D., LaVail, M.M., 1979. Rods and cones in the mouse retina. I. Structural analysis using light and electron microscopy. J Comp Neurol 188, 245-262.

Cayouette, M., Gravel, C., 1997. Adenovirus-mediated gene transfer of ciliary neurotrophic factor can prevent photoreceptor degeneration in the retinal degeneration (rd) mouse. Hum Gene Ther 8, 423-430.

Chalfie, M., Tu, Y., Euskirchen, G., Ward, W.W., Prasher, D.C., 1994. Green fluorescent protein as a marker for gene expression. Science 263, 802-805.

Chang, B., Dacey, M.S., Hawes, N.L., Hitchcock, P.F., Milam, A.H., Atmaca-Sonmez, P., Nusinowitz, S., Heckenlively, J.R., 2006. Cone photoreceptor function loss-3, a novel mouse model of achromatopsia due to a mutation in Gnat2. Invest Ophthalmol Vis Sci 47, 5017-5021.

Charbel Issa, P., Singh, M.S., Lipinski, D.M., Chong, N.V., Delori, F.C., Barnard, A.R., Maclaren, R.E., 2011. Optimization of in vivo confocal autofluorescence imaging of the ocular fundus in mice and its application to models of human retinal degeneration. Invest Ophthalmol Vis Sci.

Chen, J., Flannery, J.G., LaVail, M.M., Steinberg, R.H., Xu, J., Simon, M.I., 1996. bcl-2 overexpression reduces apoptotic photoreceptor cell death in three different retinal degenerations. Proc Natl Acad Sci U S A 93, 7042-7047.

Cheng, L., Toyoguchi, M., Looney, D.J., Lee, J., Davidson, M.C., Freeman, W.R., 2005. Efficient gene transfer to retinal pigment epithelium cells with long-term expression. Retina 25, 193-201.

Chong, N.H., Alexander, R.A., Waters, L., Barnett, K.C., Bird, A.C., Luthert, P.J., 1999. Repeated injections of a ciliary neurotrophic factor analogue leading to long-term photoreceptor survival in hereditary retinal degeneration. Invest Ophthalmol Vis Sci 40, 1298-1305.

Cook, B., Lewis, G.P., Fisher, S.K., Adler, R., 1995. Apoptotic photoreceptor degeneration in experimental retinal detachment. Invest Ophthalmol Vis Sci 36, 990-996.

Corish, P., Tyler-Smith, C., 1999. Attenuation of green fluorescent protein half-life in mammalian cells. Protein Eng 12, 1035-1040.

Daniels, D.M., Shen, W.Y., Constable, I.J., Rakoczy, P.E., 2003. Quantitative model demonstrating that recombinant adeno-associated virus and green fluorescent protein are non-toxic to the rat retina. Clin Experiment Ophthalmol 31, 439-444.

Davies, W.L., Carvalho, L.S., Hunt, D.M., 2007. SPLICE: a technique for generating in vitro spliced coding sequences from genomic DNA. Biotechniques 43, 785-789.

Davis, R.J., Tosi, J., Janisch, K.M., Kasanuki, J.M., Wang, N.K., Kong, J., Tsui, I., Cilluffo, M., Woodruff, M.L., Fain, G.L., Lin, C.S., Tsang, S.H., 2008. Functional rescue of degenerating photoreceptors in mice homozygous for a hypomorphic cGMP phosphodiesterase 6 b allele (Pde6bH620Q). Invest Ophthalmol Vis Sci 49, 5067-5076.

Davis, S., Aldrich, T.H., Ip, N.Y., Stahl, N., Scherer, S., Farruggella, T., DiStefano, P.S., Curtis, R., Panayotatos, N., Gascan, H., et al., 1993. Released form of CNTF receptor alpha component as a soluble mediator of CNTF responses. Science 259, 1736-1739.

Deeb, S.S., 2006. Genetics of variation in human color vision and the retinal cone mosaic. Curr Opin Genet Dev 16, 301-307.

Delyfer, M.N., Forster, V., Neveux, N., Picaud, S., Leveillard, T., Sahel, J.A., 2005a. Evidence for glutamate-mediated excitotoxic mechanisms during photoreceptor degeneration in the rd1 mouse retina. Mol Vis 11, 688-696.

Delyfer, M.N., Simonutti, M., Neveux, N., Leveillard, T., Sahel, J.A., 2005b. Does GDNF exert its neuroprotective effects on photoreceptors in the rd1 retina through the glial glutamate transporter GLAST? Mol Vis 11, 677-687.

Demaison, C., Parsley, K., Brouns, G., Scherr, M., Battmer, K., Kinnon, C., Grez, M., Thrasher, A.J., 2002. High-level transduction and gene expression in hematopoietic repopulating cells using a human immunodeficiency [correction of imunodeficiency] virus type 1-based lentiviral vector containing an internal spleen focus forming virus promoter. Hum Gene Ther 13, 803-813.

Di Pasquale, G., Davidson, B.L., Stein, C.S., Martins, I., Scudiero, D., Monks, A., Chiorini, J.A., 2003. Identification of PDGFR as a receptor for AAV-5 transduction. Nat Med 9, 1306-1312.

Dimos, J.T., Rodolfa, K.T., Niakan, K.K., Weisenthal, L.M., Mitsumoto, H., Chung, W., Croft, G.F., Saphier, G., Leibel, R., Goland, R., Wichterle, H., Henderson, C.E., Eggan, K., 2008. Induced pluripotent stem cells generated from patients with ALS can be differentiated into motor neurons. Science 321, 1218-1221.

Dodt, E., 1951. Cone electroretinography by flicker. Nature 168, 738.

Doi, K., Hargitai, J., Kong, J., Tsang, S.H., Wheatley, M., Chang, S., Goff, S., Gouras, P., 2002. Lentiviral transduction of green fluorescent protein in retinal epithelium: evidence of rejection. Vision Res 42, 551-558.

Douglas, R.M., Alam, N.M., Silver, B.D., McGill, T.J., Tschetter, W.W., Prusky, G.T., 2005. Independent visual threshold measurements in the two eyes of freely moving rats and mice using a virtual-reality optokinetic system. Vis Neurosci 22, 677-684.

Dreyer, E.B., Vorwerk, C.K., Zurakowski, D., Simon, P.D., Bennett, J., 1999. Infection with adeno-associated virus may protect against excitotoxicity. Neuroreport 10, 2887-2890.

Duan, D., Yue, Y., Yan, Z., Engelhardt, J.F., 2003. Trans-splicing vectors expand the packaging limits of adeno-associated virus for gene therapy applications. Methods Mol Med 76, 287-307.

Ekesten, B., Gouras, P., Salchow, D.J., 2001. Ultraviolet and middle wavelength sensitive cone responses in the electroretinogram (ERG) of normal and Rpe65 -/- mice. Vision Res 41, 2425-2433.

Erickson, P.A., Fisher, S.K., Anderson, D.H., Stern, W.H., Borgula, G.A., 1983. Retinal detachment in the cat: the outer nuclear and outer plexiform layers. Invest Ophthalmol Vis Sci 24, 927-942.

Esteller, M., 2011. Non-coding RNAs in human disease. Nat Rev Genet 12, 861-874.

Evans, M., 2005. Ethical sourcing of human embryonic stem cells--rational solutions? Nat Rev Mol Cell Biol 6, 663-667.

Fei, Y., 2003. Development of the cone photoreceptor mosaic in the mouse retina revealed by fluorescent cones in transgenic mice. Mol Vis 9, 31-42.

Fei, Y., Hughes, T.E., 2001. Transgenic expression of the jellyfish green fluorescent protein in the cone photoreceptors of the mouse. Vis Neurosci 18, 615-623.

Fishman, G.A., American Academy of Ophthalmology., 2001. Electrophysiologic testing in disorders of the retina, optic nerve, and visual pathway, 2nd ed. Foundation of the American Academy of Ophthalmology, San Francisco.

Flannery, J.G., Zolotukhin, S., Vaquero, M.I., LaVail, M.M., Muzyczka, N., Hauswirth, W.W., 1997. Efficient photoreceptor-targeted gene expression in vivo by recombinant adeno-associated virus. Proc Natl Acad Sci U S A 94, 6916-6921.

Forrester, J.V., Dick, A.D., McMenamin, P.G., Roberts, F., 2008. The Eye - Basic Sciences in Practice, 3rd ed. Elsevier, Philadelphia.

Fuhrmann, S., Kirsch, M., Heller, S., Rohrer, H., Hofmann, H.D., 1998. Differential regulation of ciliary neurotrophic factor receptor-alpha expression in all major neuronal cell classes during development of the chick retina. J Comp Neurol 400, 244-254.

Gao, G., Vandenberghe, L.H., Wilson, J.M., 2005. New recombinant serotypes of AAV vectors. Curr Gene Ther 5, 285-297.

Gehrig, A., Felbor, U., Kelsell, R.E., Hunt, D.M., Maumenee, I.H., Weber, B.H., 1998. Assessment of the interphotoreceptor matrix proteoglycan-1 (IMPG1) gene localised to 6q13-q15 in autosomal dominant Stargardt-like disease (ADSTGD), progressive bifocal chorioretinal atrophy (PBCRA), and North Carolina macular dystrophy (MCDR1). J Med Genet 35, 641-645.

Godley, B.F., Tiffin, P.A., Evans, K., Kelsell, R.E., Hunt, D.M., Bird, A.C., 1996. Clinical features of progressive bifocal chorioretinal atrophy: a retinal dystrophy linked to chromosome 6q. Ophthalmology 103, 893-898.

Gorbatyuk, M.S., Knox, T., LaVail, M.M., Gorbatyuk, O.S., Noorwez, S.M., Hauswirth, W.W., Lin, J.H., Muzyczka, N., Lewin, A.S., 2010. Restoration of visual function in P23H rhodopsin transgenic rats by gene delivery of BiP/Grp78. Proc Natl Acad Sci U S A 107, 5961-5966.

Gruter, O., Kostic, C., Crippa, S.V., Perez, M.T., Zografos, L., Schorderet, D.F., Munier, F.L., Arsenijevic, Y., 2005. Lentiviral vector-mediated gene transfer in adult mouse photoreceptors is impaired by the presence of a physical barrier. Gene Ther 12, 942-947.

Guidry, C., 2005. The role of Muller cells in fibrocontractive retinal disorders. Prog Retin Eye Res 24, 75-86.

Haim, M., 2002. Epidemiology of retinitis pigmentosa in Denmark. Acta Ophthalmol Scand Suppl 233, 1-34.

Haimann, M.H., Burton, T.C., Brown, C.K., 1982. Epidemiology of retinal detachment. Arch Ophthalmol 100, 289-292.

Harada, T., Harada, C., Kohsaka, S., Wada, E., Yoshida, K., Ohno, S., Mamada, H., Tanaka, K., Parada, L.F., Wada, K., 2002. Microglia-Muller glia cell interactions control neurotrophic factor production during light-induced retinal degeneration. J Neurosci 22, 9228-9236.

Hartong, D.T., Berson, E.L., Dryja, T.P., 2006. Retinitis pigmentosa. Lancet 368, 1795-1809.

Haruta, M., 2005. Embryonic stem cells: potential source for ocular repair. Semin Ophthalmol 20, 17-23.

Harvey, R.J., De'Sperati, C., Strata, P., 1997. The early phase of horizontal optokinetic responses in the pigmented rat and the effects of lesions of the visual cortex. Vision Res 37, 1615-1625.

Hauck, S.M., Kinkl, N., Deeg, C.A., Swiatek-de Lange, M., Schoffmann, S., Ueffing, M., 2006. GDNF family ligands trigger indirect neuroprotective signaling in retinal glial cells. Mol Cell Biol 26, 2746-2757.

Hauswirth, W.W., Berns, K.I., 1977. Origin and termination of adeno-associated virus DNA replication. Virology 78, 488-499.

Haverkamp, S., Wassle, H., Duebel, J., Kuner, T., Augustine, G.J., Feng, G., Euler, T., 2005. The primordial, blue-cone color system of the mouse retina. J Neurosci 25, 5438-5445.

Heys, J.J., Barocas, V.H., 2002. A boussinesq model of natural convection in the human eye and the formation of Krukenberg's spindle. Ann Biomed Eng 30, 392-401.

Hirami, Y., Osakada, F., Takahashi, K., Okita, K., Yamanaka, S., Ikeda, H., Yoshimura, N., Takahashi, M., 2009. Generation of retinal cells from mouse and human induced pluripotent stem cells. Neurosci Lett 458, 126-131.

Hobbelen, J.F., Collewijn, H., 1971. Effect of cerebro-cortical and collicular ablations upon the optokinetic reactions in the rabbit. Doc Ophthalmol 30, 227-236.

Hua, J., Spee, C., Kase, S., Rennel, E.S., Magnussen, A.L., Qiu, Y., Varey, A., Dhayade, S., Churchill, A.J., Harper, S.J., Bates, D.O., Hinton, D.R., 2010. Recombinant human VEGF165b inhibits experimental choroidal neovascularization. Invest Ophthalmol Vis Sci 51, 4282-4288.

Huang, W.Y., Aramburu, J., Douglas, P.S., Izumo, S., 2000. Transgenic expression of green fluorescence protein can cause dilated cardiomyopathy. Nat Med 6, 482-483.

Humphries, M.M., Rancourt, D., Farrar, G.J., Kenna, P., Hazel, M., Bush, R.A., Sieving, P.A., Sheils, D.M., McNally, N., Creighton, P., Erven, A., Boros, A., Gulya, K., Capecchi, M.R., Humphries, P., 1997. Retinopathy induced in mice by targeted disruption of the rhodopsin gene. Nat Genet 15, 216-219.

Ikeda, Y., Goto, Y., Yonemitsu, Y., Miyazaki, M., Sakamoto, T., Ishibashi, T., Tabata, T., Ueda, Y., Hasegawa, M., Tobimatsu, S., Sueishi, K., 2003. Simian immunodeficiency virus-based lentivirus vector for retinal gene transfer: a preclinical safety study in adult rats. Gene Ther 10, 1161-1169.

Ikeda, Y., Yonemitsu, Y., Miyazaki, M., Kohno, R., Murakami, Y., Murata, T., Goto, Y., Tabata, T., Ueda, Y., Ono, F., Suzuki, T., Ageyama, N., Terao, K., Hasegawa, M., Sueishi, K., Ishibashi, T., 2009. Acute toxicity study of a simian immunodeficiency virus-based lentiviral vector for retinal gene transfer in nonhuman primates. Hum Gene Ther 20, 943-954.

Jacobs, G.H., Neitz, J., Deegan, J.F., 2nd, 1991. Retinal receptors in rodents maximally sensitive to ultraviolet light. Nature 353, 655-656.

Jacobs, G.H., Neitz, J., Krogh, K., 1996. Electroretinogram flicker photometry and its applications. J Opt Soc Am A Opt Image Sci Vis 13, 641-648.

Jacobs, G.H., Williams, G.A., 2007. Contributions of the mouse UV photopigment to the ERG and to vision. Doc Ophthalmol 115, 137-144.

Jacobson, S.G., Acland, G.M., Aguirre, G.D., Aleman, T.S., Schwartz, S.B., Cideciyan, A.V., Zeiss, C.J., Komaromy, A.M., Kaushal, S., Roman, A.J., Windsor, E.A., Sumaroka, A., Pearce-Kelling, S.E., Conlon, T.J., Chiodo, V.A., Boye, S.L., Flotte, T.R., Maguire, A.M., Bennett, J., Hauswirth, W.W., 2006a. Safety of recombinant adeno-associated virus type 2-RPE65 vector delivered by ocular subretinal injection. Mol Ther 13, 1074-1084.

Jacobson, S.G., Boye, S.L., Aleman, T.S., Conlon, T.J., Zeiss, C.J., Roman, A.J., Cideciyan, A.V., Schwartz, S.B., Komaromy, A.M., Doobrajh, M., Cheung, A.Y., Sumaroka, A., Pearce-Kelling, S.E., Aguirre, G.D., Kaushal, S., Maguire, A.M., Flotte, T.R., Hauswirth, W.W., 2006b. Safety in nonhuman primates of ocular AAV2-RPE65, a candidate treatment for blindness in Leber congenital amaurosis. Hum Gene Ther 17, 845-858.

Jaissle, G.B., May, C.A., Reinhard, J., Kohler, K., Fauser, S., Lutjen-Drecoll, E., Zrenner, E., Seeliger, M.W., 2001. Evaluation of the rhodopsin knockout mouse as a model of pure cone function. Invest Ophthalmol Vis Sci 42, 506-513.

Jefferson, A., Volpi, E.V., 2010. Fluorescence in situ hybridization (FISH) for genomic investigations in rat. Methods Mol Biol 659, 409-426.

Jeon, C.J., Strettoi, E., Masland, R.H., 1998. The major cell populations of the mouse retina. J Neurosci 18, 8936-8946.

Ji, J.Z., Elyaman, W., Yip, H.K., Lee, V.W., Yick, L.W., Hugon, J., So, K.F., 2004. CNTF promotes survival of retinal ganglion cells after induction of ocular hypertension in rats: the possible involvement of STAT3 pathway. Eur J Neurosci 19, 265-272.

Johnson, T.V., Martin, K.R., 2008. Development and characterization of an adult retinal explant organotypic tissue culture system as an in vitro intraocular stem cell transplantation model. Invest Ophthalmol Vis Sci 49, 3503-3512.

Kajiwara, K., Hahn, L.B., Mukai, S., Travis, G.H., Berson, E.L., Dryja, T.P., 1991. Mutations in the human retinal degeneration slow gene in autosomal dominant retinitis pigmentosa. Nature 354, 480-483.

Kaludov, N., Handelman, B., Chiorini, J.A., 2002. Scalable purification of adeno-associated virus type 2, 4, or 5 using ion-exchange chromatography. Hum Gene Ther 13, 1235-1243.

Kalyanasundaram, T.S., Black, G.C., O'Sullivan, J., Bishop, P.N., 2009. A novel peripherin/RDS mutation resulting in a retinal dystrophy with phenotypic variation. Eye (Lond) 23, 237-239.

Kashiwakura, Y., Tamayose, K., Iwabuchi, K., Hirai, Y., Shimada, T., Matsumoto, K., Nakamura, T., Watanabe, M., Oshimi, K., Daida, H., 2005. Hepatocyte growth factor receptor is a coreceptor for adeno-associated virus type 2 infection. J Virol 79, 609-614.

Kassen, S.C., Thummel, R., Campochiaro, L.A., Harding, M.J., Bennett, N.A., Hyde, D.R., 2009. CNTF induces photoreceptor neuroprotection and Muller glial cell proliferation through two different signaling pathways in the adult zebrafish retina. Exp Eye Res 88, 1051-1064.

Kilian, E.G., Eifert, S., Beiras-Fernandez, A., Daebritz, S., Reichenspurner, H., Reichart, B., 2008. Adeno-associated virus-mediated gene transfer in a rabbit vein graft model. Circ J 72, 1700-1704.

Kong, J., Kim, S.R., Binley, K., Pata, I., Doi, K., Mannik, J., Zernant-Rajang, J., Kan, O., Iqball, S., Naylor, S., Sparrow, J.R., Gouras, P., Allikmets, R., 2008. Correction of the disease phenotype in the mouse model of Stargardt disease by lentiviral gene therapy. Gene Ther 15, 1311-1320.

Konopatskaya, O., Churchill, A.J., Harper, S.J., Bates, D.O., Gardiner, T.A., 2006. VEGF165b, an endogenous C-terminal splice variant of VEGF, inhibits retinal neovascularization in mice. Mol Vis 12, 626-632.

Kroll, A.J., Machemer, R., 1969a. Experimental retinal detachment and reattachment in the rhesus monkey. Electron microscopic comparison of rods and cones. Am J Ophthalmol 68, 58-77.

Kroll, A.J., Machemer, R., 1969b. Experimental retinal detachment in the owl monkey. V. Electron microscopy of the reattached retina. Am J Ophthalmol 67, 117-130.

Krukenberg, F., 1899. Beiderseitige angeborene Melanose der Hornhaut. Klin Mbl Augenheilkd 37, 254-258.

Lai, Y., Yue, Y., Liu, M., Ghosh, A., Engelhardt, J.F., Chamberlain, J.S., Duan, D., 2005. Efficient in vivo gene expression by trans-splicing adeno-associated viral vectors. Nat Biotechnol 23, 1435-1439.

LaVail, M.M., Unoki, K., Yasumura, D., Matthes, M.T., Yancopoulos, G.D., Steinberg, R.H., 1992. Multiple growth factors, cytokines, and neurotrophins rescue photoreceptors from the damaging effects of constant light. Proc Natl Acad Sci U S A 89, 11249-11253.

LaVail, M.M., Yasumura, D., Matthes, M.T., Lau-Villacorta, C., Unoki, K., Sung, C.H., Steinberg, R.H., 1998. Protection of mouse photoreceptors by survival factors in retinal degenerations. Invest Ophthalmol Vis Sci 39, 592-602.

Le Meur, G., Stieger, K., Smith, A.J., Weber, M., Deschamps, J.Y., Nivard, D., Mendes-Madeira, A., Provost, N., Pereon, Y., Cherel, Y., Ali, R.R., Hamel, C., Moullier, P., Rolling, F., 2007. Restoration of vision in RPE65-deficient Briard dogs using an AAV serotype 4 vector that specifically targets the retinal pigmented epithelium. Gene Ther 14, 292-303.

Leaver, S.G., Cui, Q., Bernard, O., Harvey, A.R., 2006. Cooperative effects of bcl-2 and AAV-mediated expression of CNTF on retinal ganglion cell survival and axonal regeneration in adult transgenic mice. Eur J Neurosci 24, 3323-3332.

Lebherz, C., Maguire, A., Tang, W., Bennett, J., Wilson, J.M., 2008. Novel AAV serotypes for improved ocular gene transfer. J Gene Med 10, 375-382.

Lee, H., Chung, H., Arnouk, H., Lamoke, F., Hunt, R.C., Hrushesky, W.J., Wood, P.A., Lee, S.H., Jahng, W.J., 2010. Cleavage of the retinal pigment epithelium-specific protein RPE65 under oxidative stress. Int J Biol Macromol 47, 104-108.

Leonard, K.C., Petrin, D., Coupland, S.G., Baker, A.N., Leonard, B.C., LaCasse, E.C., Hauswirth, W.W., Korneluk, R.G., Tsilfidis, C., 2007. XIAP protection of photoreceptors in animal models of retinitis pigmentosa. PLoS One 2, e314.

Leveillard, T., Mohand-Said, S., Lorentz, O., Hicks, D., Fintz, A.C., Clerin, E., Simonutti, M., Forster, V., Cavusoglu, N., Chalmel, F., Dolle, P., Poch, O., Lambrou, G., Sahel, J.A., 2004. Identification and characterization of rod-derived cone viability factor. Nat Genet 36, 755-759.

Leveillard, T., Sahel, J.A., 2010. Rod-derived cone viability factor for treating blinding diseases: from clinic to redox signaling. Sci Transl Med 2, 26ps16.

Lewis, G.P., Charteris, D.G., Sethi, C.S., Fisher, S.K., 2002. Animal models of retinal detachment and reattachment: identifying cellular events that may affect visual recovery. Eye (Lond) 16, 375-387.

Liang, F.Q., Dejneka, N.S., Cohen, D.R., Krasnoperova, N.V., Lem, J., Maguire, A.M., Dudus, L., Fisher, K.J., Bennett, J., 2001. AAV-mediated delivery of ciliary neurotrophic factor prolongs photoreceptor survival in the rhodopsin knockout mouse. Mol Ther 3, 241-248.

Lipinski, D.M., Singh, M.S., Maclaren, R.E., 2011a. Assessment of cone survival in response to CNTF, GDNF and VEGF165b in a novel ex vivo model of end-stage retinitis pigmentosa. Invest Ophthalmol Vis Sci.

Lipinski, D.M., Thake, M., Maclaren, R.E., 2012. Clinical applications of retinal gene therapy. Prog Retin Eye Res.

Lipinski, D.M., Thake, M., MacLaren, R.E., 2013. Clinical applications of retinal gene therapy. Prog Retin Eye Res 32, 22-47.

Lipinski, D.M., Yusuf, M., Barnard, A.R., Damant, C., Charbel Issa, P., Singh, M.S., Lee, E., Davies, W.L., Volpi, E.V., Maclaren, R.E., 2011b. Characterization of a dominant cone degeneration in a green fluorescent protein-reporter mouse with disruption of Loci associated with human dominant retinal dystrophy. Invest Ophthalmol Vis Sci 52, 6617-6623.

Liu, H.S., Jan, M.S., Chou, C.K., Chen, P.H., Ke, N.J., 1999. Is green fluorescent protein toxic to the living cells? Biochem Biophys Res Commun 260, 712-717.

Lois, N., Wong, D., 2003. Pseudophakic retinal detachment. Surv Ophthalmol 48, 467-487.

Ludwig, G.V., Kondig, J.P., Smith, J.F., 1996. A putative receptor for Venezuelan equine encephalitis virus from mosquito cells. J Virol 70, 5592-5599.

Lyles, D.S., Rupprecht, C.E., 2006. Rhabdoviridae, Fifth ed. Lippincot-Williams & Wilkins, New York.

Lyubarsky, A.L., Chen, C., Simon, M.I., Pugh, E.N., Jr., 2000. Mice lacking G-protein receptor kinase 1 have profoundly slowed recovery of cone-driven retinal responses. J Neurosci 20, 2209-2217.

Lyubarsky, A.L., Falsini, B., Pennesi, M.E., Valentini, P., Pugh, E.N., Jr., 1999. UV- and midwave-sensitive cone-driven retinal responses of the mouse: a possible phenotype for coexpression of cone photopigments. J Neurosci 19, 442-455.

Lyubarsky, A.L., Lem, J., Chen, J., Falsini, B., Iannaccone, A., Pugh, E.N., Jr., 2002. Functionally rodless mice: transgenic models for the investigation of cone function in retinal disease and therapy. Vision Res 42, 401-415.

MacLaren, R.E., Buch, P.K., Smith, A.J., Balaggan, K.S., MacNeil, A., Taylor, J.S., Osborne, N.N., Ali, R.R., 2006a. CNTF gene transfer protects ganglion cells in rat retinae undergoing focal injury and branch vessel occlusion. Exp Eye Res 83, 1118-1127.

MacLaren, R.E., Pearson, R.A., MacNeil, A., Douglas, R.H., Salt, T.E., Akimoto, M., Swaroop, A., Sowden, J.C., Ali, R.R., 2006b. Retinal repair by transplantation of photoreceptor precursors. Nature 444, 203-207.

Magnussen, A.L., Rennel, E.S., Hua, J., Bevan, H.S., Beazley Long, N., Lehrling, C., Gammons, M., Floege, J., Harper, S.J., Agostini, H.T., Bates, D.O., Churchill, A.J., 2010. VEGF-A165b is cytoprotective and antiangiogenic in the retina. Invest Ophthalmol Vis Sci 51, 4273-4281.

Maier, K., Rau, C.R., Storch, M.K., Sattler, M.B., Demmer, I., Weissert, R., Taheri, N., Kuhnert, A.V., Bahr, M., Diem, R., 2004. Ciliary neurotrophic factor protects retinal ganglion cells from secondary cell death during acute autoimmune optic neuritis in rats. Brain Pathol 14, 378-387.

Malik, P., Arumugam, P.I., Yee, J.K., Puthenveetil, G., 2005. Successful correction of the human Cooley's anemia beta-thalassemia major phenotype using a lentiviral vector flanked by the chicken hypersensitive site 4 chromatin insulator. Ann N Y Acad Sci 1054, 238-249.

Malygin, A.A., Bondarenko, E.I., Ivanisenko, V.A., Protopopova, E.V., Karpova, G.G., Loktev, V.B., 2009. C-terminal fragment of human laminin-binding protein contains a receptor domain for venezuelan equine encephalitis and tick-borne encephalitis viruses. Biochemistry (Mosc) 74, 1328-1336.

May, C., Rivella, S., Callegari, J., Heller, G., Gaensler, K.M., Luzzatto, L., Sadelain, M., 2000. Therapeutic haemoglobin synthesis in beta-thalassaemic mice expressing lentivirus-encoded human beta-globin. Nature 406, 82-86.

McGee Sanftner, L.H., Abel, H., Hauswirth, W.W., Flannery, J.G., 2001. Glial cell line derived neurotrophic factor delays photoreceptor degeneration in a transgenic rat model of retinitis pigmentosa. Mol Ther 4, 622-629.

McGill, T.J., Prusky, G.T., Douglas, R.M., Yasumura, D., Matthes, M.T., Nune, G., Donohue-Rolfe, K., Yang, H., Niculescu, D., Hauswirth, W.W., Girman, S.V., Lund, R.D., Duncan, J.L., LaVail, M.M., 2007. Intraocular CNTF reduces vision in normal rats in a dose-dependent manner. Invest Ophthalmol Vis Sci 48, 5756-5766.

McLaughlin, S.K., Collis, P., Hermonat, P.L., Muzyczka, N., 1988. Adeno-associated virus general transduction vectors: analysis of proviral structures. J Virol 62, 1963-1973.

Megason, S., Amsterdam, A., Hopkins, N., Lin, S., 2006. Uses of GFP in transgenic vertebrates. Methods Biochem Anal 47, 285-303.

Mendes, H.F., van der Spuy, J., Chapple, J.P., Cheetham, M.E., 2005. Mechanisms of cell death in rhodopsin retinitis pigmentosa: implications for therapy. Trends Mol Med 11, 177-185.

Michalakis, S., Muhlfriedel, R., Tanimoto, N., Krishnamoorthy, V., Koch, S., Fischer, M.D., Becirovic, E., Bai, L., Huber, G., Beck, S.C., Fahl, E., Buning, H., Paquet-Durand, F., Zong, X., Gollisch, T., Biel, M., Seeliger, M.W., 2010. Restoration of cone vision in the CNGA3-/- mouse model of congenital complete lack of cone photoreceptor function. Mol Ther 18, 2057-2063.

Michaud, J.L., Boucher, F., Melnyk, A., Gauthier, F., Goshu, E., Levy, E., Mitchell, G.A., Himms-Hagen, J., Fan, C.M., 2001. Sim1 haploinsufficiency causes hyperphagia, obesity and reduction of the paraventricular nucleus of the hypothalamus. Hum Mol Genet 10, 1465-1473.

Mitry, D., Charteris, D.G., Fleck, B.W., Campbell, H., Singh, J., 2010a. The epidemiology of rhegmatogenous retinal detachment: geographical variation and clinical associations. Br J Ophthalmol 94, 678-684.

Mitry, D., Fleck, B.W., Wright, A.F., Campbell, H., Charteris, D.G., 2010b. Pathogenesis of rhegmatogenous retinal detachment: predisposing anatomy and cell biology. Retina 30, 1561-1572.

Miyoshi, H., Takahashi, M., Gage, F.H., Verma, I.M., 1997. Stable and efficient gene transfer into the retina using an HIV-based lentiviral vector. Proc Natl Acad Sci U S A 94, 10319-10323.

Mori, S., Wang, L., Takeuchi, T., Kanda, T., 2004. Two novel adeno-associated viruses from cynomolgus monkey: pseudotyping characterization of capsid protein. Virology 330, 375-383.

Mussolino, C., della Corte, M., Rossi, S., Viola, F., Di Vicino, U., Marrocco, E., Neglia, S., Doria, M., Testa, F., Giovannoni, R., Crasta, M., Giunti, M., Villani, E., Lavitrano, M., Bacci, M.L., Ratiglia, R., Simonelli, F., Auricchio, A., Surace, E.M., 2011. AAV-mediated photoreceptor transduction of the pig cone-enriched retina. Gene Ther 18, 637-645.

Naarendorp, F., Esdaille, T.M., Banden, S.M., Andrews-Labenski, J., Gross, O.P., Pugh, E.N., Jr., 2010. Dark light, rod saturation, and the absolute and incremental sensitivity of mouse cone vision. J Neurosci 30, 12495-12507.

Naldini, L., Blomer, U., Gallay, P., Ory, D., Mulligan, R., Gage, F.H., Verma, I.M., Trono, D., 1996. In vivo gene delivery and stable transduction of nondividing cells by a lentiviral vector. Science 272, 263-267.

Nicoud, M., Kong, J., Iqball, S., Kan, O., Naylor, S., Gouras, P., Allikmets, R., Binley, K., 2007. Development of photoreceptor-specific promoters and their utility to investigate EIAV lentiviral vector mediated gene transfer to photoreceptors. J Gene Med 9, 1015-1023.

Nikonov, S.S., Kholodenko, R., Lem, J., Pugh, E.N., Jr., 2006. Physiological features of the S- and M-cone photoreceptors of wild-type mice from single-cell recordings. J Gen Physiol 127, 359-374.

Nishijima, K., Ng, Y.S., Zhong, L., Bradley, J., Schubert, W., Jo, N., Akita, J., Samuelsson, S.J., Robinson, G.S., Adamis, A.P., Shima, D.T., 2007. Vascular endothelial growth factor-A is a survival factor for retinal neurons and a critical neuroprotectant during the adaptive response to ischemic injury. Am J Pathol 171, 53-67.

Nour, M., Quiambao, A.B., Al-Ubaidi, M.R., Naash, M.I., 2004. Absence of functional and structural abnormalities associated with expression of EGFP in the retina. Invest Ophthalmol Vis Sci 45, 15-22.

Odom, J.V., Reits, D., Burgers, N., Riemslag, F.C., 1992. Flicker electroretinograms: a systems analytic approach. Optom Vis Sci 69, 106-116.

Ohnaka, M., Miki, K., Gong, Y.Y., Stevens, R., Iwase, T., Hackett, S.F., Campochiaro, P.A., 2012. Long-term expression of glial cell line-derived neurotrophic factor slows, but does not stop retinal degeneration in a model of retinitis pigmentosa. J Neurochem 122, 1047-1053.

Okoye, G., Zimmer, J., Sung, J., Gehlbach, P., Deering, T., Nambu, H., Hackett, S., Melia, M., Esumi, N., Zack, D.J., Campochiaro, P.A., 2003. Increased expression of brain-derived neurotrophic factor preserves retinal function and slows cell death from rhodopsin mutation or oxidative damage. J Neurosci 23, 4164-4172.

Pagon, R.A., Daiger, S.P., 2005. Retinitis pigmentosa overview. University of Washington Press, Seattle.

Pang, J., Cheng, M., Haire, S.E., Barker, E., Planelles, V., Blanks, J.C., 2006. Efficiency of lentiviral transduction during development in normal and rd mice. Mol Vis 12, 756-767.

Pang, J., Lei, B., Mao, S., Everhart, D., Deng, W., Lieu, L., Li, Q., Chang, B., Barlow, R., Hauswirth, W.W., 2009. Long term rescue following AAV-mediated cone targeting gene therapy to cpfl5 mice, a model of human achromatopsia 2 with CNGA3 mutation, ARVO 2009 Annual Meeting, Fort Lauderdale, FL.

Pang, J.J., Alexander, J., Lei, B., Deng, W., Zhang, K., Li, Q., Chang, B., Hauswirth, W.W., 2010. Achromatopsia as a potential candidate for gene therapy. Adv Exp Med Biol 664, 639-646.

Pang, J.J., Chang, B., Hawes, N.L., Hurd, R.E., Davisson, M.T., Li, J., Noorwez, S.M., Malhotra, R., McDowell, J.H., Kaushal, S., Hauswirth, W.W., Nusinowitz, S., Thompson, D.A., Heckenlively, J.R., 2005. Retinal degeneration 12 (rd12): a new, spontaneously arising mouse model for human Leber congenital amaurosis (LCA). Mol Vis 11, 152-162.

Park, I.H., Arora, N., Huo, H., Maherali, N., Ahfeldt, T., Shimamura, A., Lensch, M.W., Cowan, C., Hochedlinger, K., Daley, G.Q., 2008. Disease-specific induced pluripotent stem cells. Cell 134, 877-886.

Pawliuk, R., Westerman, K.A., Fabry, M.E., Payen, E., Tighe, R., Bouhassira, E.E., Acharya, S.A., Ellis, J., London, I.M., Eaves, C.J., Humphries, R.K., Beuzard, Y., Nagel, R.L., Leboulch, P., 2001. Correction of sickle cell disease in transgenic mouse models by gene therapy. Science 294, 2368-2371.

Peachey, N.S., Ball, S.L., 2003. Electrophysiological analysis of visual function in mutant mice. Doc Ophthalmol 107, 13-36.

Peachey, N.S., Goto, Y., al-Ubaidi, M.R., Naash, M.I., 1993. Properties of the mouse cone-mediated electroretinogram during light adaptation. Neurosci Lett 162, 9-11.

Pearson, R.A., Barber, A.C., Rizzi, M., Hippert, C., Xue, T., West, E.L., Duran, Y., Smith, A.J., Chuang, J.Z., Azam, S.A., Luhmann, U.F., Benucci, A., Sung, C.H., Bainbridge, J.W., Carandini, M., Yau, K.W., Sowden, J.C., Ali, R.R., 2012. Restoration of vision after transplantation of photoreceptors. Nature 485, 99-103.

Pease, M.E., Zack, D.J., Berlinicke, C., Bloom, K., Cone, F., Wang, Y., Klein, R.L., Hauswirth, W.W., Quigley, H.A., 2009. Effect of CNTF on retinal ganglion cell survival in experimental glaucoma. Invest Ophthalmol Vis Sci 50, 2194-2200.

Peterson, W.M., Wang, Q., Tzekova, R., Wiegand, S.J., 2000. Ciliary neurotrophic factor and stress stimuli activate the Jak-STAT pathway in retinal neurons and glia. J Neurosci 20, 4081-4090.

Poeschla, E.M., Wong-Staal, F., Looney, D.J., 1998. Efficient transduction of nondividing human cells by feline immunodeficiency virus lentiviral vectors. Nat Med 4, 354-357.

Punzo, C., Kornacker, K., Cepko, C.L., 2009. Stimulation of the insulin/mTOR pathway delays cone death in a mouse model of retinitis pigmentosa. Nat Neurosci 12, 44-52.

Qing, K., Mah, C., Hansen, J., Zhou, S., Dwarki, V., Srivastava, A., 1999. Human fibroblast growth factor receptor 1 is a co-receptor for infection by adeno-associated virus 2. Nat Med 5, 71-77.

Redmond, T.M., Yu, S., Lee, E., Bok, D., Hamasaki, D., Chen, N., Goletz, P., Ma, J.X., Crouch, R.K., Pfeifer, K., 1998. Rpe65 is necessary for production of 11-cis-vitamin A in the retinal visual cycle. Nat Genet 20, 344-351.

Rennel, E., Waine, E., Guan, H., Schuler, Y., Leenders, W., Woolard, J., Sugiono, M., Gillatt, D., Kleinerman, E., Bates, D., Harper, S., 2008. The endogenous anti-angiogenic VEGF isoform, VEGF165b inhibits human tumour growth in mice. Br J Cancer 98, 1250-1257.

Renwick, J., Narang, M.A., Coupland, S.G., Xuan, J.Y., Baker, A.N., Brousseau, J., Petrin, D., Munger, R., Leonard, B.C., Hauswirth, W.W., Korneluk, R.G., Tsilfidis, C., 2006. XIAP-mediated neuroprotection in retinal ischemia. Gene Ther 13, 339-347.

Saint-Geniez, M., Maharaj, A.S., Walshe, T.E., Tucker, B.A., Sekiyama, E., Kurihara, T., Darland, D.C., Young, M.J., D'Amore, P.A., 2008. Endogenous VEGF is required for visual function: evidence for a survival role on muller cells and photoreceptors. PLoS One 3, e3554.

Sakuma, T., Barry, M.A., Ikeda, Y., 2012. Lentiviral vectors: basic to translational. Biochem J 443, 603-618.

Schlichtenbrede, F.C., da Cruz, L., Stephens, C., Smith, A.J., Georgiadis, A., Thrasher, A.J., Bainbridge, J.W., Seeliger, M.W., Ali, R.R., 2003a. Long-term evaluation of retinal function in Prph2Rd2/Rd2 mice following AAV-mediated gene replacement therapy. J Gene Med 5, 757-764.

Schlichtenbrede, F.C., MacNeil, A., Bainbridge, J.W., Tschernutter, M., Thrasher, A.J., Smith, A.J., Ali, R.R., 2003b. Intraocular gene delivery of ciliary neurotrophic factor results in significant loss of retinal function in normal mice and in the Prph2Rd2/Rd2 model of retinal degeneration. Gene Ther 10, 523-527.

Schmidt, T.M., Taniguchi, K., Kofuji, P., 2008. Intrinsic and extrinsic light responses in melanopsin-expressing ganglion cells during mouse development. J Neurophysiol 100, 371-384.

Shamu, C.E., 1997. Splicing together the unfolded-protein response. Curr Biol 7, R67-70.

Shan, H., Ji, D., Barnard, A.R., Lipinski, D.M., You, Q., Lee, E.J., Kamalden, T.A., Sun, X., MacLaren, R.E., 2011. AAV-mediated gene transfer of human X-linked inhibitor of apoptosis protects against oxidative cell death in human RPE cells. Invest Ophthalmol Vis Sci 52, 9591-9597.

Singh, M.S., Charbel Issa, P., Butler, R., Martin, C., Lipinski, D.M., Sekaran, S., Barnard, A.R., Maclaren, R.E., 2013. Reversal of end-stage retinal degeneration and restoration of visual function by photoreceptor transplantation. Proc Natl Acad Sci U S A 110, 1101-1106.

Small, K.W., 1998. North Carolina macular dystrophy: clinical features, genealogy, and genetic linkage analysis. Trans Am Ophthalmol Soc 96, 925-961.

Small, K.W., Udar, N., Yelchits, S., Klein, R., Garcia, C., Gallardo, G., Puech, B., Puech, V., Saperstein, D., Lim, J., Haller, J., Flaxel, C., Kelsell, R., Hunt, D., Evans, K., Lennon, F., Pericak-Vance, M., 1999. North Carolina macular dystrophy (MCDR1) locus: a fine resolution genetic map and haplotype analysis. Mol Vis 5, 38.

Solomon, S.G., Lennie, P., 2007. The machinery of colour vision. Nat Rev Neurosci 8, 276-286.

Spear, I.S., Fife, K.H., Hauswirth, W.W., Jones, C.J., Berns, K.I., 1977. Evidence for two nucleotide sequence orientations within the terminal repetition of adeno-associated virus DNA. J Virol 24, 627-634.

Srivastava, A., Lusby, E.W., Berns, K.I., 1983. Nucleotide sequence and organization of the adeno-associated virus 2 genome. J Virol 45, 555-564.

Stockman, A., Sharpe, L.T., Ruther, K., Nordby, K., 1995. Two signals in the human rod visual system: a model based on electrophysiological data. Vis Neurosci 12, 951-970.

Strack, R.L., Strongin, D.E., Bhattacharyya, D., Tao, W., Berman, A., Broxmeyer, H.E., Keenan, R.J., Glick, B.S., 2008. A noncytotoxic DsRed variant for whole-cell labeling. Nat Methods 5, 955-957.

Streichert, L.C., Birnbach, C.D., Reh, T.A., 1999. A diffusible factor from normal retinal cells promotes rod photoreceptor survival in an in vitro model of retinitis pigmentosa. J Neurobiol 39, 475-490.

Summerford, C., Bartlett, J.S., Samulski, R.J., 1999. AlphaVbeta5 integrin: a co-receptor for adeno-associated virus type 2 infection. Nat Med 5, 78-82.

Summerford, C., Samulski, R.J., 1998. Membrane-associated heparan sulfate proteoglycan is a receptor for adeno-associated virus type 2 virions. J Virol 72, 1438-1445.

Sun, H., Macke, J.P., Nathans, J., 1997. Mechanisms of spectral tuning in the mouse green cone pigment. Proc Natl Acad Sci U S A 94, 8860-8865.

Talcott, K.E., Ratnam, K., Sundquist, S.M., Lucero, A.S., Lujan, B.J., Tao, W., Porco, T.C., Roorda, A., Duncan, J.L., 2011. Longitudinal Study of Cone Photoreceptors during Retinal Degeneration and in Response to Ciliary Neurotrophic Factor Treatment. Invest Ophthalmol Vis Sci 52, 2219-2226.

Tour, O., Meijer, R.M., Zacharias, D.A., Adams, S.R., Tsien, R.Y., 2003. Genetically targeted chromophore-assisted light inactivation. Nat Biotechnol 21, 1505-1508.

Travis, G.H., Christerson, L., Danielson, P.E., Klisak, I., Sparkes, R.S., Hahn, L.B., Dryja, T.P., Sutcliffe, J.G., 1991. The human retinal degeneration slow (RDS) gene: chromosome assignment and structure of the mRNA. Genomics 10, 733-739.

Vandenberghe, L.H., Bell, P., Maguire, A.M., Cearley, C.N., Xiao, R., Calcedo, R., Wang, L., Castle, M.J., Maguire, A.C., Grant, R., Wolfe, J.H., Wilson, J.M., Bennett, J., 2011. Dosage thresholds for AAV2 and AAV8 photoreceptor gene therapy in monkey. Sci Transl Med 3, 88ra54.

Wang, G., Slepushkin, V., Zabner, J., Keshavjee, S., Johnston, J.C., Sauter, S.L., Jolly, D.J., Dubensky, T.W., Jr., Davidson, B.L., McCray, P.B., Jr., 1999. Feline immunodeficiency virus vectors persistently transduce nondividing airway epithelia and correct the cystic fibrosis defect. J Clin Invest 104, R55-62.

Wang, J., Faust, S.M., Rabinowitz, J.E., 2011. The next step in gene delivery: molecular engineering of adeno-associated virus serotypes. J Mol Cell Cardiol 50, 793-802.

Wiedenmann, J., Oswald, F., Nienhaus, G.U., 2009. Fluorescent proteins for live cell imaging: opportunities, limitations, and challenges. IUBMB Life 61, 1029-1042.

Williams, D., Sekiguchi, N., Brainard, D., 1993. Color, contrast sensitivity, and the cone mosaic. Proc Natl Acad Sci U S A 90, 9770-9777.

Williams, G.A., Daigle, K.A., Jacobs, G.H., 2005. Rod and cone function in coneless mice. Vis Neurosci 22, 807-816.

Wu, P., Xiao, W., Conlon, T., Hughes, J., Agbandje-McKenna, M., Ferkol, T., Flotte, T., Muzyczka, N., 2000. Mutational analysis of the adeno-associated virus type 2 (AAV2) capsid gene and construction of AAV2 vectors with altered tropism. J Virol 74, 8635-8647.

Yan, Z., Zhang, Y., Duan, D., Engelhardt, J.F., 2000. Trans-splicing vectors expand the utility of adeno-associated virus for gene therapy. Proc Natl Acad Sci U S A 97, 6716-6721.

Yang, Y., Mohand-Said, S., Danan, A., Simonutti, M., Fontaine, V., Clerin, E., Picaud, S., Leveillard, T., Sahel, J.A., 2009. Functional cone rescue by RdCVF protein in a dominant model of retinitis pigmentosa. Mol Ther 17, 787-795.

Yin, L., Greenberg, K., Hunter, J.J., Dalkara, D., Kolstad, K.D., Masella, B.D., Wolfe, R., Visel, M., Stone, D., Libby, R.T., Diloreto, D., Jr., Schaffer, D., Flannery, J., Williams, D.R., Merigan, W.H., 2011. Intravitreal injection of AAV2 transduces macaque inner retina. Invest Ophthalmol Vis Sci 52, 2775-2783.

Yokoyama, S., Radlwimmer, F.B., Kawamura, S., 1998. Regeneration of ultraviolet pigments of vertebrates. FEBS Lett 423, 155-158.

Zadro-Lamoureux, L.A., Zacks, D.N., Baker, A.N., Zheng, Q.D., Hauswirth, W.W., Tsilfidis, C., 2009. XIAP effects on retinal detachment-induced photoreceptor apoptosis [corrected]. Invest Ophthalmol Vis Sci 50, 1448-1453.

Zhang, K., Hopkins, J.J., Heier, J.S., Birch, D.G., Halperin, L.S., Albini, T.A., Brown, D.M., Jaffe, G.J., Tao, W., Williams, G.A., 2011. Ciliary neurotrophic factor delivered by encapsulated cell intraocular implants for treatment of geographic atrophy in age-related macular degeneration. Proc Natl Acad Sci U S A 108, 6241-6245.

Zincarelli, C., Soltys, S., Rengo, G., Rabinowitz, J.E., 2008. Analysis of AAV serotypes 1-9 mediated gene expression and tropism in mice after systemic injection. Mol Ther 16, 1073-1080.

Zolotukhin, S., 2005. Production of recombinant adeno-associated virus vectors. Hum Gene Ther 16, 551-557.

Zufferey, R., Dull, T., Mandel, R.J., Bukovsky, A., Quiroz, D., Naldini, L., Trono, D., 1998. Self-inactivating lentivirus vector for safe and efficient in vivo gene delivery. J Virol 72, 9873-9880.

Appendix

Publications written by or contributed to throughout the duration of this thesis

Tolmachova, T., Tolmachov, O.E., Barnard, A.R., de Silva, S.R., **Lipinski**,**D**.**M**.,, Walker, N.J., MacLaren, R.E.& Seabra, M.C. Funtional expression of Rab Escort Protein following AAV2-mediated gene delivery in the retina of choroideremia mice and human cells ex vivo. Mol. Med., 2013 (In press)

Singh, M., Charbel Issa, P., Butler, R., Martin, C., **Lipinski**,**D**.**M**., Sekaran, S., Barnard, A.R.& MacLaren, R.E.Reversal of end-stage retinal degeneration and restoration of visual function by photoreceptor transplantation. Proc. Natl. Acad. Sci. USA, 2013

Lipinski,**D**.**M**.*****, Thake, M., & MacLaren R.E. Clinical Applications of Retinal Gene Therapy. Prog Retin Eye Res, 2012. 32: 22-47

Charbel Issa, P., Singh, M.S., **Lipinski**,**D**.**M**., Chong, N.V., Delori, F.C., Barnard, A.R. & MacLaren, R.E. Optimization of in vivo confocal autofluosecence imaging of the ocular fundus in mice and its application to models of human retinal degeneration.Invest Ophthalmol Vis Sci, 2011. 53(2): 1066-75

Yusuf, M., Bauer, D.L.V., **Lipinski**,**D**.**M**., MacLaren, R.E., Wade-Martins, R., Mir, K. & Volpi, E.V. Combined M-FISH and Quantum Dot Technology for Fast Chromosomal Assignment of Transgene Insertions. BMCBiotechnol, 2011. 11(1): 121

Shan, H., Ji, D., Barnard, A.R., **Lipinski**,**D**.**M**., You, Q., Lee, E., Tengku Kamalden, T.A., Sun, X-H., & MacLaren, R.E. AAV-mediated gene transfer of human X-linked inhibitor of apoptosis protects against oxidative cell death in human RPE cells. Invest Ophthalmol Vis Sci, 2011 52(13): 9591-7

Lipinski,**D**.**M**.*****, Singh, M. & MacLaren, R.E. Quantification of cone photoreceptor survival in a novel in vitromodel of retinitis pigmentosa following administration of CNTF, GDNF and VEGF 165b. Invest OphthalmolVis Sci, 2011. 52(10): 7340-6

Lipinski,**D**.**M**.*****, Yusuf, M., Barnard, A.R., Damant, C., Charbel Issa, P., Singh, M., Lee, E., Davies, W. L., Volpi, E. & MacLaren, R.E. Characterization of a dominant cone degeneration in a GFP-reporter mouse with disruption of loci associated with human dominant retinal dystrophy. Invest Ophthalmol Vis Sci, 2011. 52(9):6617-23

*****denotes principal or sole author of the manuscript

Awards or honours received for work carried out as part of this thesis

2012 - The Master's Prize (Ruskell Medal). Awarded for an outstanding first contribution in the field of ophthalmology – Worshipful Company of Spectacle Makers, London, UK

2012 - AFER/NIHR Biomedical Resource Centre for Ophthalmology Traval Grant – ARVO annual conference

2011 - Young Investigators Award in Visual Science – AsiaARVO biennial conference